PhD degree in Molecular Medicine

European School of Molecular Medicine (SEMM),

University of Milan and University of Naples "Federico II"

Faculty of Medicine

Settore disciplinare: BIO/10

Role of vitronectin interaction in the biology of the urokinase receptor

Valentina Pirazzoli

IFOM-IEO Campus, Milan

Matricola n. R06821

Supervisor: Dr. Nicolai Sidenius

IFOM-IEO Campus, Milan

Anno accademico 2009-2010

Index

List of abbreviations

APCs: antigen presenting cells
ATF: amino-terminal fragment of uPA
CHO cells: Chinese hamster ovary cells
D1: domain 1 of uPAR
D2: domain 2 of uPAR
D3: domain 3 of uPAR
D2D3: uPAR fragment composed of domains 2 and 3
DCs: dendritic cells
DIC: Differential Interference Contrast microscopy
DMEM: Dulbecco's Modified Eagle's Medium
EC: Endothelial cell
ECM: extracellular matrix
ERK1/2: extracellular signal-regulated kinases 1 and 2
F-actin: filamentous actin
FA: focal adhesion
FACS: fluorescence activated cell sorter
FN: fibronectin
GPI: glycosyl-phosphatidylinositol
GFP: green fluorescent protein
HEK293 cells: human embryonic kidney 293 cell line
MMP: matrix metalloproteases
p130Cas: Crk-associated substrate (molecular weight: 130 kDa)
PA: plasminogen activation
PAI-1: plasminogen activator inhibitor type-1
PBS: phosphate-buffered saline
PECAM: platelet endothelial cell adhesion molecule
Phalloidin-FITC: Fluoresceinyl-aminomethyldithiolano-phalloidin (stains F-actin)
Plg: plasminogen
PmT: Polyoma middle T
RGD-motif: three residues (^{47}RGD) within the Vn responsible for integrin binding
SMB: somatomedin B domain
suPAR: soluble urokinase-type plasminogen activator receptor
uPA: urokinase-type plasminogen activator
uPAR: urokinase-type plasminogen activator receptor
VE-cadherin: Vascular endothelial cadherin
VN: vitronectin
VN(1-66): truncated VN encoding residues 1-66
VN(1-66)^{RAD}: truncated VN encoding residues 1-66, with one point mutant, G48A

Figure index

List of Publications

1. Taddei A, Giampietro C, Conti A, Orsenigo F, Breviario F, Pirazzoli V, Potente M, Daly C, Dimmeler S, Dejana E. Endothelial adherens junctions control tight junctions by VE-cadherin-mediated upregulation of claudin-5. Nat Cell Biol. 2008 Aug; 10(8): 923-34.

2. Pirazzoli V, Sidenius N. Urokinase plasminogen activator receptor interacts with vitronectin to influence cancer growth. In preparation

Abstract

Expression of uPAR has been extensively correlated with the malignant progression and metastasis of cancer; however, little evidence for a causal connection between increased uPAR expression and these processes has been documented to date. A complete functional alanine scan of human uPAR, pinpointed the extracellular matrix protein vitronectin (VN) as the critical uPAR-interactor required to induce cell adhesion, migration, and signaling *in vitro*, identifying this molecular interaction as a possible target for anti-cancer therapy (Madsen et al., 2007).

The same study helped to determine the binding epitope in uPAR responsible for its interaction to VN in an integrin-independent fashion. The composite epitope is fully conserved in mouse and included three amino acids (W32, R58, I63) in domain 1 (D1) and 2 amino acids (R92, Y93) in the linker region between D1 and D2.

We substituted these residues with alanine by site directed mutagenesis and analyzed the biological activity of resulting receptor variants in CHO Flp-In cells as compared to wild-type muPAR.

All the mutant receptors displayed a deficiency for the binding to VN, preserving the receptor binding to its natural ligand uPA. They also failed to induce muPAR-induced cell morphology changes. These changes include the formation of actin-rich lamellipodia, loss of stress fibers, reduced cell-cell contact as well as a complete failure to form colonies when seeded at low density. The mouse uPAR^{W32A} (muPAR^{W32A}) was chosen for further experiments since it did not show folding problems. Moreover the W32 position is not a part of the receptor chemotactic epitope and is not involved in the receptor cleavage.

Additional experiments using recombinant soluble muPAR confirmed the impaired VN-binding and a normal uPA-binding.

To determine if uPAR and/or VN are involved in tumor formation and progression, and more specifically, if the direct uPAR/VN-interaction is important in this process, we exploited a xenograft mouse model. For this purpose muPAR or muPAR^{W32A} or a muPAR variant lacking of the D1, required for both VN and uPA binding (muPAR$^{\Delta D1}$), were expressed in HEK293 Flp-In GFP positive cells and injected in the fourth mammary fat pad of immunodeficient mice.

In parallel the cells were tested for some *in vitro* assays. We demonstrated that HEK293 cells expressing muPAR are more proliferating and less apoptotic than the other cells. The interaction with VN is required to increased cell proliferation and to prevent from apoptosis. Moreover, muPAR-VN interaction induced cell spreading and migration.

muPAR expressing cells formed palpable tumors earlier than cells expressing the mutant receptors and the tumor growth was significantly faster. Despite the expression of the muPAR^{W32A} didn't affect the timing of the primary tumor formation, it drastically slowed down the growth of the primary tumor mass.

Finally we conducted *in vitro* studies to determine the molecular mechanisms underlying the possible role of the uPAR/VN-interaction *in vivo*. From these tests emerged that VN may act as an adhesion "bridge" between different cells expressing uPAR and VN-integrins or cells expressing both uPAR, suggesting a possible role of the uPAR/VN-interaction not only in cell-ECM interactions but also in cell-cell adhesion events including the extravasation of metastatic cancer cells.

Introduction

A fundamental property of living systems is to respond to external stimuli. The extracellular matrix (ECM) provides signaling cues that regulate cell behavior and orchestrate functions of cells in tissue formation and homeostasis. The ECM is the defining feature of connective tissue and includes the interstitial matrix, found in the intercellular spaces among various cells, and the basement membrane. The interstitial space consists of protein fibers embedded in an amorphous mixture of huge proteoglycan molecules and acts as a compression buffer against the stress placed on the ECM. Basement membranes are sheet-like depositions of ECM on which various epithelial cells rest.

Many cell types contribute to the production of the various ECM components thus determine the properties of the connective tissue. The majority of these components are produced by resident cells and secreted into the ECM via exocytosis. Due to its diverse nature and composition, the ECM can serve many functions, such as providing support and anchorage for cells, segregating tissues from one another, and regulating intercellular communication. In addition, it sequesters a wide range of cellular growth factors, and acts as a local *reservoir* for them.

The normal formation and function of multicellular tissues require correct expression and function of genes that control interactions of cells with the ECM. Misregulation of cell–ECM interactions can contribute to many diseases, including developmental, immune, haemostasis, degenerative and malignant disorders. The role of the ECM in cancer is a long-standing topic of investigation. In the ECM, there appears to be a proteolytic cascade that is involved in clearance of molecules from the ECM, interstitial fluid dynamics and turnover of individual ECM components as well as remodeling of tissue. This remodeling process is also critical in tumor invasion, for the

creation of space for cellular growth, and in metastasis formation, that often involves the destruction of extracellular matrix.

The urokinase-type plasminogen activator receptor (uPAR), first cloned in 1985, through the binding of urokinase plasminogen activator (uPA) guides the conversion of plasminogen into the active serine-protease plasmin at the leading edge of cells. For this reason, it was initially believed that the primary function of uPAR at the leading edge of migrating cells was to regulate invasive cell migration by virtue of its ability to promote degradation of the ECM. Indeed uPAR has been detected in invadopodia (Artym et al., 2002) and in the invasive front of many human tumors (Dano et al., 2005; Nielsen et al., 2007) and its expression on tumor cells strongly correlates with their migratory and invasive phenotype (Wang, 2001). However, it is becoming evident that uPAR also elicits a plethora of non-proteolytic functions, and its involvement in cell proliferation and migration is now well documented (Blasi and Carmeliet, 2002).

Aim of the work

In this thesis I will investigate the importance of the interaction of uPAR and VN, an ECM component, in a xenograft mouse model of tumorigenesis. In the view of that the VN-binding site of mouse uPAR will be investigated to better understand uPAR-VN interaction and to further produce a mutant muPAR receptor having an impaired VN-binding site.

In vitro experiments will be also conducted to understand how uPAR-VN interaction can occur *in vivo* and what can be the *in vivo* relevance of their binding.

Urokinase-type plasminogen activator receptor (uPAR)

uPAR expression

uPAR is a glycosyl-phosphatidylinositol (GPI)-anchored cell surface receptor expressed by many different tissues and cell types including epithelial (Limongi et al., 1995), keratinocytes (Romer et al., 1994), endothelial (Pepper et al., 1993), fibroblasts (Anichini et al., 1994), megakaryocytes (Wohn et al., 1997), podocytes (Wei et al., 2008), placental trophoblasts (Pierleoni et al., 1998) and most haematopoietic cells counting; peripheral monocytes/macrophages (Miles and Plow, 1987; Nykjaer et al., 1990), neutrophils (Plesner et al., 1994a), granulocytes (Miles and Plow, 1987), natural killer cells (Nykjaer et al., 1992), activated T-lymphocytes (Nykjaer et al., 1994) as well as osteoblasts and osteoclasts (Daci et al., 1999; Rabbani et al., 1997). Under normal physiological conditions basal expression levels of uPAR are rather low in all the various homeostatic mouse tissues that have been examined. However, uPAR expression is upregulated during certain tissue remodeling processes (Romer et al., 1994; Solberg et al., 2001), in host response to infection (Coleman et al., 2001; Speth et al., 1998), during inflammation and in many human diseases, including, Alzheimer's disease (Walker et al., 2002), rheumatoid arthritis (Del Rosso et al., 1999), multiple sclerosis (Balabanov et al., 2001), atherosclerosis (Okada et al., 1998) and cancer. uPAR is over-expressed in numerous human tumors, including leukemias (Lanza et al., 1998; Mustjoki et al., 1999; Plesner et al., 1994b), breast (Carriero et al., 1997), lung (Morita et al., 1998), bladder (Hudson and McReynolds, 1997), colon (Pyke et al., 1991), liver (De Petro et al., 1998), pleura (Shetty and Idell, 1998b), pancreas (Taniguchi et al., 1998) and brain (Yamamoto et al., 1994). Its expression levels correlated with poor prognosis and an unfavorable outcome, due to the increased risk of tumor recurrence and metastatic formations in patients (Ganesh et al., 1994; Grondahl-

Hansen et al., 1995; Pedersen et al., 1994; Sidenius and Blasi, 2003; Stephens et al., 1999).

uPAR gene

The human uPAR gene, located to chromosome 19q13.2 (Borglum et al., 1992), is made of seven exons separated by six introns and occupies about 21.23 kb (Wang et al., 1995). The seven exons of the gene are 101-, 111-, 144-, 162-, 135-, 147- and 563 bp long, respectively and encode 19, 37, 48, 54, 45, 49 and 83 amino acids residues, respectively. Exons 2+3 encode domain I, 4+5 encode D2, while exons 6+7 encodes for D3. Each domain is separated from the next by an intron. Part of the exon 1 encodes most of the hydrophobic leader sequence whereas the hydrophobic sequence necessary for GPI-anchor attachment is encoded in exon 7 (Roldan et al., 1990).

The six introns of the uPAR gene are approximately 2.04, 2.62, 8.42, 0.906, 3.10 and 2.78 kb long, respectively. They begin with GT and end in AG. The proximal promoter region of the uPAR gene lacks conventional TATA and CAAT boxes but contains a CpG-rich island and several putative *cis*-regulatory elements (AP1, AP2, SP1 and NF-κB) (Fig.1). Primer extension experiments demonstrated that the transcription start site is located at 50 bp upstream of the translation site (ATG) of the human gene (Wang et al., 1995).

Promoter analyses in transgenic mice have shown that uPAR expression in different tissues is controlled at a transcriptional level (Wang et al., 2003). Cytokines such as TNF-α or TGF-β and phorbol esters stimulate transcription (Lund et al., 1995; Lund et al., 1991a; Lund et al., 1991b; Niiya et al., 1998; Picone et al., 1989; Wang et al., 1994), while mRNA binding proteins regulates the stability of the uPAR mRNA (Lund et al., 1995; Lund et al., 1991a; Niiya et al., 1998; Shetty and Idell, 1998a; Shetty et al., 1997; Wang et al., 1998). In addition tumor-specific transcription factors have

been documented to bind the promoter in gastrointestinal cancer (Schewe et al., 2003). The uPAR mRNA stability is partly regulated by the phosphoglycerate kinase (PGK), which recognizes a short fragment within the uPAR coding region (Shetty et al., 2004). Despite the expression of uPAR during early embryogenesis, it is surprising that gene targeting of uPAR in mice is compatible with normal development and fertility (Bugge et al., 1995).

The uPAR cDNAs from other species including mouse (Kristensen et al., 1991), bovine (Reuning et al., 1993) and rat (Rabbani et al., 1994) have been also isolated and found to have similar sequence coding for the three domains of uPAR. The interspecies conservation of the individual domains is more than 60% (Kratzschmar et al., 1993).

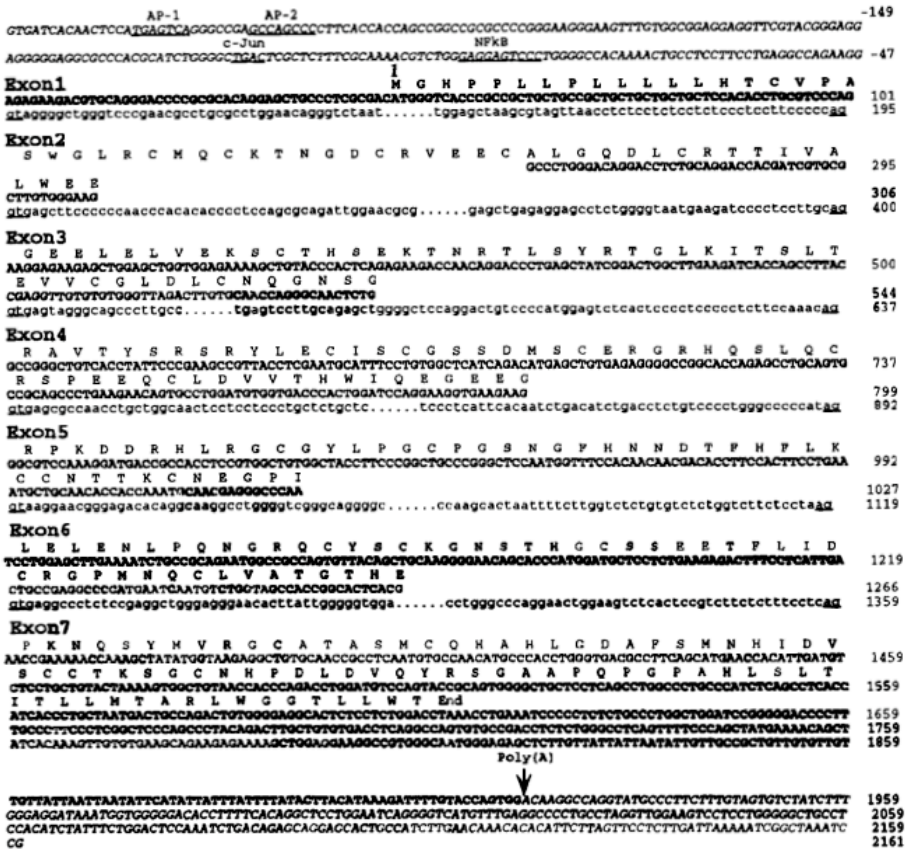

Figure 1: Nucleotide sequence of the human uPAR gene.

The complete amino acid sequence (single letter code) is shown above the first nucleotide of each codon. Exons are designated by upper-case and bold face letters and introns designated by lower-case letters. The

5'-flanking region and the 3'end sequence obtained from genomic clones are indicated by italics. The sequence is numbered and the translation-start site of known cDNA is considered as position 1. The beginning and the end of each intron and the putative transcription-factor-binding sites are underlined. The poly(A) attachment site is indicated by an arrowhead. Figure taken from (Wang et al., 1995).

uPAR protein

The nascent uPAR is translated as a 313 amino acids polypeptide, preceded by a 22 amino acid signal peptide. This signal peptide together with a C-terminal GPI-anchoring peptide (30 residues) are excised from the nascent protein during posttranslational processing, generating a 283 amino acid single chain polypeptide, linked to the outer membrane leaflet by a GPI-anchor (Moller et al., 1992; Ploug et al., 1991). The fact that uPAR is tethered to the cell surface by a glycolipid renders it predisposed for cleavage by phospholipases (Ploug et al., 1991; Wilhelm et al., 1999) and soluble uPAR (suPAR) has been observed *in vitro* as well as *in vivo* (Pedersen et al., 1993). This process is called uPAR shedding. Full-length suPAR binds uPA at an indistinguishable affinity from GPI-anchored full-length uPAR (Ploug et al., 1994). The mature uPAR protein is a single-chain protein of 55-60 kDA. It consists of three homologous domains, determed DI (residues 1-87), D2 (residues 88-191) and D3 (residues 192-283). The first domain contains the major binding region to uPAR natural ligand uPA (Huai et al., 2006) and is also required for uPAR-mediated cell binding to VN (Sidenius and Blasi, 2000). The other two domains have no detectable uPA binding activity. However, they might be important for high affinity uPA-binding as the purified first domain has a 1,500-fold lower ligand affinity than the original three-domain uPAR (Ploug et al., 1994; Riittinen et al., 1996).

The mature uPAR protein is highly glycosylated and decreases to Mr of 35 kDa upon deglycosylation (Behrendt et al., 1990; Nielsen et al., 1988). The N-linked glycosylation profile is highly heterogeneous and dependent on cell type and differentiation state (Behrendt et al., 1990; Lund et al., 1995). According to the sequence

it is predicted that human uPAR has five N-linked glycosylation sites (Asn52, Asn162, Asn172, Asn200 and Asn233) (Roldan et al., 1990). However, studies using recombinant uPAR (1-277) produced and secreted by CHO cells, demonstrated that only the first four of these sites are actually being glycosylated (Ploug et al., 1998). Interestingly these glycosylation sites exhibit site-specific heterogeneity (Ploug et al., 1998).

Relationship between uPAR and the Ly-6 gene family

Protein database searching using the consensus sequence of the putative domains of uPAR revealed homology to a diverse group of single domain glycoproteins (Behrendt et al., 1991). This group includes a gene family of murine leukocyte antigens collectively known as Ly-6 and the human regulatory complement component CD59. Like uPAR these are all glycolipid-anchored membrane proteins and have gene organization comparable to those segments of the uPAR gene encoding the individual domains (Ploug and Ellis, 1994). Moreover uPAR, Ly-6 and CD59 genes show a similar three-dimensional folding motif. The biological significance of the similarity between uPAR and members of the Ly-6 family genes is not clear at present.

uPAR structure

The crystal structure of soluble uPAR (suPAR) was first solved in association with a competitive inhibitor (AE147) of the uPA-uPAR interaction (suPAR/AE147) (Llinas et al., 2005). The structure of uPAR bound to the catalytic inactive amino-terminal fragment of uPA (ATF) was solved later on, first in a ternary complex (ATF/suPAR/ATN615), where ATF was bound to uPAR using a Fab fragment of the monoclonal antibody (ATN615) binding domain III of uPAR (Huai et al., 2006) and then in a binary complex (ATF/suPAR), where suPAR was bound directly to the ATF of uPA (Barinka et al., 2006). Finally the crystal structure of uPAR in complex with

both ATF and the SMB domain of VN was determined (suPAR-ATF-SMB) (Huai et al., 2008).

The solved crystal structure revealed that the uPAR three domains adopt a typical three-finger fold with three adjacent loops rich in β-pleated sheets and a small C-terminal loop. The secondary structure of each domain is composed by three consecutive β-sheets; D1 and D2 having six β-strands and D3 having five β-strands (Fig. 2). Altogether, uPAR possesses 17 antiparallel β-strands and 3 short helical stretches at the edge of loop 3 of D3. This fold possesses four disulphide bonds in D1 and five disulphide bonds in D2 and D3. The three domains of uPAR are assembled in a circular manner generating an almost globular receptor with a breach between D1 and D3. This topology creates a central cavity (19 Å deep) that accommodates uPA; the top of the cavity is widely open (21-25 Å large) while gradually tightening towards the bottom. This characteristic shape of the uPAR complex creates a large external surface containing the interdomain linker regions and the five N-glycosylation sites, permitting interactions with other proteins, such as vitronectin (Wei et al., 1994), or even oligomerization of the uPAR molecule (Cunningham et al., 2003).

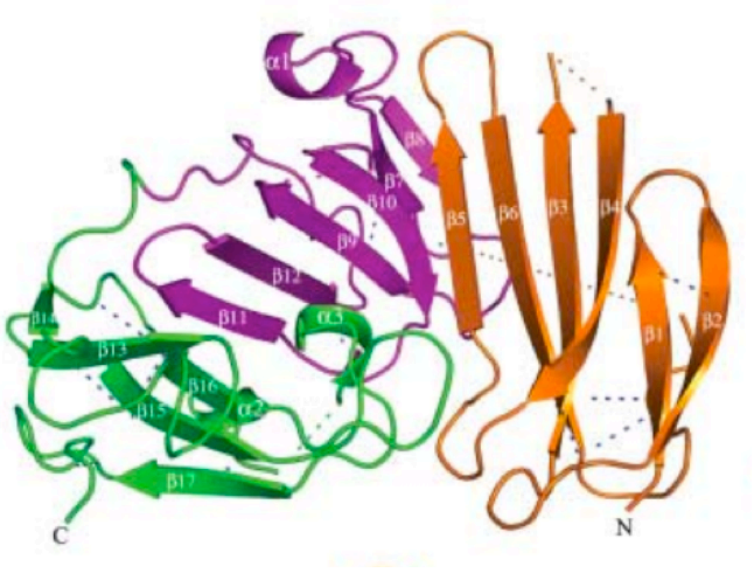

Figure 2: uPAR structure.

Domain structure of suPAR in the ATF/suPAR/ATN615 complex. The D1 domain (orange, residues 1 to 80) contains six β strands (β1, residues 2 to 7; β2, 10 to 16; β3, 23 to 32; β4, 38 to 46; β5, 53 to 58; β6, 63 to 71). The D2 domain (magenta, residues 93 to 191) contains six β strands (β7, 94 to 99; β8, 111 to 114; β9, 121 to 128; β10, 143 to 149; β11, 156 to 161; β12, 164 to 171) and a short α helix (α1, 104 to 107). The D3 domain (green, residues 192 to 283) contains five β strands (β13, 193 to 198; β14, 211 to 214; β15, 220 to 226; β16, 237 to 242; β17, 262 to 266) and two short α helices (α2, 244 to 246 and α3, 253 to 256). Disulfide bonds are shown in dashed lines (blue). The disordered loops are connected by the dash line colored as is the backbone to which they belong. Copy taken from the published crystal structure of the ATF/suPAR/ATN615 complex (Huai et al., 2006).

Important for the globular conformation of uPAR are the non-covalent interfaces between the three domains (interdomain interfaces). The interdomain interfaces provide flexibility to the structure and are greatly affected upon uPA binding (Huai et al., 2006).

The aperture of the D3-D1 interdomain interface (476 $Å^2$) is brought together by three hydrogen bonds between these two domains (His47-Asn259, Lys50-Asp254, and Arg53-Asp254) (Huai et al., 2006). Interestingly these three hydrogen bonds are not observed in the D3-D1 interface of suPAR/AE147 complex indicating that the binding of ATF invokes closure of the bowl-like structure by eliciting changes of the individual domains. This is supported by the larger D3-D1 interface observed upon ATF binding (476 $Å^2$ vs. 169 $Å^2$). In the ATF/suPAR/ATN615 complex the angle between D1 and D2 is reduced by ~20° due to conformational shift (9.5Å) centered on the corresponding interdomain β-strands (Huai et al., 2006). Another alteration observed

upon ATF binding was found in the connecting linker region (residues 78-92) between D1 and D2 (Barinka et al., 2006). Upon the binding of ATF this linker region is immobilized in its open conformation distanced by more than 14 Å from the receptor body, as observed in the binary ATF/suPAR complex. The immobilization of the flexible linker region is interesting as this stretch of residues is susceptible to proteolytic cleavage by various proteases including uPA, plasmin, elastase, cathepsin G and pro-matrix metalloproteases (MMPs) (Andolfo et al., 2002; Beaufort et al., 2004; Hoyer-Hansen et al., 1997). The physiological outcome upon cleavage includes loss of D1, deficient uPA -and VN binding (Hoyer-Hansen et al., 1997) and, depending on the exact cleavage sites, exposure of a chemotactically active fragment (Fazioli et al., 1997; Gargiulo et al., 2005). Taken together, uPAR seems to accommodate its corresponding ligand through a great conformational plasticity.

The functional epitope for uPA has been identified for the human uPAR by systematic alanine scanning mutagenesis (Gardsvoll et al., 2006). In details, nine residues in uPAR D1 (Arg25, Thr27, Leu40, Lys50, Thr51, Arg53, Leu55, Tyr57 and Leu66), eleven residues of D2 (Asp102, Ser104, Glu106, Val125, Thr127, Asp140, His143, Leu150, Pro151 and Leu168) and three residues of D3 (Met219, Gly227 and Phe256) displayed a ≥ 2.5 fold increase in the dissociation rate constant upon alanine substitution. This analysis clearly emphasized the important role of uPAR D2 in uPA binding.

The similarity of the ternary complex suPAR-ATF-SMB with the suPAR-ATF structure confirmed the notion that SMB binding doesn't perturb the structure of suPAR-uPA interface (Huai et al., 2008). The structure showed in fact that uPA occupies the central cavity of the receptor, whereas SMB binds the outer site. On the other hand the receptor occupancy by uPA does affect the binding of SMB to uPAR, as the suPAR-vitronectin affinity in the absence of uPA is reduced (Gardsvoll and Ploug,

2007; Sidenius et al., 2002). uPAR oligomerization was proposed to explain this uPA effect on VN binding to uPAR (Sidenius et al., 2002). However it is possible that uPA has a role in stabilizing the active conformation of uPAR, and this may explain the effect of uPA on SMB binding. The VN-binding surface of uPAR was previously mapped using a single-site alanine-scanning point mutation library of either purified suPAR (Gardsvoll and Ploug, 2007) or full-length uPAR expressed on HEK 293 cells (Madsen et al., 2007). In both studies, uPAR residues Try32, Arg58, Ile63 of D1 and Arg91, Tyr92 of the D1-D2 linker region were identified as key residues for SBM binding in the presence of uPA (Fig. 3). These results were consistent with the suPAR-ATF-SMB structural model.

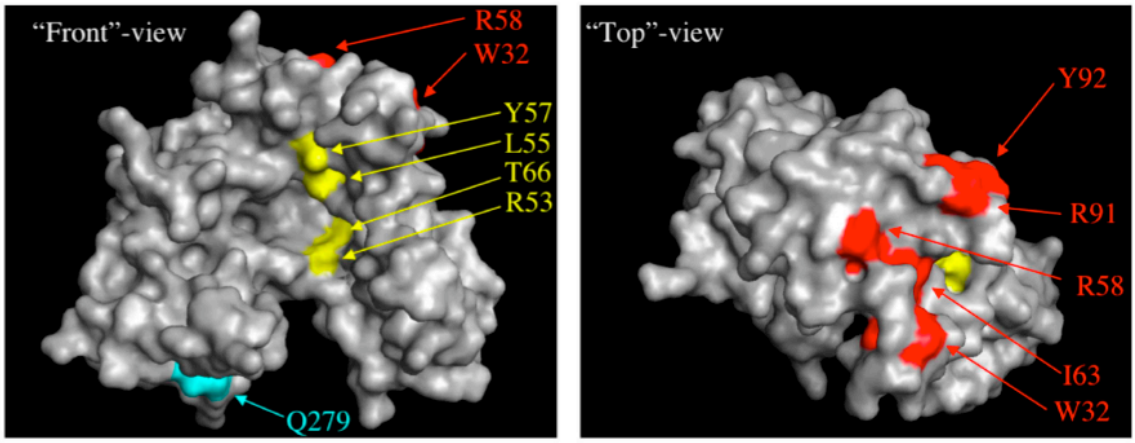

Figure 3: Location of the VN-binding site on the crystal structure of uPAR.

A surface representation of the uPAR structure is shown in gray, and the positions of the alanine-substituted residues that cause a strong reduction in VN binding using purified proteins are indicated in red. For comparison, a series of residues located in the uPAR ligand binding cavity and known to be involved in uPA binding are indicated in yellow. The most C-terminal residue (Q279) that is likely to be located close to the GPI anchor of membrane-tethered uPAR is indicated in cyan. The left panel is a "front" view of the uPA-binding cavity and the right panel is a "top" view (front view rotated 90° toward the observer). The images were constructed using the coordinates deposited in the Protein Data Bank (PDB) with the code number 1YWH and the MacPyMOL software (http://pymol.sourceforge.net). Figure taken from (Madsen et al., 2007).

Species selectivity of the uPA-uPAR interaction

Whereas SMB binding is not compromised by species differences (Lin et al., 2010), biochemical analysis of the binding properties for human and murine components revealed that the uPA-uPAR interaction exhibits species specificity. This species barrier has to be taken into account when testing the functional role of uPAR in proteolysis and signaling *in vivo*, i.e. during cancer invasion and metastasis using xenotransplanted tumor models. A detailed analysis of the ligand-binding interface in the crystal structure solved of human and murine uPA-uPAR complexes helped to identify the uPA residues responsible for the species selectivity (Lin et al., 2010). The mATF-muPAR crystal structure revealed that the interaction between uPAR and uPA is governed by the burial of the β-hairpin from the growth factor-like domain (GFD) module of ATF. Within this region just four positions differ between man and mouse, i.e. Asn27/Arg28 and His29/Arg30 (site 1) Asn22/Tyr23 and the Trp30/Arg31 (site 2). The humanization of just two of these positions, i.e. Tyr23→Asn and Arg31→Trp was able to swap the kinetic rate constants for the interactions between muPA and human or murine uPAR, thus demonstrating a clear structure-activity relationship for site 2 (Lin et al., 2010). Concordantly, it was also possible to graft the reciprocal species selectivity by introducing the equivalent mutations in huPA (Asn22→ Tyr, Trp30→Arg) (Lin et al., 2010).

As reported in the previously described crystal structure, uPA-binding occupies a large cavity that requires all three uPAR domains for its assembly. Despite this, just a mutation of the residue Glu31 in muPAR to Leu, the corresponding amino acid in huPAR, was sufficient to increase the receptor affinity for huPA. Glu31, in fact, forms a hydrogen bond to the essential Arg31 at site 2 of the bond mGFD, giving stability to the muPA-muPAR complex. This Glu31→Leu mutation in muPAR also rescued completely the loss of high affinity binding muPA Arg31→Try (Lin et al., 2010).

Vitronectin (VN)

Vitronectin expression

VN was discovered as the "serum spreading factor" (Holmes, 1967). The main site of VN biosynthesis is the liver; however, VN can also be produced by platelets (Preissner et al., 1989) and monocytes/macrophages (Hetland et al., 1989). VN is circulating in the blood stream at high concentration of 200-500 μg/ml (Preissner et al., 1985). VN in the blood exists as a monomer, but is converted into a multimeric form when incorporated into the ECM. VN is found in loose connective tissue of many organs, blood vessel walls, lymph nodes, and in the stroma of lymphatic tissue (Hayman et al., 1983), (Reilly and Nash, 1988). Increased VN deposition is found in reactive and fibrotic tissue (Reilly and Nash, 1988), atherosclerotic plaques (Niculescu et al., 1989) and in several tumors (Loridon-Rosa et al., 1988), (Gladson and Cheresh, 1991), (Gladson et al., 1995), (Maenpaa et al., 1997). Accordingly, VN has been implicated in a variety of physiological and pathological processes, including haemostasis (Thiagarajan and Kelly, 1988), angiogenesis (Brooks et al., 1994a), (Brooks et al., 1994b; Brooks et al., 1995), rheumatoid arthritis (Tomasini-Johansson et al., 1998) and tumor cell invasion (Desgrosellier and Cheresh; Nip et al., 1992).

Vitronectin gene

The human VN gene is composed of 4.5-5 kb pairs and contains eight exons and seven introns, from which a 1.7 kb pair transcript is derived. It encodes a molecule of 459 amino acids, which are preceded by a 19 amino acid signal peptide. The molecular weight of human VN is 75 kDa and contains three glycosylation sites (Schvartz et al., 1999). VN is post-translationally modified by sulfatation (Jenne et al., 1989),

phosphorylation (Schvartz et al., 2002; Seger et al., 1998; Seger et al., 2001), and N-linked glycosylation (Sano et al., 2007).

Despite the expression during embryogenesis, it should be noted that deletion of the VN gene in mice is compatible with normal development and fertility (Zheng et al., 1995).

Structure of vitronectin

The VN molecule is composed of several domains and binding epitopes (Fig 4). The N-terminal part of VN contains a SMB domain (residue 1-44), holding the high affinity-binding site for both uPAR and PAI-1 (residues D22, L24, Y27, Y28) (Fig. 4) (Schroeck et al., 2002; Seiffert and Loskutoff, 1991), followed by a region containing an Arg-Gly-Asp (RGD) motif (residues 45-47), which mediates the attachment and spreading of cells to the ECM through the binding to specific integrins (αvβ1, αvβ3, αvβ5, αIIbβ3) (Humphries et al., 2006; Preissner, 1991). Adjacent to the RGD motif occurs a highly acidic region (residues 53-64), containing the binding site for the antithrombin III complex (TAT) and the collagen-binding domain (Izumi et al., 1988). An ionic interaction between this acidic region and the basic region (residues 348-379) at the carboxyl-terminal domain is probably involved in stabilizing the three-dimensional structure of VN, and in the formation of its multimers. The major part of vitronectin contains seven hemopexin-type repeats (Jenne and Stanley, 1987) that accommodates in the carboxyl-terminal edge the binding site to heparin (Liang et al., 1997), glycosaminoglycans (Cardin and Weintraub, 1989) and plasminogen (Kost et al., 1992).

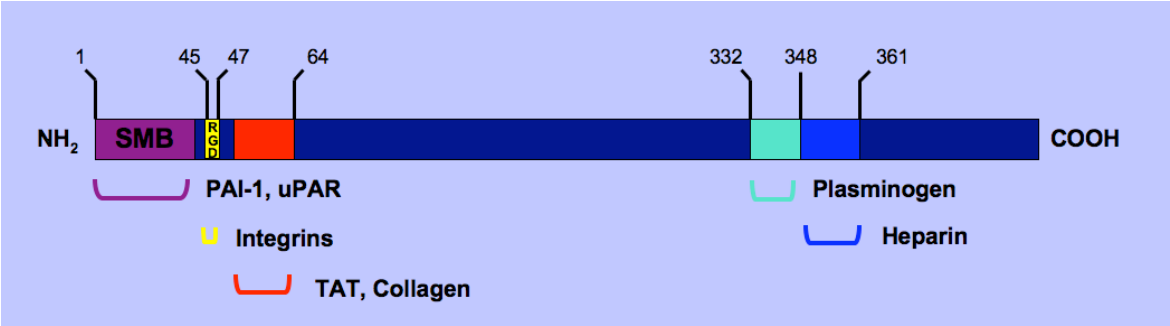

Figure 4: Vitronectin structure.

Localization of the binding domains of vitronectin towards various ligands; the binding sites for plasminogen activator inhibitor-1 (PAI-1), urokinase receptor (uPAR), integrins, thrombin±antithrombin III complex (TAT) and collagen are located in the N-terminus of the molecule, while the binding domains for plasminogen, heparin and PAI-1 are located in the carboxyl terminal edge. Figure adapted from (Schvartz et al., 1999).

The crystal structure of PAI-1 in complex with the SMB domain of VN has been solved and suggests that PAI-1 binding to VN may sterically interfere with integrin binding (Zhou et al., 2003). Indeed, in systems using purified proteins the interaction between integrins and VN can be fully blocked by PAI-1; however endothelial -and smooth muscle cell adhesion to VN is only partially inhibited by PAI-1; suggesting contemporaneous binding of PAI-1 and integrins to VN (Stefansson et al., 2007). Then again, formation of the ternary VN-PAI-1-αvβ3-complex in endothelial -and smooth muscle cells did not occur after treatment with cytochalasin D, a drug disrupting the actin cytoskeleton. This suggests a model in which integrins within focal adhesions (FA) sites are rigidly held by the cytoskeleton thus generating sufficient force to access the RGD-motif in VN by physically displacing PAI-1 without entirely removing it from the adjacent SMB domain (Stefansson et al., 2007).

VN exists as monomers and multimers (Stockmann et al., 1993), of which the latter is considered to be the active form, as defined by its ability to bind heparin, PAI-1 and uPAR. Multimeric VN exists predominantly incorporated into the ECM and is

recognized by cell surface receptors, like integrins and uPAR, where it supports cell adhesion, migration and invasion. On the contrary, these binding sites are inaccessible on monomeric VN, which accounts for the majority of VN in the plasma (Preissner and Seiffert, 1998). It is estimated that only 2% of plasma VN exist in an activated form, although it is not clear whether these 2% is able to bind ligands (Izumi et al., 1989). Interesting however, is the fact that VN inside the α-granules of platelets, when released by exocytosis, is presented in an active form (Seiffert and Schleef, 1996). Consequently, the biological functions of VN, and its binding properties to different ligands and cells, are tightly dependent on its conformational state(s). The exact structural alterations responsible for its many functions are still poorly understood; however, it is believed that partially cryptic binding sites in monomeric VN become exposed upon multimerization i.e. the SMB domain and the RGD motif. The transition from the monomeric to the multimeric form is often induced by interactions with heparin, PAI-1 (Seiffert and Loskutoff, 1996), and the thrombin-antithrombin complexes, and is believed to involve conformational changes in both the N-terminal acidic part and the C-terminal basic part of the molecule (Preissner and Seiffert, 1998). Likewise, phosphorylation (Seger et al., 2001), glycosylation (Sano et al., 2007) and proteolytic degradation of vitronectin (Chain et al., 1991) have been shown to modulate its conformation and function. The assembled multimers are deposited at sites of increased vascular permeability or injury (Seiffert, 1997) where they interact with various binding partners i.e. collagen, glycosaminoglycans, PAI-1, uPAR and integrins.

uPAR and the plasminogen activation system

Proteolytic degradation of the extracellular matrix plays a crucial role in cancer progression. The malignant progress of tumor invasion and metastasis requires the extensive making and breaking of the cell-cell and cell-ECM contacts as well as the degradation of ECM components that poses the physical barrier in the direction of invasion and migration. This degradative interplay often mimics the one observed in the tissue of origin during non-neoplastic remodeling processes, insinuating that cancer invasion may be regarded as uncontrolled tissue remodeling (Dano et al., 1999).

Proteolytic remodeling of the ECM involves a complex interplay between cancer cells and stromal cells and it is accomplished by a number of proteases with different activities and substrate specificities. Best known are the plasminogen (Plg) activation system that leads to the formation of the serine protease plasmin. In mammals, two different plasminogen activators have been identified, urokinase-type and the tissue-type plasminogen activators (uPA and tPA). Even though both plasminogen activators catalyzed the same reaction, uPA is thought to be more important in tissue remodeling and tPA in vascular fibronolysis.

uPA is released from the cells as an inactive proenzime, pro-uPA. Pro-uPA is a single glycoprotein chain of 52 kDa, composed of three crucial regions: the growth factor-like domain (GFD, residues 10 to 43) and the kringle domain (residues 50 to 132) that together form the N-terminal domain (ATF), which binds uPAR, and the C-terminal domain (CTF), which is endowed with catalytic activity. uPAR binds both pro-uPA and uPA with high affinity (0.1-1 nM) (Ellis et al., 1989). Once activated, uPA is able to convert the plasminogen to active plasmin, which than breaks down ECM components directly or indirectly through activation of pro-matrix metalloproteases (pro-MMPs) (Fig. 5).

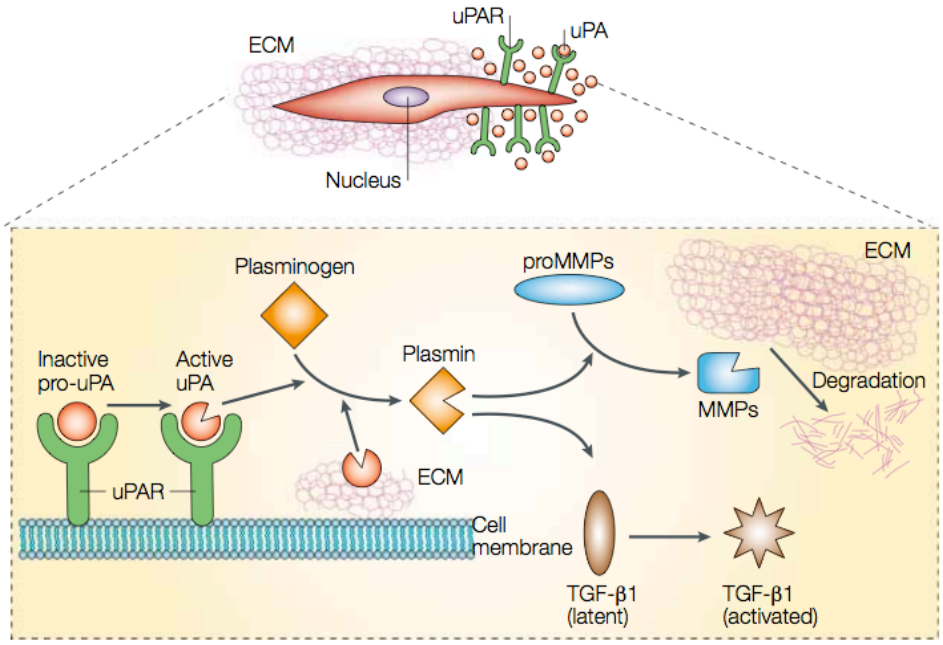

Figure 5: Schematic representation of the role of uPAR as a proteinase receptor.

At the leading edge of migrating cells uPAR binds pro-uPA, which is than converted to active uPA. Active uPA proteolytically converts the inactive zymogen plasminogen to active plasmin, which breaks down ECM components or activates latent growth factors such as transforming growth factor β1 (TGF-β1). Plasmin can also degrade the ECM indirectly through the activation of pro-MMPs. Figure taken from (Blasi and Carmeliet, 2002).

It is interesting that several components of the fibrinolytic pathway modulate uPAR activity. For instance, uPA, plasmin or MMPs, are all able to cleave membrane bound and soluble uPAR (Andolfo et al., 2002; Hoyer-Hansen et al., 1997) (Fig. 6). The result of the proteolytic cleavage of uPAR is the release of the D1 fragment from the rest of the receptor. This phenomenon impairs plasminogen activation as the co-localization between plasminogen and pro-uPA is lost and produces the uPAR fragment D2D3 fragment, which exploits a potent chemotactic activity (Fazioli et al., 1997) (Fig.6).

The plasminogen activator inhibitor-1 (PAI-1) also binds and regulates uPAR functions (Cubellis et al., 1989; Ellis et al., 1990). Indeed PAI-1 binds active uPA and

forms a uPA:PAI-1 covalent complex. This complex interacts with uPAR and another transmembrane receptor, a member of the low-density lipoprotein (LDL)-receptor-related protein (LRP)-protein family, which than drives the internalization of the uPAR-uPA:PAI-1 complex. In this process the uPA:PAI-1 complex is degraded (Cubellis et al., 1990), (Olson et al., 1992) and uPAR is recycled to the cell surface (Nykjaer et al., 1997).

The ECM not only determines tissue architecture but also serves as a reservoir for growth factors (Aumailley and Gayraud, 1998), contributing to organ formation, growth, apoptosis and most likely cancer dissemination (Liotta and Kohn, 2001). Thus the proteolytic degradation of the ECM contributes to the release of matrix-bound growth factors and signaling molecules (Ramirez and Rifkin, 2003). Of particular interest is the activation of bFGF (Saksela and Rifkin, 1990), FGF-2 (Ribatti et al., 1999), TGF-β1 (Lyons et al., 1990) (Fig. 5), HGF (Naldini et al., 1992) and IGFBP-4 (Remacle-Bonnet et al., 1997), which all can be activated by the PA system.

Besides concentrating pro-uPA to the cell surface, uPAR is capable of localizing the protein to specific sites where plasminogen activation is required, since uPAR is usually localized at the leading edge of migrating cells (Estreicher et al., 1990; Romer et al., 1994).

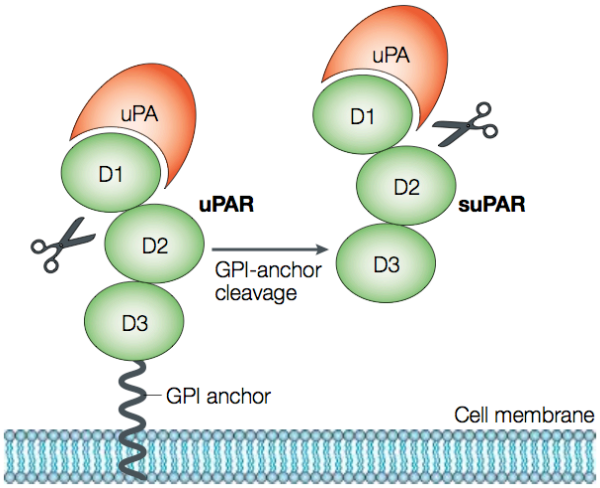

Figure 6: uPAR cleavage and shedding.

The urokinase receptor (uPAR) consists of three internally disulphide bounded domains and is attached to the cell surface by a GPI-anchor. Soluble uPAR (suPAR) is released from the plasma membrane by cleavage of the GPI anchor (uPAR shedding). Both uPAR and suPAR can be cleaved in the region that links domains D1 and D2 (scissors) to yield a D1 and D2D3 fragment (uPAR cleavage). Figure taken from (Blasi and Carmeliet, 2002).

Another player in the plasminogen activation system is the ECM protein vitronectin (VN). PAI-1 binds with high affinity to VN in a reaction that stabilized PAI-1 in its active conformation (Knudsen and Nachman, 1988). VN bound PAI-1 can still bind and inactivate uPA, but the formed uPA:PAI-1 complex has only low affinity for VN and is rapidly released (Deng et al., 1996). The binding sites for PAI-1 on VN overlaps with the one for uPAR, also capable of binding VN, and the binding of these two proteins is competitive and mutually exclusive (Deng et al., 1996), (Seiffert and Loskutoff, 1991). Numerous studies indicate that the uPA-system is involved in cancer. uPAR and uPA are over-expressed in human tumors (Dano et al., 2005). During tissue remodeling and cancer invasion functional redundancy is observed between extracellular proteases and often a synergistic effect is observed (Dano et al., 2005).

Besides this, proteolysis-independent cancer invasion have been observed by the ability of cancer cells to switch from a mesenchymal to an amoeboid type of migration surpassing the need of ECM degradation (Sahai and Marshall, 2003), (Wolf et al., 2003).

uPAR and signaling

In addition to regulating proteolysis, many studies show that uPAR is also a signaling receptor that promotes cell motility, invasion, proliferation and survival (Fig. 7). Although signaling through uPAR can involve uPA-uPAR binding, it is typically independent of uPA proteolytic activity. Another PA system player that takes part in the uPAR signaling is VN. Studies using alanine scanning mutagenesis have shown that only the residues of the VN-binding site are essential for uPAR to stimulate the actin cytoskeletal rearrangements required for cell spreading and migration (Madsen et al., 2007). However, lacking transmembrane and intracellular domains, uPAR must cooperate with transmembrane receptors to activate intracellular signaling. Considerable evidence suggested integrins to be uPAR-signaling co-receptors. Integrins are a large family of heterodimeric adhesion receptors that mediate cell attachment to several ECM components, including VN. uPAR co-immunoprecipitates with integrins and integrin-associated signaling molecules such as FAK and Src family kinases (Wei et al., 1996). Moreover, binding of different integrins to uPAR confers specificity to the signaling output of uPAR, activating one pathway instead of another. Even if all these approaches associate integrin pathways to uPAR, they do not prove a physical interaction between uPAR and integrins. uPAR binding to VN is independent of integrin engagement with VN, as mutation of the RGD motif into RAD still supports cell adhesion (Madsen et al.,

2007). Additionally, treatment with integrin-blocking antibodies, EDTA, and RGD-blocking peptides fail to inhibit uPAR-mediated cell adhesion to VN (Wei et al., 1994). The uPAR affinity for VN is often increased by concurrent binding of uPA or ATF (Sidenius et al., 2002). Accordingly, cells expressing low levels of uPAR adhere poorly to VN unless saturated with exogenous uPA, while cell expressing high levels of endogenous uPAR adhere independently of receptor occupancy (Sidenius and Blasi, 2000).

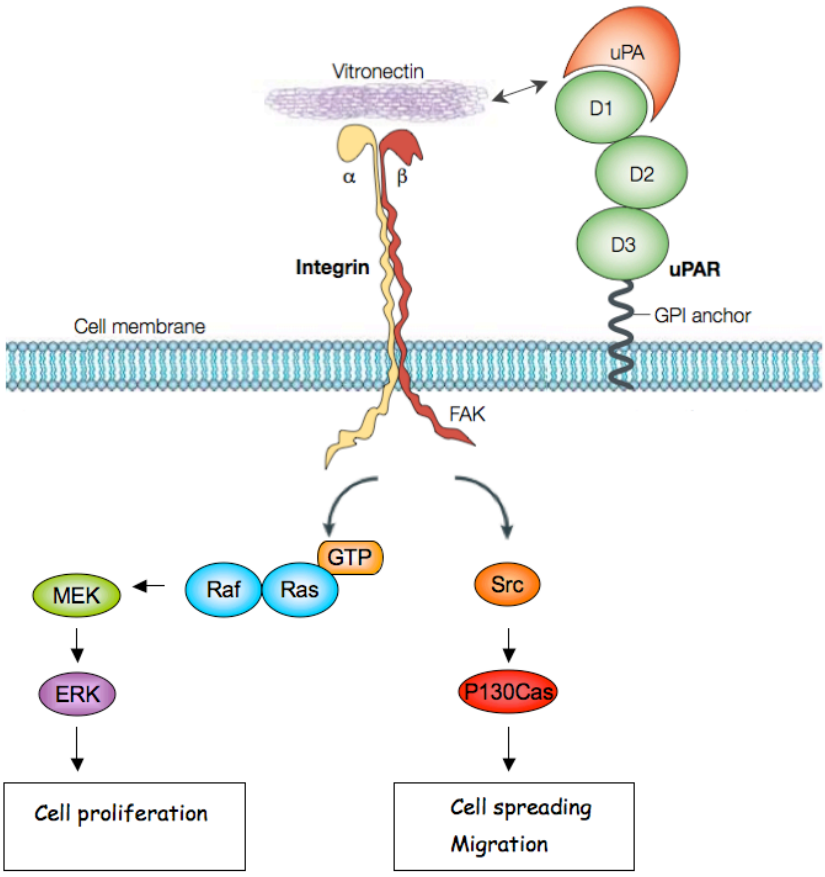

Figure 7: Role of uPAR as signaling receptor.

The urokinase receptor (uPAR) binds uPA and VN. uPAR lacks a cytosolic domain but transmits intracellular signals through its association with transmembrane integrins. Figure adapted from (Blasi and Carmeliet, 2002).

The first uPAR-integrin colocalization to be described involved MAC1, expressed in leukocytes, where it regulates migration, differentiation and phagocytosis. uPAR expression stimulates MAC1-driven neutrophil and monocyte chemotaxis *in vitro* (Gyetko et al., 1994). In addition, uPAR-deficient mice displayed impaired neutrophil infiltration of the lungs in models of pulmonary infection (Gyetko et al., 2000). uPAR-MAC1 signaling can contribute to the adhesion of macrophages and neutrophils to endothelial cells, a prerequisite for extravasation (Gyetko et al., 2000; May et al., 1998).

These findings are particularly interesting within the tumor scenario, which is often rich in leukocytes such as macrophages and neutrophils, as such tumor-associated leukocytes are important drivers of tumor behavior, including metastasis (Mantovani and Pierotti, 2008).

uPAR has also been found to co-localized with β1 and β3 integrins (Smith and Marshall, 2009). Several studies emphasized the distinct roles of uPAR-β1 integrin and uPAR-β3 integrin signaling. uPAR- β1 integrin is linked to ERK-dependent tumor cell proliferation. Chicken chorioallantoic membrane assay showed that signaling through α5β1 integrin is enhanced by uPA-uPAR interaction, leading tumor cell proliferation. Interestingly, in the same system, cells lacking uPAR entered a dormant state (Aguirre Ghiso et al., 1999; Aguirre-Ghiso et al., 2001), which suggests an important role for uPAR in determining whether tumor cells proliferate or become dormant. The uPAR-β3 integrin complex is proposed to initiate a pathway that involves Src activation and p130Cas phosphorylation, thus stimulating actin polymerization and cell protrusion that lead to cell motility. VN is often co-expressed with uPAR and β3 integrin in tumors (Loridon-Rosa et al., 1988); moreover, in tumor cells and podocytes, uPAR-β3 integrin signaling is VN-dependent. This is consistent with the fact that both uPAR and β3 integrins can bind VN.

Role of uPAR and uPA in *in vivo* fibrinolysis

The fibrinolytic system, also called plasminogen/plasmin system, has been claimed to play a role in a variety of phenomena associated with proteolysis, including blood clot dissolution (thrombolysis), ovulation, embryo implantation, embryogenesis, and cell invasion (Collen and Lijnen, 1991; Vassalli et al., 1991).

The availability of gene targeted mice deficient in the urokinase type plasminogen activator (uPA), urokinase receptor (uPAR), tissue-type plasminogen activator (tPA), and plasminogen (Plg) permitted a critical, genetic-based analysis of the physiological and pathological roles of the two mammalian plasminogen activators uPA and tPA.

Plg deficient mice are predisposed to severe thrombosis and secondary tissue damage but complete embryonic development, survive to adulthood, and are capable of reproduction.

Like Plg-/- mice, mice with combined deficiency in uPA and tPA suffer extensive spontaneous fibrin deposition but develop to term, grow to adulthood and reproduce (Carmeliet et al., 1994).

Remarkably, despite the fact that tPA appears to be of primary importance in vascular fibrinolysis via its fibrin binding property, mice lacking only tPA experience essentially no thrombotic problems (Carmeliet et al., 1994). Similarly mice lacking only uPA are generally healthy, but these mice occasionally develop hepatic fibrin deposition and ischemic rectal lesions (Carmeliet et al., 1994). Together these findings support that fibrinolysis may be the only physiological process for which Plg is essential and both uPA and tPA are complementary proteases that are individually capable of effectively clearing spontaneous vascular and extravascular fibrin.

The uPA receptor concentrates uPA-mediated proteolysis on the cell surface and it is well established that the rates of both pro-uPA and Plg activation *in vitro* are dramatically accelerated by the binding of uPA to uPAR (Ellis and Dano, 1991). Despite these evidences, uPAR deficient mice do not develop the spontaneous hepatic fibrin deposit, ischemic rectal ulcerations, or rectal prolapses observed in uPA-/- mice (Carmeliet et al., 1994). Moreover mice with combined uPAR and tPA deficiency do not exhibit the wide-range spread fibrin deposition, extensive multi-organ tissue damage and severe impairment of wound healing observed in mice with combined uPA and tPA deficiency and Plg-/- mice (Bugge et al., 1996). These findings demonstrate that receptor-bound uPA plays a role in fibrinolysis but it is effective in general fibrin clearance and can support wound healing in a uPAR- and tPA- independent manner.

Elucidation of the specific functions of uPA-uPAR interaction *in vivo* has been difficult because uPA has important physiological functions that are independent of binding to uPAR and because uPAR engages multiple ligands. In a recent study Connolly et al. (Connolly et al., 2010) generated a new mouse strain Plau $^{GDFhu/GDFhu}$ in which the uPA-uPAR interaction is selectively abrogated, while other functions of the protease and its cellular receptor are retained. Analysis of Plau $^{GDFhu/GDFhu}$ mice revealed an unanticipated role of the uPA-uPAR interaction in suppressing inflammation secondary to fibrin deposition. In contrast, leukocyte recruitment and tissue regeneration were unaffected by the loss of uPA binding to uPAR (Connolly et al., 2010). The obtained results clearly demonstrated that fibrin surveillance by uPA is a uPAR-dependent process that cannot be fully compensated by either uPAR-independent Plg activation (Bugge et al., 1996) or by activation of Plg by tPA (Carmeliet et al., 1994). Moreover the novel mouse-strain developed will be a most valuable tool for further functional dissection of the uPAR molecule.

uPAR and cancer

There is abundant experimental and clinical evidence in the literature supporting a role for the PA system in cancer progression. Neoplastic tumors in mice deficient in either plasminogen or uPA exhibit slower growth and show less tumor progression than similar lesions in wild-type mice (Gutierrez et al., 2000). Transfection of uPAR in HEK293 cells enhances metastasis into the lungs of immunodeficient mice in an uPA independent fashion (Jo et al., 2009) (Fig. 8). Furthermore, antibodies and inhibitors against components of the PA system prevent or reduced metastasis (Ossowski and Reich, 1983; Ploug et al., 2001).

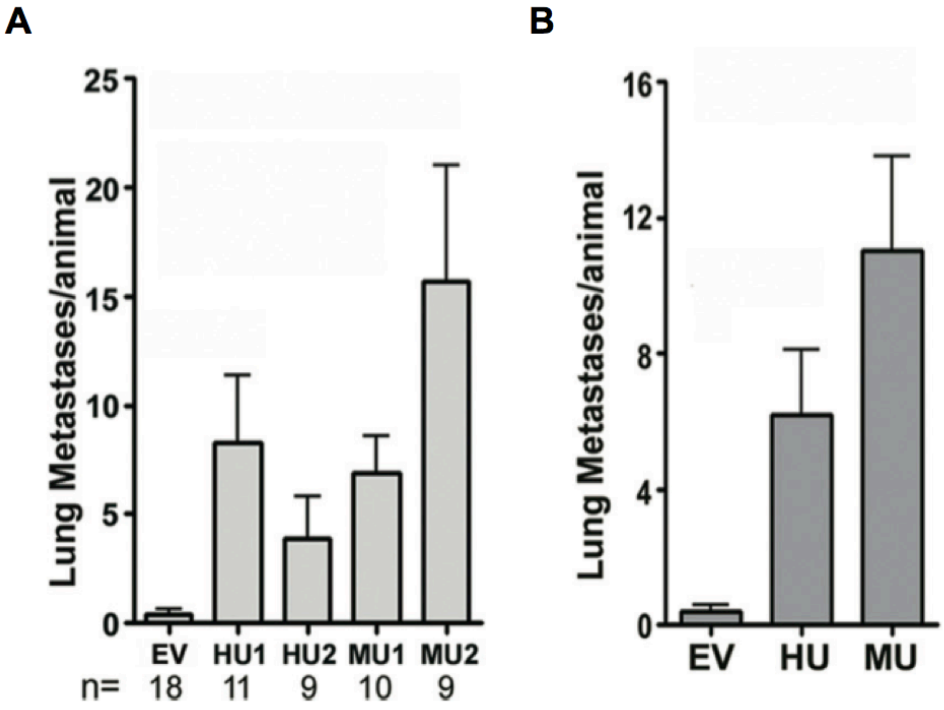

Figure 8: uPAR promotes HEK-293 cell metastasis in mice.

A: The number of discernable metastasis to the lungs is plotted for mice injected with empty vector (EV), human uPAR-expressing cells (HU1, HU2) or mouse uPAR-expressing cells (MU1, MU2). Lung metastasis were determined by counting green fluorescent foci that are at least 100 μm in maximum diameter on the surfaces of each lobe (mean ± s.e.m., $P<0.01$, P value determined by one-way analysis of variance test). **B:** Results obtained with HU1 and HU2 cells or MU1 and MU2 cells were pooled. Figure taken from (Jo et al., 2009).

The reason that the PA system is an attractive target for cancer therapy is that this system is quantitatively more expressed in tumor tissue. High uPAR, uPA and PAI-I levels have been shown to be adverse prognostic markers in several types of tumors. In early studies it was taken for granted that the proteases in tumor tissue were produced by the cancer cells. However, further findings suggested that the expression of components of the PA system in tumors can occur in tumor cells and/or tumor associated stromal cells. Precisely, which cell type synthesizes each of these molecules is different in different types of human cancer. In ductal breast cancer and in colon cancer uPA is expressed by fibroblast (Nielsen et al., 2001), in prostate cancer by macrophages (Pyke et al., 1991; Usher et al., 2005). In contrast, uPA is expressed by cancer cells in skin squamous cell carcinomas (Romer et al., 1991). The expression pattern of uPAR also differs between different cancers. uPAR is expressed by both cancer cells and macrophages in colon cancer (Pyke et al., 1991), primarily by macrophages in ductal breast cancer (Pyke et al., 1993), by cancer cells in skin squamous cell carcinoma and by macrophages in prostate cancer (Usher et al., 2005). Interestingly, the correlation between poor prognosis and expression of protein of the PA system is independent of the cell types in which the molecules are produced. These evidences suggest that cancer invasion is the result of an interaction between cancer cells and stromal cells. The cancer cells that invade are the initiators and probably the organizers, but each cell type contributes in a distinct way to the overall process.

Only few experimental studies on the functional role of stromal cells expression and components of the proteolytic system in cancer have been reported, probably because this phenomenon is generally poorly mimicked by transplanted tumors and there are few good animal models of spontaneous cancer available for study. However, studies conducted in genetically induced breast cancer in transgenic mice, that resemble the human ductal breast cancer, including the uPA expression by tumor-associated

stromal cells, reported as the absence of uPA leads to pronounced decrease in lung and lymph node metastasis, indicating an important role of stromally derived of uPA in this process (Almholt et al., 2005).

Since uPAR was discovered to be able to promote cell signaling through the interaction with members of the ECM and transmembrane proteins, therapeutic targeting of uPAR in cancer could not only interrupt the proteolytic cascade but also block the intracellular signaling responsible for the tumor-promoting functions of the stroma.

Targeting the PA system in cancer

uPAR discovery as a signaling molecule is relatively recent; for this reason most of therapies against cancer have been developed to target the proteolytic systems. Established therapeutic strategies to inhibit the uPA system are different and include inhibitor of the interaction between uPAR and uPA, inhibitor of the uPAR/VN/integrin interface and attenuation of uPA activity. Furthermore, transcriptional and post-transcriptional silencing of uPA system components are novel strategies for inhibition of tumor growth.

Some studies have investigated the antineoplastic effectiveness of anti-uPAR antibodies. A syngenic tumor model was produced by inoculation of rat breast carcinoma cells Mat B-III overexpressing uPAR into a syngenic rat, which then received a polyclonal antibody against the ligand-binding N-terminal domain of rat uPAR (Rabbani and Gladu, 2002). Treated rats showed a strong decrease of tumor progression. Similar results were obtained from an orthopic mouse model of human

pancreatic carcinoma, whose treatment with anti-uPAR monoclonal antibody decreased tumor growth and metastasis (Bauer et al., 2005).

The ATF portion of uPA lacks enzymatic activity and competes with naturally occurring uPA for uPAR binding. Transfection of human ATF cDNA in human lung carcinoma cells was shown to significantly reduce their invasive capacity in vitro and to prevent lung progression in a spontaneous metastasis model (Zhu et al., 2001). Similar results were demonstrated by another study using a defective adenovirus conveying a secretable version of the ATF of uPA (AdmATF) (Li et al., 1998). In this study, intratumoral injection of AdmATF into pre-established human breast cancer grafted in athymic mice exhibited an important reduction of tumor neovascularization, together with an inhibition of tumor growth.

Besides ATF, synthetic linear and cyclic peptides reproducing the receptor-binding region of ATF have been designed. An early study demonstrated the ability of murine uPA-derived peptides (residues 17-34) to inhibit metastatic colonization of murine Lewis Lung carcinoma cells inoculated subcutaneously into syngenic mice (Kobayashi et al., 1994). In another study, treatment of nude mice with cyclo^{19,31}-uPA$_{19-31}$, a cyclic form of the minimal essential peptide uPA$_{19-31}$, reduced the growth of human MDA-MB231 breast cancer cells when compared with the vehicle-treated control group (Sperl et al., 2001).

The use of recombinant soluble truncated forms of uPAR (suPAR) was another strategy to prevent tumor-associated proteolysis. In xenogenic mouse models, a reduction of primary tumor growth, tumor spread and metastasis occurred for ovarian cancer as well as breast cancer (Kruger et al., 2000).

Results to disclose the possibility of inhibiting tumor growth by suppression of uPA activity were achieved with anti-uPA antibodies and synthetic small molecules inhibiting the uPA system. Inhibition of receptor-bound uPA by specific anti-uPA

antibodies caused a significant suppression of proliferation in human melanoma cell line GUBSB (Kirchheimer et al., 1989). The WX-UK1, is one of the most potent uPA inhibitors described so far. First studies demonstrated that WX-UK1significantly reduced the number of metastatic lesions and tumor progression in a resected, spontaneously metastasizing rat mammary tumor model (Kirchheimer et al., 1989). WX-UK1 is currently under evaluation in phase II.

Many cytokines and growth factors induce the expression of components of the uPA system. Inhibition of cytokines and growth factors binding to their receptors or inhibition of their intracellular signaling may prevent uPA/uPAR-dependent processes. An example is given by studies of compounds blocking the EGFR activity. The EGFR family is overexpressed in a lot of human cancers and it is known to be involved in the transduction of uPAR stimuli. Results obtained with prostate cancer lines documented that tyrosine kinase inhibitors competitively bind the ATP pocket of EGFR, inducing a drastic reduction of uPA and uPAR mRNA and protein levels. This effect was associated with the inhibition of invasion potential of tumor cells and metastasis formation in nude mice studies (Festuccia et al., 2005).

In other faces of oncology, the uPA/uPAR system has been targeted with gene therapies such antisense nucleotide inhibition and siRNA.

Down-regulation of uPAR levels by antisense strategy using an adenovirus construct (Ad-uPAR) inhibited tumor cell invasion and metastasis in non-small cell lung cancer cell lines (Lakka et al., 2001). In vivo antisense uPAR mRNA also impaired colon cancer metastasis (Wang et al., 2001). Intraperitoneal and intratumoral administration of interfering RNA plasmid targeting uPAR demonstrated remarkable regression of pre-established breast tumors in mice (Fig. 9) (Kunigal et al., 2007).

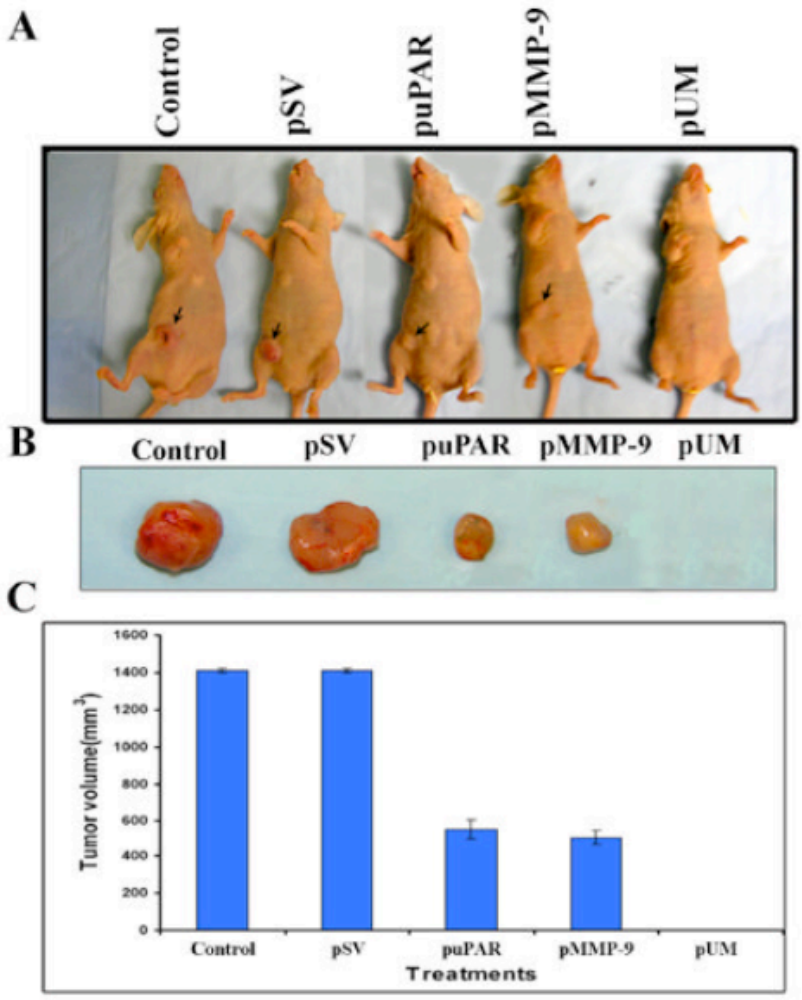

Figure 9: Therapeutic Effect of siRNA for uPAR and MMP-9.

MDA-MB231 cells (5-6×106 cells in 100 μL of phosphate-buffered saline or serum-free medium) were injected into the breast pad of nude mice and kept under observation for tumor growth. Tumors were allowed to grow until they reached 5 to 6 mm. At this point, tumors were randomized into several groups receiving treatment with SV, puPAR, pMMP-9, or pUM (plasmid siRNA vector for uPAR and MMP-9) (150 μg of each vector was injected intratumorally). **A**: Animals injected with various constructs. **B**: Tumors from these animals were dissected 4 weeks after injection with these constructs. **C**: Semiquantification of tumor volume in control, SV, puPAR, pMMP-9, and pUM-treated groups at 4 to 6 weeks after treatment. Data shown are mean ± S.D. values from 5 to 6 animals from each group. Figure taken from (Kunigal et al., 2007).

Virus- and toxin-associated anticancer therapies are new and promising approaches for the treatment of cancer.

An example of oncolytic virus engineered to specifically target tumor cells is given by Jing and co-workers. The authors characterized a novel Edmonston vaccine

strain oncolytic MV (MV-Edm) fully retargeted against uPAR. More precisely, they display the uPAR-binding ATF of either human (MV-h-uPA) or murine (MV-m-uPA) uPA into the COOH- terminus of mutant MV-H glycoprotein, which lacks the ability to attach to its endogenous receptors. They showed that MV-h-uPA significantly delayed tumor progression and improved survival in a breast cancer xenograft model. Moreover, MV-m-uPA was able to target tumor capillaries *in vivo* (Jing et al., 2009).

Among the new therapeutic strategies that have been exploited to achieve tumor-restriction action, one of the most common is the conjugation of antibodies, cytokines and growth factors with bacterial or plant toxins. Liu and colleagues (Liu et al., 2001) constructed mutated anthrax toxin-protective antigen (PrAg) proteins in which the furin cleavage site is replaced by sequences cleaved specifically by uPA. These uPA-targeted PrAg proteins were activated selectively on the surface of uPAR-expressing tumor cells in the presence pro-uPA and plasminogen. The activated PrAg proteins caused internalization of a recombinant cytotoxin, thereby killing the uPAR-expressing tumor cells. Data obtained from *in vivo* studies of uPA-activated PrAg proteins were extremely encouraging. In fact, engineered PrAg had a strong anti-tumor activity when injected adjacent to tumor nodules. These evidences strongly support the mutated PrAg proteins as a new therapeutic agent for cancer treatment (Liu et al., 2005).

PA system in innate and adaptive immunity

Levels of various components of the PA system are upregulated during severe infections. This evidence supports a role for this system in both innate and adaptive immune-mediated responses.

Indeed, bacterial products, such as endotoxin, as well as pro inflammatory cytokines, including IL-1β and TNF-α, whose release is increased in case of severe infection, elicit uPA expression and secretion by several cells, such as epithelial and endothelial cells monocytes and neutrophils (Blasi, 1993).

uPAR also participates in the initiation of the innate immune response by regulating cell adhesion and migration. In uPAR deficient mice, macrophages and neutrophils failed to infiltrate the lungs of mice infected with *Streptococcus pneumonia* (Rijneveld et al., 2002) or *Pseudomonas aeruginosa* (Gyetko et al., 2000) (Fig. 10).

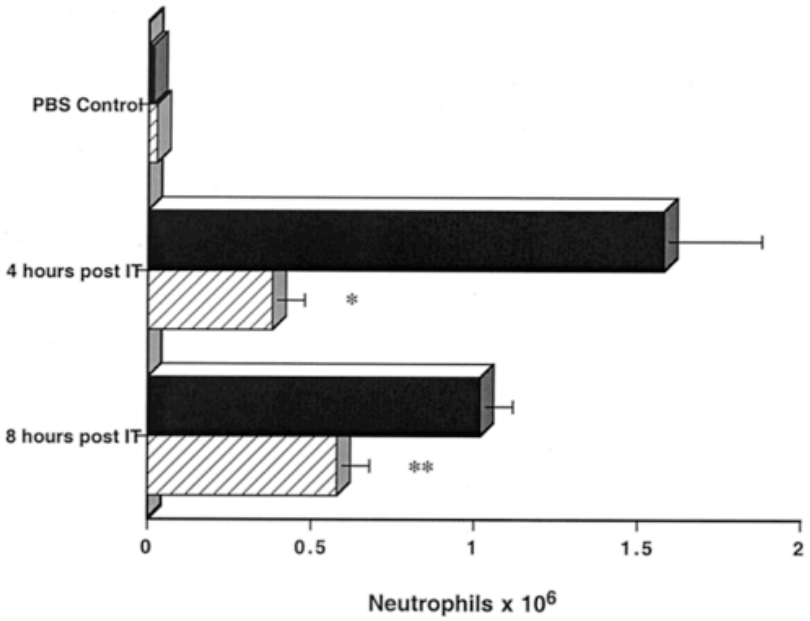

Figure 10: Comparison of neutrophil recruitment in WT and uPAR-/- mice in response to *P. aeruginosa* pneumonia.

WT and uPAR-/- mice were IT inoculated with PBS or *P. aeruginosa,* and the numbers of neutrophils present in BAL fluid were determined 4 and 8 h later. Neutrophils in PBS-inoculated mice were quantified at 4 h post-IT inoculation. In black columns WT mice; in stripped columns, uPAR-/-. Data are expressed as the mean ±s.e.m., *, p=0.0003 (n=12); **, p =0.0011 (n=5). Figure taken from (Gyetko et al., 2000).

The observation that uPAR-dependent cell recruitment was in some cases independent of uPA (Gyetko et al., 2001; May et al., 1998), and that uPAR- and uPA-knockout mice have different susceptibilities to several pathogen infections (Gyetko et

al., 2000; Rijneveld et al., 2002), indicates that uPAR and uPA might operate at different steps and by different pathways. Furthermore, the finding that PA1-1 or plasminogen deficient mice showed optimal inflammatory cell migration and host defense during *Pneumococcal pneumoniae* infection (Rijneveld et al., 2003) indicates that uPA and uPAR favor innate immune responses mostly by promoting inflammatory cell activation and migration rather than through their fibrinolytic function.

uPA and uPAR also participate in the initiation of adaptive immune responses. T-cells expression of both uPA and uPAR are rapidly upregulated during T-cell activation (Bianchi et al., 1996; Nykjaer et al., 1994). Moreover uPAR is expressed by antigen presenting cells (APCs), such as dendritic cells (DCs), monocytes and macrophages (Blasi, 1999; Plesner et al., 1997). Thus the concomitant expression of uPA and uPAR by T-cell and APC supports the possibility that the PA system participates in T-cell priming. This possibility is supported by data obtained both *in vitro* and *in vivo*. In fact, splenocytes derived from uPA-deficient mice elicit only suboptimal T-cell activation and proliferation *in vitro* (Gyetko et al., 1999). Moreover, blocking uPAR on the surface of DCs and monocytes lowers the co-stimulatory capabilities of these cells (Stonehouse et al., 1999; Woodhead et al., 2000). Furthermore, in absence of uPA, T helper effetor lymphocytes fail to differentiate in response to pathogen challenge *in vivo* (Gyetko et al., 2002), (Gyetko et al., 2004). uPA-uPAR could also promote T-cell effector function at the site of infection. For instance, uPA can activate latent proinflammatory cytokines, such as pro-TGF-β, pro-IL-1 and pro-IL-6, or MMPs, and thus favor the local inflammatory reaction (Vaday and Lider, 2000). Finally, uPA-dependent fibrinolysis and tissue remodeling, by eliciting the degradation of several tissues components, might favor antigen presentation, and thus T-cell re-activation in situ. By contrast uPAR might favor the recruitment of activated T cells in infected tissues. Indeed, blockade of uPAR expression by antisense nucleotides

hampers leukocyte migration *in vitro* (Gyetko et al., 1994). *In vivo*, T-cell recruitment to the lung is defective in uPAR-Knockout mice (Gyetko et al., 2001) (Fig. 11).

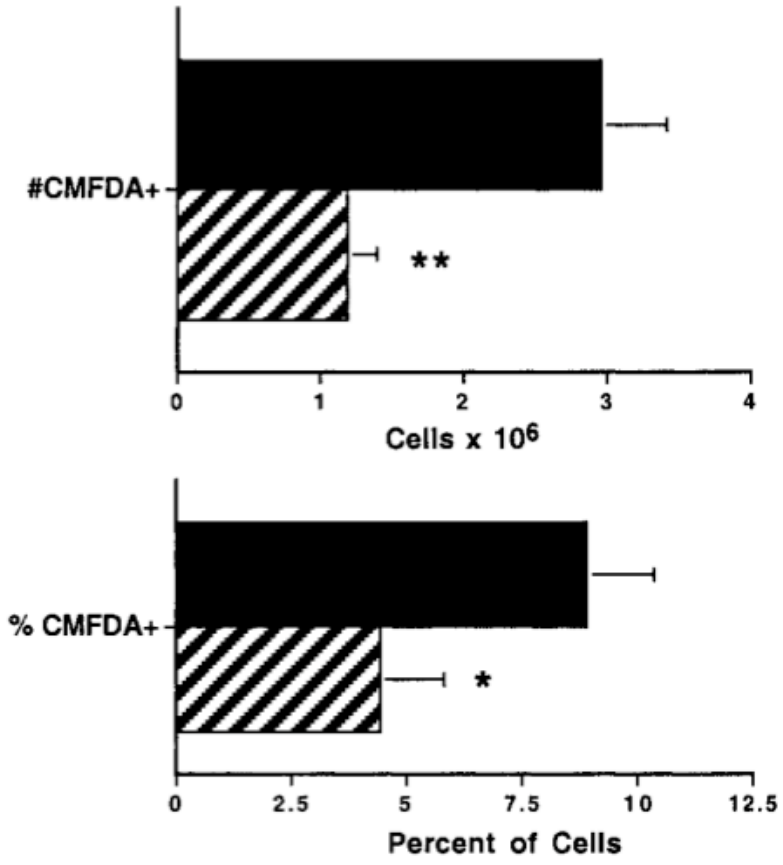

Figure 11: Comparison of recruitment of WT and uPAR-/- lymphoblast to the lungs of WT recipient mice.

WT or uPAR-/- CMFDA-labeled lymphoblasts were i.v. infused into SRBC-primed WT mice 3 days after they were inoculated with SRBC IT. Eighteen hours later the number and percentage of CMFDA+ lymphocytes recruited to the lungs of the WT recipient mice were determined. WT lymphocytes recruited to the lungs of the WT recipient mice were determined. WT lymphoblasts are represented by the filled bars and uPAR-/- lymphoblast are represented by the hatched bars. Data are represented as mean ±s.e.m., *, p=0.05; **, p =0.007 (n=6). Figure taken from (Gyetko et al., 2001).

Material and Methods

Antibodies

Polyclonal antibody against muPAR (SI420), muPAR D1 (BR 4.8) and muPAR D1D2 (AK 17.1) were used in FACS analysis and Western blot (Tjwa et al., 2009). Rat monoclonal anti-mouse F4/80 FITC-conjugated (Abcam) was used for Bone Marrow-derived macrophages IF. Polyclonal antibodies against total and phosphorylated ERK1/2, pY410-p130Cas, and secondary antibodies anti–mouse HRP and anti-rabbit HRP were from Cell Signaling Technology. Antibody against mouse vinculin was from Sigma-Aldrich. Hamster anti-mouse CD31/PECAM was from Millipore. Goat anti-mouse VE-cadherin (C-19) was from Santa Cruz. Donkey anti-mouse-IgG-Cy3, Donkey anti-mouse-IgG-Cy5, Donkey anti-Goat-FITC and Goat anti-Hamster-Cy3 were from Jackson ImmunoResearch Laboratories. Phalloidin-FITC and biotinylated-AnnexinV were from Sigma-Aldrich. SA-APC was from eBioscience.

Cloning of mouse uPAR and expression vectors construction

A full-length mouse uPAR cDNA (muPAR, (Kristensen et al., 1991)) was amplified with primers mupKpn/muPARre and cloned KpnI/NotI in pcDNA5/FRT-TO (Invitrogen) generating the expression vector pFRT/TO-muPAR. The muPAR$^{\Delta D1}$ deletion mutant was generated by co-amplification (primers mupKpn/muPARre) of two PCR products generated using primer-pairs mupKpn/mD1rev and mD1/muPARre and cloning as described for full-length mouse uPAR. This procedure deletes the D1-coding region (residues 1-84) generating a truncated D2D3-receptor having the same N-terminal (Gly85) as that generated by uPA or limited plasmin cleavage of the D1-D2 linker region (Andolfo et al., 2002).

The VN(1–66)/Fc fusion protein was generated by attaching the first 66 amino acids of mature human VN to a constant region of a human IgG. Primers and templates were as follows: a vector containing part of the VN cDNA (pTrx-VN(1–97) (Deng et al., 1996)) were amplified with oligonucleotides VN(1–66)u and VN(1–66)d and a vector containing an Fc region of human IgG (pIG-1 (Fawcett et al., 1992)) were amplified with primers FcU and FcD. The VN(1–66) (Kpn1–Xho1) and Fc (Xho1–Not) fragments were assembled in Kpn1–Not1 digested pcDNA5/FRT-TO (Madsen et al., 2007). The correct sequences of the complete coding regions of all constructs were verified by sequencing.

The primers are shown in appendix A.

Site directed mutagenesis

Alanine substitutions were generated by site-directed mutagenesis according to the QuickChange II Site-directed mutagenesis protocol (Stratagene). Multiple rounds of mutagenesis were used to generate constructs carrying multiple substitutions. Expression vectors encoding soluble uPAR variants were generated by a second round of site-directed mutagenesis changing codon 284 of uPAR into a stop-codon (oligo pair A284Stop). Oligos used to generate muPAR mutants are shown in appendix A.

For the generation of cell lines with constitutive expression of the different uPAR-variants the coding regions were transferred KpnI/NotI to the pcDNA5/FRT vector (Invitrogen).

Cell Lines

Chinese Hamster Ovary (CHO) cells

Parental CHO cells Flp-In were cultured in vitro by subconfluent passage in Ham's F12 medium (Invitrogen), supplemented with 10% Fetal Calf Serum (FCS, Hyclone), 100U/ml penicillin, 100U/ml streptomycin, 5mM Glutamine (EuroClone) and 100 μg/ml zeocin (Invitrogen) at 37°C in 5% CO2.

Transfections were performed with a 1:10 ratio of pcDNA5/FRT/TO-based expression vector and the Flp recombinase expression vector pOG44 (Invitrogen) using FuGENE 6 (Roche). When cotransfected with the pcDNA5/FRT plasmid into a Flp-In mammalian host cell line, the Flp recombinase expressed from pOG44 mediates integration of the pcDNA5/FRT vector containing the gene of interest into the genome via Flp Recombination Target (FRT) sites.

Stable CHO Flp-In transfectants were selected in medium lacking zeocin using 300 μg/ml ml hygromycin B (Roche).

HEK293 Flp-In T-Rex cells

Parental HEK293 Flp-In T-Rex cells were cultured in Dulbecco's Modified Eagle Medium (DMEM, BioWhittaker), supplemented as for CHO Flp-In cells, but plus 5 μg/ml Blasticidin (Invitrogen). The procedure of transfection was the same as CHO Flp-In cells, but stable transfectants were selected in medium lacking zeocin using 150 μg/ml hygromycin B. Expression in HEK293 Flp-In T-Rex was induced by adding 1 μg/ml tetracycline (Sigma-Aldrich) to the medium overnight.

For *in vivo* experiments, parental HEK293 Flp-In T-Rex cells were transfected with cytosolic GFP expression vector (pEGFP-N1, Clonetech) and subjected to single cell cloning by adding 1 mg/ml G-418 (Invitrogen) to the medium. These cells were further transfected with pcDNA5/FRT/TO-based expression vector, containing full-

length muPAR, muPAR^{W32A}, muPAR$^{\Delta D1}$ or with empty vector (mock), as previously described, and selected in 150 μg/ml hygromycin B.

Rat smooth muscle cells (RSMC)

RSMC were a kind gift of Dr. Bernard Degryse. RSMC culture medium consisted of DMEM supplemented with 10% FCS, 100 U/ml penicillin, 100 U/ml streptomycin, 5 mM Glutamine.

Lung endothelial cell (EC) derivation and culture

Lungs of uPAR+/+ and uPAR-/- adult mice were removed aseptically, rinsed in PBS, minced and than digested in DMEM containing collagenase A (1.5 mg/ml, Roche) and DNaseI (25 mg/ml, Roche). The enzymatic digestion was performed in agitation at 37°C for 4 h. The resulting cell suspension was further dissociated by gentle pipetting, filtered through a sterile 70 μm nylon mesh and centrifuged at 1200 rpm for 5 minutes. Cell pellet was then incubated in 0.2% NaCl for 1 minute to lyse red blood cells and than overlaid with 1.8% NaCl to restore physiological conditions. After 3 washes in PBS, the cells were plated in culture medium on 24-well plates (0.5 to 1 x 10^6 cells/well) plate for 1 lung) pre-coated with 0.1% gelatin and incubated in 37°C, 5% CO_2 incubator. After 48 h cells were immortalized with polyoma middle T (PmT) as previously described (Garlanda et al., 1994). Briefly, cells were incubated with 300 μl/well of PmT supernatant in the presence of 8μg/ml polybrene (Sigma-Aldrich). The virus-containing medium was replaced 3 h later with fresh complete medium.

Cells were routinely cultured in DMEM supplemented with 20% FCS, 100U/ml penicillin, 100U/ml streptomycin, 5mM Glutamine, endothelial cell growth supplement (5mg/ml, home-made from calf brain) and heparin (100 mg/ml, Sigma-Aldrich), on 0.1% gelatin (Difco)-coated tissue culture plates.

Isolation and culture of bone marrow-derived macrophages (BMMs)

BMMs were isolated from mice whose genotypes were uPAR+/+ (Wt) and uPAR-/- (Ko). Red blood cells lysis was performed as for EC. Cells were seeded at $1x10^6$ cells per 100mm dish (Corning) in 5ml of macrophage growth medium, consisting of DMEM medium supplemented with 20% FCS, 100U/ml penicillin, 100U/ml streptomycin, 5mM Glutamine (EuroClone), 1mM sodium pyruvate (Gibco), 50 μM 2-mercaptoethanol (Invitrogen) supplemented with 30% L929 cell-conditioned medium (L-cell) as a source of CSF-1. After 3 days, non-adherent cells were collected, and either cryogenically stored in macrophage growth medium containing 10% dimethyl sulphoxide (DMSO, Euroclone) or seeded at 10^5 cells/ml in bacteriological plates (Falcon), and grown for 5 days before use. Cells were then harvested using Versene (1:5000), centrifuged at 1200 rpm for 5 minutes and resuspended in macrophage growth medium. Freezing did not detectably modify the characteristics or the behavior of the macrophages that were obtained. All the results described here are from cells that had been cultured for no more than a total of 2 weeks.

Expression and purification of recombinant proteins

For the production of soluble uPAR mutants, semi-confluent CHO Flp-In cells stably transfected with the relevant expression vectors was washed in PBS and incubated for 7–10 days in CHO protein-free medium (Sigma-Aldrich). The conditioned medium was used for in vitro binding assays without further purification. Recombinant Fc-fusion proteins were expressed in the same way, but were purified by standard Protein A affinity chromatography. The SMB used in adhesion and in vitro binding assays a fusion protein between VN (amino acid 1-66) and EGFP. It was purified from CHO cells

conditioned medium by mAb153 (anti-SMB) by affinity chromatography (Nicolai Sidenius, unpublished).

Quantification of Fc-tagged mouse uPAR variants

The concentration of Fc-tagged mouse uPAR variants in the conditioned medium of transfected CHO cells was measured by an ELISA-type assay using a polyclonal anti-human Fc antibody (Sigma) for capturing and a monoclonal Eurobium-labeled anti-human Fc antibody (Perkin Elmer) for detection by time-resolved fluorescence (DELFIA). A purified human IgG1 was used as standard.

Cell Proliferation assay

Cells were seeded at the concentration of $1.5x10^3$/well on E-Plates (Roche) and their proliferation was monitored in real time by using the xCELLigence System (Roche). The system measures electrical impedance across interdigitated microelectrodes integrated on the bottom of tissue culture E-Plates. The presence of the cells on top of the electrodes affect the local ionic environment at the electrode/solution interface, leading to an increase in the electrode impedance. The more cells are attached on the electrodes, the larger the increases in electrode impedance. The first impedance variations registered by the system are index of the initial cells spreading. After 2 h, when all the cells are attached to the plate, the registered impedance correlates exclusively with cell proliferation. Cell index was followed for 96 h and measurements taken every 15 minutes. The data are represented as the mean of 3 independent wells.

FACS analysis

Cell surface expression of muPAR , muPAR D1 and muPAR D2D3 were analyzed by flow cytometry by using a polyclonal antibody directed against the full-length protein or monoclonal antibodies that recognize the D1 or D2D3 domains of muPAR. All these antibodies were used at the concentration of 5 μg/ml. Cells were stained with appropriate secondary Cy5-labelled antibody (diluted 1:50) or SAP-APC (diluted 1:800) and analyzed by flow cytometry (FACSCalibur; BD Biosciences). Apoptosis was analyzed by staining the cells with Annexin V (1:50; Sigma-Aldrich) and Propidium Iodide (PI 50μg/ml in PBS; Sigma-Aldrich).

Cell lysis and Western Blotting

Cells were washed and lysed directly on the culture dish in ice-cold lysis buffer (25 mM Tris, pH 7.6, 150 mM NaCl, 1% Triton X-100, protease inhibitor cocktail [Complete-EDTA-free], 1 mM PMSF, 1 mM EDTA, 1 mM NaF, and 1 mM Na_3VO_4) or in ice-cold RIPA buffer (50 mM Tris, pH 8.0, 150 mM NaCl, 1% Triton X-100, 0.5% sodium deoxycholate, 0.1% SDS, protease inhibitor cocktail [Complete-EDTA-free], 1 mM PMSF, 1 mM EDTA, 1 mM NaF, and 1 mM Na_3VO_4) followed by a brief sonication. The total protein content was determined using the DC-Protein assay (Bio-Rad Laboratories) with BSA as standard. Equal amounts of total protein were separated by SDS-PAGE and probed as indicated.

Cell adhesion assay

Cells were seeded at the concentration of 3 x 10^4/well on MaxiSorp 96-well plates (Nunc), coated with different substrates, and allowed to adhere in the presence or absence of pro-uPA (20 nM) and SMB (30 nM) for 30 min at 37°C. After washing, the

adherent cells were fixed, stained with crystal violet, and quantified by measuring the absorbance at 540 nm. Coatings were as follows: poly-L-lysine 100 μg/ml (Engelbreth-Holm-Swarm murine sarcoma), fibronectin 10 μg/ml (Roche), $\alpha_v\beta_3$ (Chemicon) 0,5 μg/ml, purified VN, VN^{RAD}, $VN(1\text{-}66)^{RAD}$ were all coated at 5 μg/ml. suPAR/Fc was coated 20 nM. pro-uPA was a kind gift of Jack Henkin Abbot. All measurements were done in triplicate, and the specific binding calculated by subtraction of the non-specific binding to BSA-coated wells.

Binding assay of purified proteins

In vitro binding assays were performed in black 96-well plates (Nunc MaxiSorp), coated with SMB/Fc (0,1 ml/well, 2 μg/ml in 0.05M phosphate buffer, pH 9.6) or mATF (0,1 ml/well, 1 μg/ml in 0.05M phosphate buffer, pH 9.6) over night at 4°C and blocked 1.15 ml of 2% BSA in PBS for 1 h. Subsequent incubations with smuPAR variants were performed with reagents diluted in dilution buffer (PBS containing 1% BSA) for 1 h at room temperature on a orbital shaker. Binding to SMB was induced by pre incubation with pro-uPA (100 nM). After extensive washing with PBS containing 0.1% Tween 20 (PBS-T), the wells were probed for bound smuPAR with a Eu^{3+}-labeled polyclonal anti-muPAR antibody (0.5 μg/ml) followed by the measurement of time-resolved fluorescence. All measurements were done in triplicate, and the specific binding calculated by subtraction of the non-specific binding to BSA-coated wells.

Differential Interference Contrast microscopy (DIC)

Cells were plated at the concentration of 2 x 10^4/well on coverglass chambers (Lab-TekII) and allowed to adhere for 24h. Cells were then fixed in 4% paraformaldehyde and rinsed with PBS (to maintain the requested difference of refractive indexes) and

subjected to DIC analysis. DIC imaging of cells was performed using an inverted microscope Olympus IX81. Cells were viewed through a high-aperture 60x objective lens (UIS2 60x TIRFM PlanApo N, NA 1.45; Olympus). Images were acquired using Hamamatsu Orca-ER digital camera with the software Metamorph 7.5.6.0. For cell spreading assay the cell area of 50 cells/type was measured with ImageJ 1.42q.

Phase contrast and time-lapse imaging

Phase-contrast and time-lapse live-cell imaging was performed at 37°C, 5% CO_2 with an inverted microscope (IX80; Olympus) equipped with an incubation chamber (OKOlab) to control CO_2 and temperature. Cells were plated in 12 well plates (Nunc) at the confluence of 1 x 10^5 cell/well. Time-lapse imaging was performed in serum-containing growth medium. Cells were viewed through 10x (uPlan FLN 10X Ph1, N.A. 0.30; Olympus) objective lenses and pictures were taken every 5 minutes for 5 h. The acquisition system includes a digital camera (Hamamatsu Orca-ER) and System Control Software Olympus ScanR. Adjustment of brightness/contrast, smoothening and sharpness of images was done using ImageJ 1.42q and always applied to the entire image. Cell migration speed was quantified with ImageJ 1.42q using the plug-in "manual tracking". In each experiment, 20 randomly chosen cells were tracked and their average migration speed throughout the experiment was calculated.

Immunofluorescence Microscopy

Cells were plated on 35mm dishes (Corning) and allowed to adhere overnight. Cells were washed in PBS, fixed in 4% parafolmaldehyde, permeabilized with 0.1% Triton X-100, 0.2% BSA in PBS, and blocked with 2% BSA in PBS. Cells were stained as indicated in the figures. EC were starved overnight before to proceed with the staining

in DMEM 1% BSA. Cell imaging was performed by using the full-motorized upright Olympus BX61 microscope. Cells were viewed through a 60x (uPlanApo 60x, N.A. 1.45; Olympus), 20x (uPlanApo 20X, N.A. 0.70; Olympus) or 10x (UPlanFl 10X, N.A. 0.30; Olympus) objective lens. Images were acquired using photometrics coolsnap EZ camera with the software Metamorph 7.5.6.0. Adjustment of brightness/contrast of images was done using ImajeJ 1.42q.

Transgenic Mice

Wt mice and mice lacking uPAR were used to obtain EC. Wt C57BL/6J (B6) mice were obtained from Charles River Laboratories. uPAR-/- mice were generated at Vlaams Interuniversitair Instituut (Leuven, Belgium) and inbred in B6 for 12 generations (Dewerchin et al., 1996). Mice were maintained in HEPA-filtered IVC units. All experiments were performed according to the guidelines for care and use of laboratory animals approved by the institutional ethical animal care committee.

Xenograft Studies in Mice

Anesthetized 8-weeks-old C.B-17/IcrCrl-scid-BR (Charles River Laboratories) were inoculated in the fourth mammary fat pad with 1 x 10^6 HEK293-GFP cells, suspended in 50 μl of 1:1 PBS and Matrigel (Sigma). Primary tumor growth was monitored every 2 to 3 days by caliper. The tumor volume was estimated by the formula V = (length x width^2) / 2. Mice were euthanized when the tumors were 2 cm^3 (between 2 and 4 months). Xenografts and lungs were recovered for analysis.

Mice were maintained in HEPA-filtered IVC units. All experiments were performed according to the guidelines for care and use of laboratory animals approved by the institutional ethical animal care committee.

Results

Identification and characterization of the VN binding epitope in murine uPAR (muPAR)

The VN-binding epitope in human uPAR has been identified through a complete single-site alanine scanning mutagenesis of either purified soluble human uPAR (suPAR) (Gardsvoll and Ploug, 2007) or full-length human uPAR expressed on HEK293 and CHO cells (Madsen et al., 2007). Five residues (W32, R58, I63, R91 and Y92) are critically involved. Given the high homology between the human and mouse receptors (Fig. 12), these residues were substituted with alanine by site-directed mutagenesis. The biological activity of the resulting receptor variants were then analyzed and compared to wild-type muPAR.

```
TCVPASWGLRCMQCKTNGDCRVEECALGQDLCRTTIVRLWEEGEELELVEKSCTHSEKTN   74
TCVPAS GL+CMQC++N  C VEECALGQDLCRTT++R W++  ELE+V + C HSEKTN
TCVPASQGLQCMQCESNQSCLVEECALGQDLCRTTVLREWQDDRELEVVTRGCAHSEKTN   75


RTLSYRTGLKITSLTEVVCGLDLCNQGNSG-RAVTYSRSRYLECISCGSSDMSCERGRHQ   133
RT+SYR G  I SLTE VC  +LCN+   G R   + + RYLEC SC S D SCERGR Q
RTMSYRMGSMIISLTETVCATNLCNRPRPGARGRAFPQGRYLECASCTSLDQSCERGREQ   135

SLQCRSPEEQCLDVVTHWIQEGEEGRPKDDRHLRGCGYLPGCPGSNGFHNNDTFHFLKCC   193
SLQCR P E C++VVT    +  E   KD+ + RGCG LPGCPG+ GFH+N TFHFLKCC
SLQCRYPTEHCIEVVT---LQSTERSLKDEDYTRGCGSLPGCPGTAGFHSNQTFHFLKCC   192

NTTKCNEGPILELENLPQNGRQCYSCKGNSTHGCSSEETFLIDCRGPMNQCLVATDTHGP   253
N T CN GP+L+L++  P NG QCYSC+GN+T GCSSEE  LI+CRGPMNQCLVAT
NYTHCNGGPVLDLQSFPPNGFQCYSCEGNNTLGCSSEEASLINCRGPMNQCLVATGLDVL   252

KNQSYMVRGCATASMCQHAHLGDAFSMN-HIDVSCCTKSGCNHPDLDVQYRSGAAPQPGP   312
 N+SY VRGCATAS CQ +H+ D+F  + ++ VSCC  SGCN P       +G AP+PGP
GNRSYTVRGCATASWCQGSHVADSFPTHLNVSVSCCHGSGCNSP-------TGGAPRPGP   305

AHLSLTITLL  322
A LSL  +LL
AQLSLIASLL  315
```

Figure 12: Human uPAR vs Murine uPAR alignment.

The amino acid sequence of human uPAR (aa 1-322) has been aligned with the murine uPAR sequence (aa 1-315). Five residues (W32, R58, I63, R91 and Y92) constitute the VN binding site in huPAR. The matching amino acid sequence in the middle showed the high homology between the human and mouse receptors and how the residues involved the uPAR-VN interaction (reported in yellow) are fully conserved.

For this purpose the generated muPAR variants and the muPAR wt were transfected in CHO Flp-In cells. The Flp-In system generates pools of isogenic transfectants carrying a single copy of the expression cassette, thus eliminating potential artifacts caused by clonal differences or heterogeneous expression levels. The correct expression of the mutants was checked by Western Blot analysis of total lysates (Fig. 13). All the mutants showed a band at the expected molecular weight, as compared to the muPAR wild type. Some of the mutants (I63A, R58E, R58E+W32A) showed an upper band indicating SDS-resistant protein aggregates.

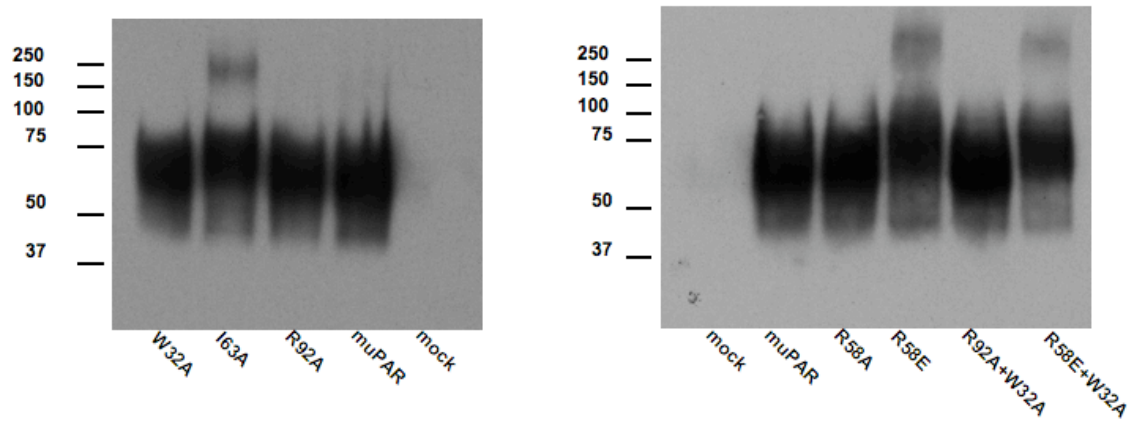

Figure 13: WB analysis of CHO cells stably expressing murine uPAR.

Cell expressing the receptor variants were lysed and muPAR expression was assayed by immunoblot. Representative western blot are shown.

Expression of human uPAR in CHO cells resulted in a strong change in morphology and F-actin cytoskeleton (Madsen et al., 2007). The phase contrast analysis showed that parental CHO cells and cells expressing the mutants had comparable cell

morphology, which was different from CHO cells expressing wild type muPAR. As an example we report the image of the muPAR^{W32A} mutant. The cells appear to grow in colonies while the muPAR wild type CHO cells are scattered (Fig. 14, upper panel). A further analysis of the morphology, by immunofluorescence microscopy, in which we stained for actin and vinculin, displayed the formation of protrusions and lamellipodia as well as the loss of stress fibers and focal adhesion dissociation only in muPAR wild type transfected cells (Fig. 14, lower panel). uPAR induced phenotype was completely reverted by the W32A and R92A point mutations, that disrupted the receptor binding to VN (Fig. 14, lower panel). Cells expressing the other receptor variants showed an intermediate phenotype.

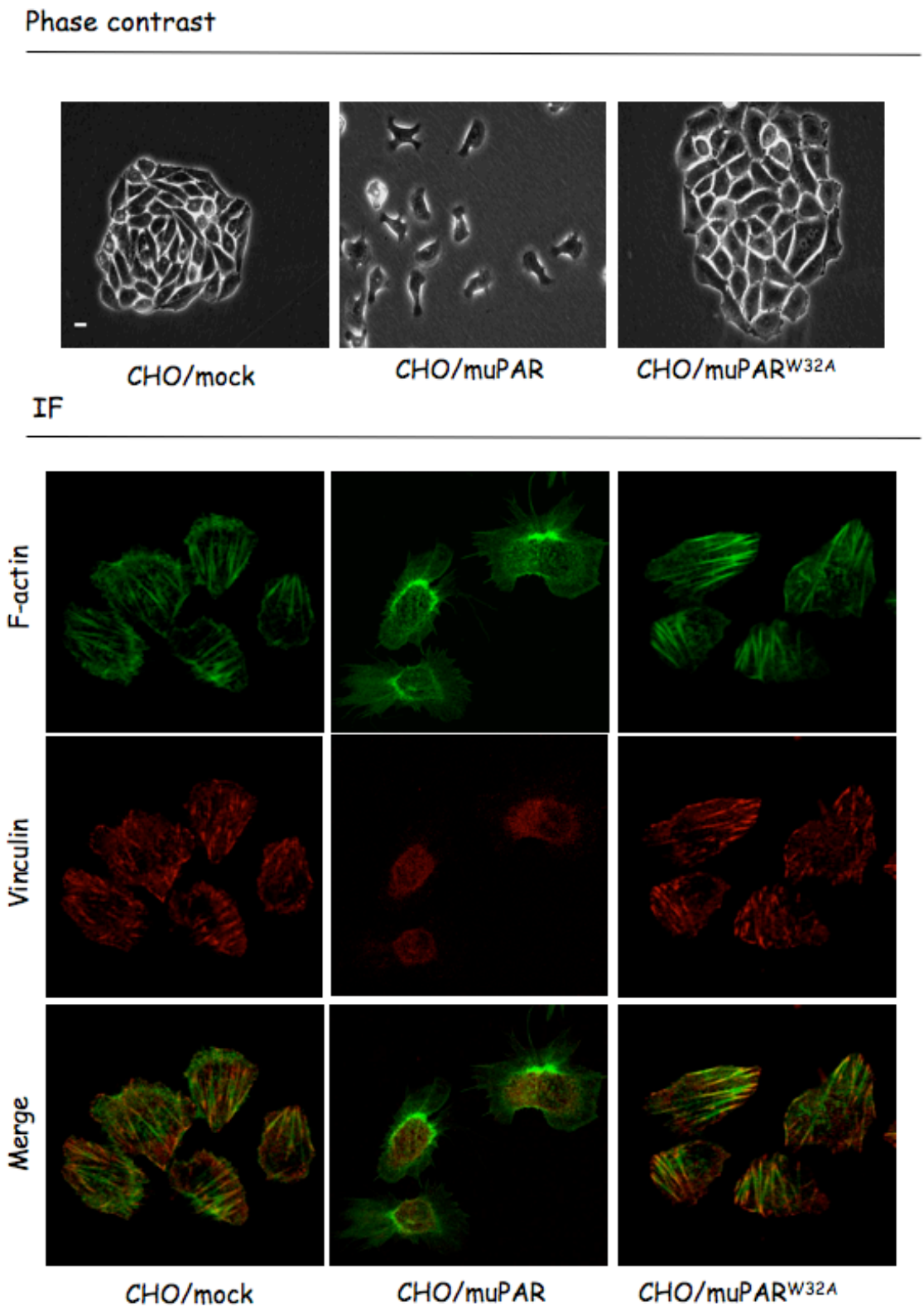

Figure 14: mPAR-induced changes in cell morphology.

CHO Flp-In cells (CHO) transfected with an empty vector (CHO/mock) or wild type muPAR (CHO/muPAR) and CHO Flp-In cells stably expressing uPAR^{W32A} mutant (CHO/muPAR-W32A) were analyzed by phase contrast microscopy (upper panels) or by confocal microscopy after fixation and staining with phalloidin-FITC and vinculin-Cy3 (lower panels).

The ability of the mutant receptors to promote cell adhesion to VN has been analyzed in cell adhesion assays to a modified VN in which the RGD sequence responsible for integrin binding has been mutated into RAD. As this modified VN does not support integrin dependent cell adhesion (Madsen et al., 2007) it allows for the direct quantification of uPAR dependent VN-adhesion. For comparison, integrin dependent adhesion to fibronectin (Fn, which is not a substrate for uPAR) was measured. All the different muPAR mutants failed to adhere to VN, maintaining a normal adhesion to Fn, demonstrating the effective loss of VN-binding to these receptors (Fig. 15).

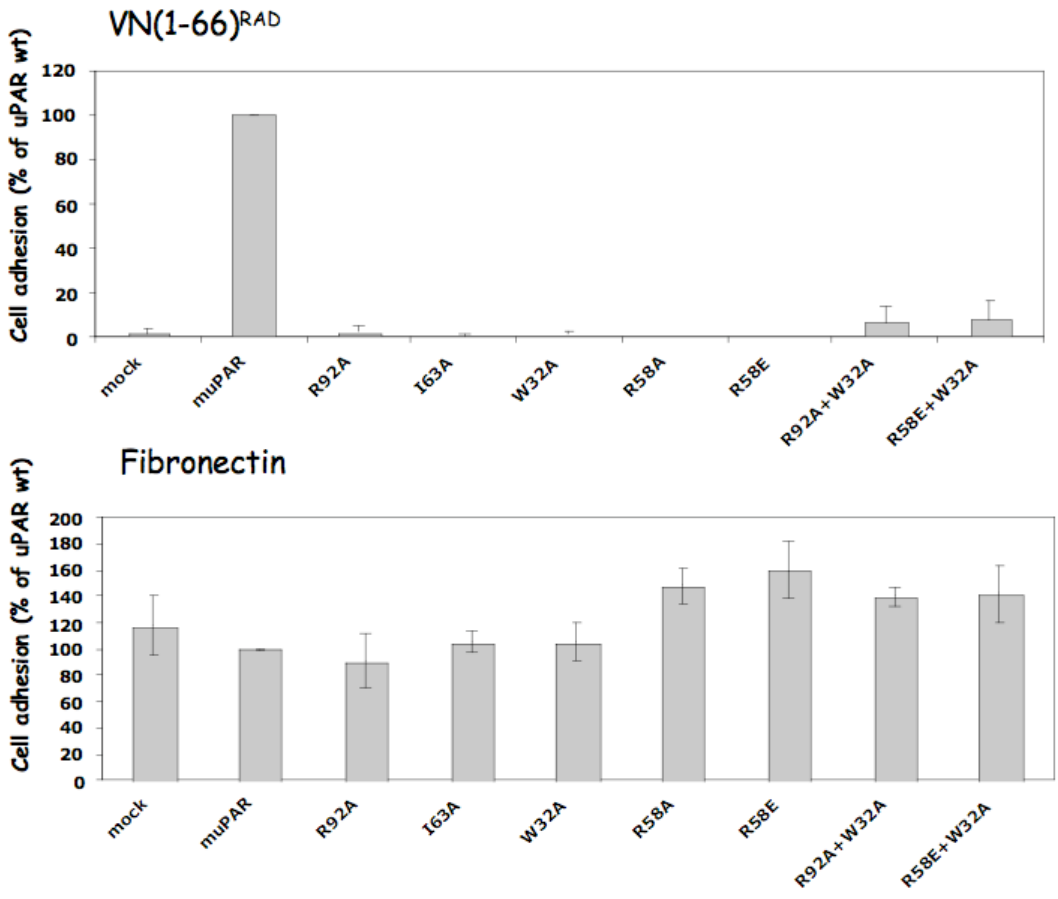

Figure 15: mPAR mutants in VN-binding epitope fail to adhere to VN.

Adhesive properties of cells expressing muPAR mutants in VN-binding site, which completely fail to induce changes in CHO morphology. Cells were plated for 30 minutes on 96 well plates coated with FN

(10 μg/ml) and VN(1-66)^{RAD} (5 μg/ml). Adherent cells were fixed and stained with crystal violet. Cell adhesion to muPAR wild type was set as 100% for each cell line. Data are expressed as mean ± s.e.m., number of independent experiments (n=3).

The direct muPAR-VN interaction was also analyzed using purified proteins in an *in vitro* binding assay. We generated expression vectors encoding soluble variants of the mutant receptors fused to the constant region (Fc) of a human IgG molecule. These expression vectors were transfected into CHO cells and the recombinant proteins purified from the conditioned medium by protein-A affinity chromatography. Proteins concentration was then measured by ELISA-type assay. *In vitro* binding assays to immobilized VN and uPA were utilized to determine the binding constants of the different receptors for these interaction partners. While the uPA binding was not affected by the point mutations in muPAR (Fig. 16, left panel), the VN-binding was effectively abrogated by either W32A or R92A point mutation (Fig. 16, right panel).

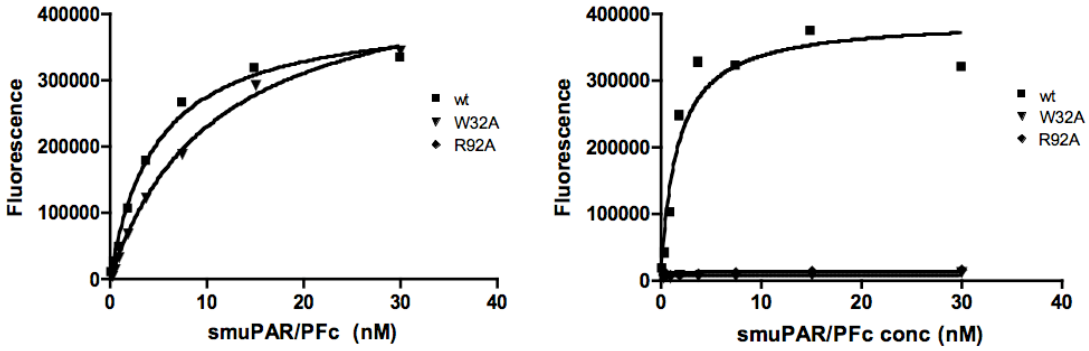

	wt	W32A
KD (nM)	4.87±0.7	10.95±1.03

	wt	W32A	R92A
KD (nM)	1.65±0.59	N.M.	N.M.

Figure 16: mPAR mutants in VN-binding epitope bind uPA.

Soluble variants of muPAR mutant receptors were generated, expressed and tested for their ability to bind immobilized ATF (left panel) or SMB domain of VN (right panel) by i*n vitro* binding assay. Representative IVB are shown.

Collectively, the data obtained from the analysis of the muPAR variants show that all the substitutions destroyed receptor binding to VN, without disturbing the binding to its natural ligand muPA. Moreover the receptors variants completely reverted the morphological phenotype resulting from the expression of muPAR in CHO cells. However, possible problems in the folding of the protein caused by some of the substitutions (see Fig. 13) reduced the number of the mutant candidates to the muPAR^{W32A} and the muPAR^{R92A}. We decided to use the muPAR^{W32A} for the next experiments, since R92 is an amino acid involved in the receptor cleavage and is a part of the uPAR chemotactic epitope (Fazioli et al., 1997).

Characterization of uPAR variants in HEK293 FlpIn cells

To determine uPAR-VN activities that may be important for cancer progression *in vivo*, we decided to express muPAR and muPAR^{W32A} receptors in HEK293 Flp-In cells. Although HEK-293 cells are not true cancer cells, due to the expression of adenoviral early region 1A, these cells are capable of forming tumors in immunodeficient mice (Graham et al., 1977). More important, these cells do not express both uPA and uPAR endogenously (Madsen et al., 2007). Besides the W32A receptor variant we decide to study another form of muPAR missing the whole D1 (muPAR$^{\Delta D1}$). This mutant receptor is not capable of both VN and uPA binding. In view of a possible progression of the xenografted tumors to form metastasis sites, HEK293 Flp-In cells were first transfected to express GFP, to better track macrometastasis, and then transfected with the empty vector (mock) or the three muPAR mutants (muPAR, muPAR^{W32A} and muPAR$^{\Delta D1}$). FACS analysis was performed to select a stable GFP expressing clone and to evaluate the receptors expression levels. All the receptor

variants and GFP were expressed at comparable levels (Fig. 17B and 17C). As expected, muPAR$^{\Delta D1}$ was not recognized by the antibody against the D1 of uPAR (Fig 17D).

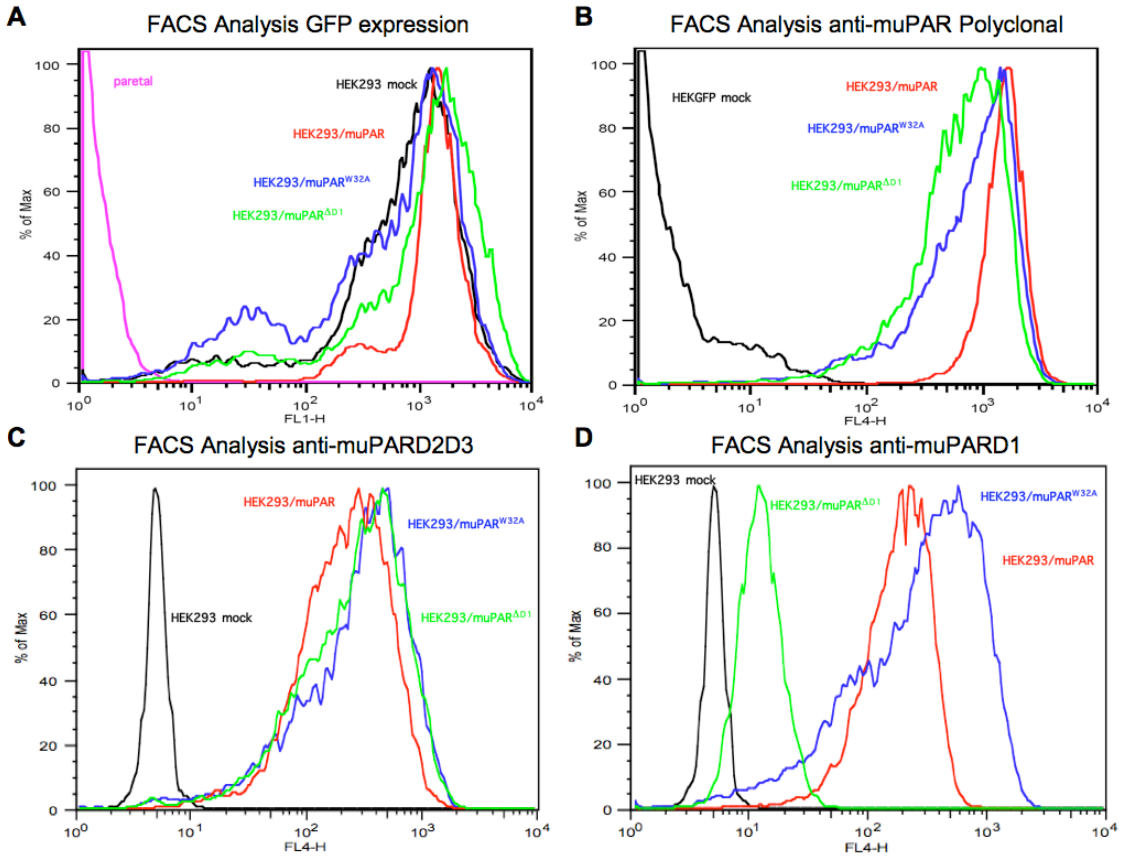

Figure 17: muPAR variants are expressed at comparable levels in HEK293 cells.

GFP and mutant receptors expression profiles were evaluated by FACS analysis. **A**: GFP expression level in HEK293 cells. Expression profiles of muPAR^{W32A} (blue) and muPAR$^{\Delta D1}$ (green), compared to muPAR (red) and mock cells (black), were detected by a polyclonal antibody against mouse uPAR (**B**), a specific anti-D2D3 antibody (**C**) and a monoclonal anti-D1 antibody (**D**). In violet parental cells.

The comparable expression level will allow us to account for eventual differences to the functionality of our receptor variants and not to their amount on the cell surface.

All the four cell lines (mock, muPAR, muPAR^{W32A} and muPAR$^{\Delta D1}$) were tested for their ability to adhere to immobilized VN and FN, in cell adhesion assay (Fig. 18). The wt receptor was able to promote cell binding to VN without disturbing the binding to Fn. Binding to VN was integrin-independent since the cells expressing muPAR adhered to VN^{RAD}. Both muPAR^{W32A} and muPAR$^{\Delta D1}$ cells showed an impaired adhesion to immobilized VN and failed to adhere to VN^{RAD}. The remaining VN-adhesion observed in muPAR^{W32A} and muPAR$^{\Delta D1}$ expressing cells is integrin-mediated as it is comparable to the one observed in mock-transfected cells.

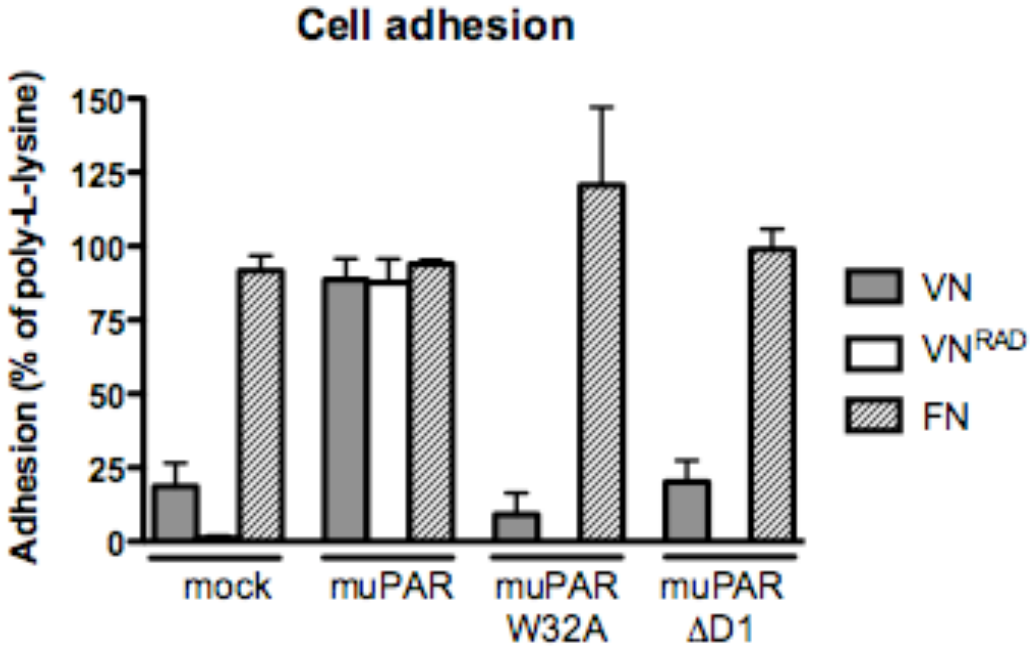

Figure 18: muPAR variants failed to promote cell adhesion to VN.

Adhesion assay: Mock, muPAR, muPAR^{W32A} and uPAR$^{\Delta D1}$ transfected HEK293 cells were plated for 30 minutes on FN (10 μg/ml), VN (5 μg/ml) and VN^{RAD} (5 μg/ml). Adherent cells were fixed and quantified by measuring GFP fluorescence on by ENVISION (PerkinElmer) plate reader. Cell adhesion to poly-D-lysine was set as 100% for each cell line. Data are expressed as mean ± s.e.m., n=3.

Moreover, uPAR expression doesn't alter cell adhesion to the FN, as all the cells adhered to FN at comparable levels (Wei et al., 2005).

The observation that uPAR is overexpressed in human tumors and that the expression levels have strong prognostic value tentatively suggest that uPAR might be involved in tumor growth. Therefore we investigated the proliferating cell signal that may be triggered by uPAR-VN interaction. Figure 19 shows that the expression of muPAR on the cell surface enhanced cell proliferation. Importantly, cell proliferating signal is a consequence of the uPAR-VN interaction. In fact, the growth of the cell expressing the receptor variants, incapable of VN-binding, was comparable to the mock-transfected cells.

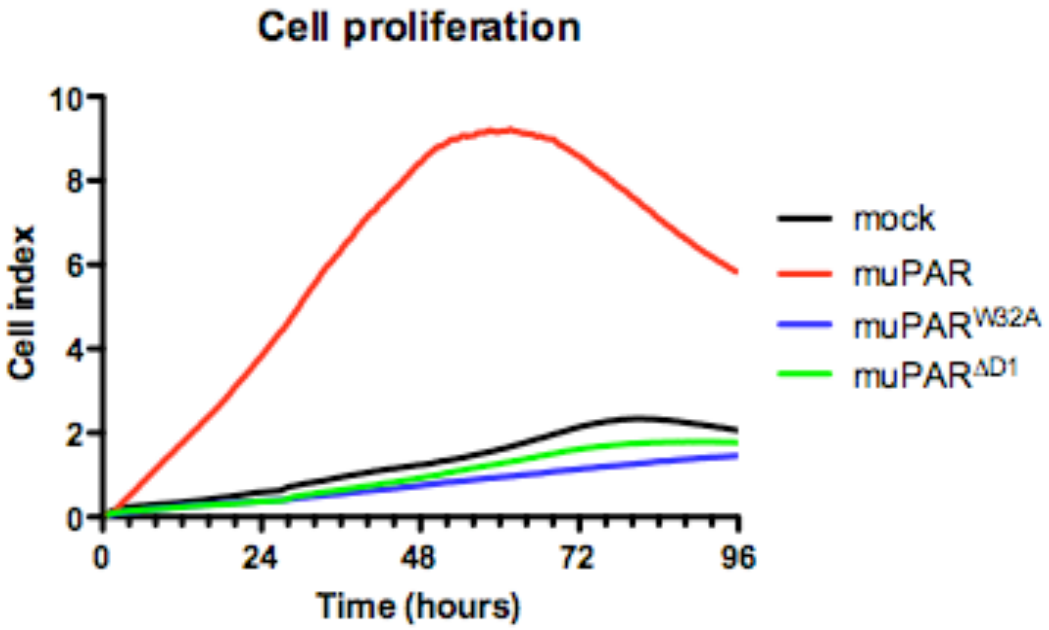

Figure 19: uPAR-Vn interaction is required to promote cell proliferation.

Dynamic monitoring of adherent cell proliferation. HEK293 muPAR (red), muPAR^{W32A} (blue), muPAR^{DD1} (green) and mock (black) cells were seeded at 1500/well cell density on E-Plates. The cell growth curves were automatically recorded on the xCELLigence System in real time. Cell index was followed for 96 h (measurements every 15 minutes). Data represent the mean of 3 independent wells. For clarity SD is not shown.

To further investigate the proliferative signal transduction induced by uPAR-VN interaction we assayed the ERK1/2 activation by Western blot. Serum starved HEK293/muPAR cells displayed higher level of ERK1/2 phosphorylation, compared to mock transfected cells. Activation of ERK1/2 in mock and the receptor variants expressing cells was comparable (Fig. 20).

Taken together these results demonstrated that uPAR-VN interaction triggers MAPK activation that is presumably responsible for the differences in cell growth observed in the proliferation assay.

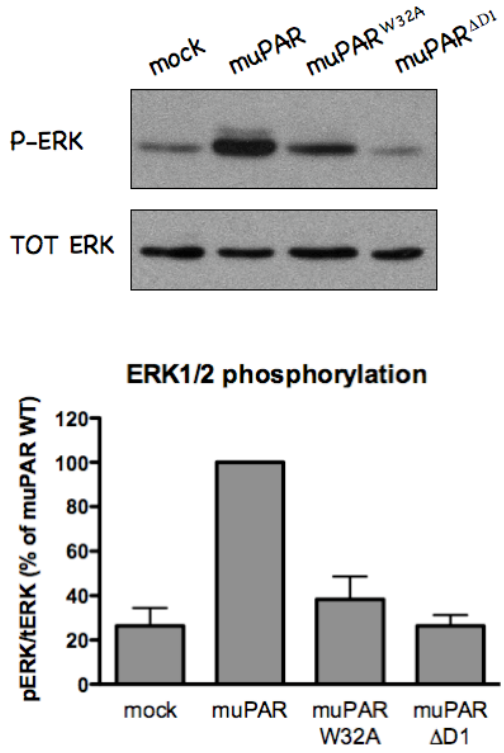

Figure 20: uPAR-VN interaction induces ERK1/2 activation.

Immunoblot analysis of ERK1/2 phosphorylation upon uPAR-VN interaction. Western blot (upper panel) and densitometric analysis (lower panel) are shown. Cells were serum starved for 4 hours prior to lysis. Blots were first probed for phosphorylated ERK1/2 (top blot) then stripped and reprobed for total ERK1/2 (bottom blot). The graph shows the mean ± s.e.m. increase in the ratio between phosphorylated and total ERK1/2 (n=5). Ratio of muPAR wild type (WT) expressing cells was set as 100%. Representative western blot are shown.

HEK293 cells are poorly adherent cells. uPAR-VN interaction could increase the integrins binding to the ECM (Madsen et al., 2007), thus preventing cell apoptosis induced by loss of anchorage, a phenomenon also known as anoikis. After initiation of apoptosis, most cell types translocate the membrane phospholipid PS from the inner surface of the plasma membrane to the outside. PS can be detected by staining with Annexin V that binds naturally to PS. During programmed cell death, PS externalization precedes membrane bleb formation and DNA fragmentation. Figure 21 shows Annexin V staining in conjugation with PI staining performed in all four cell lines.

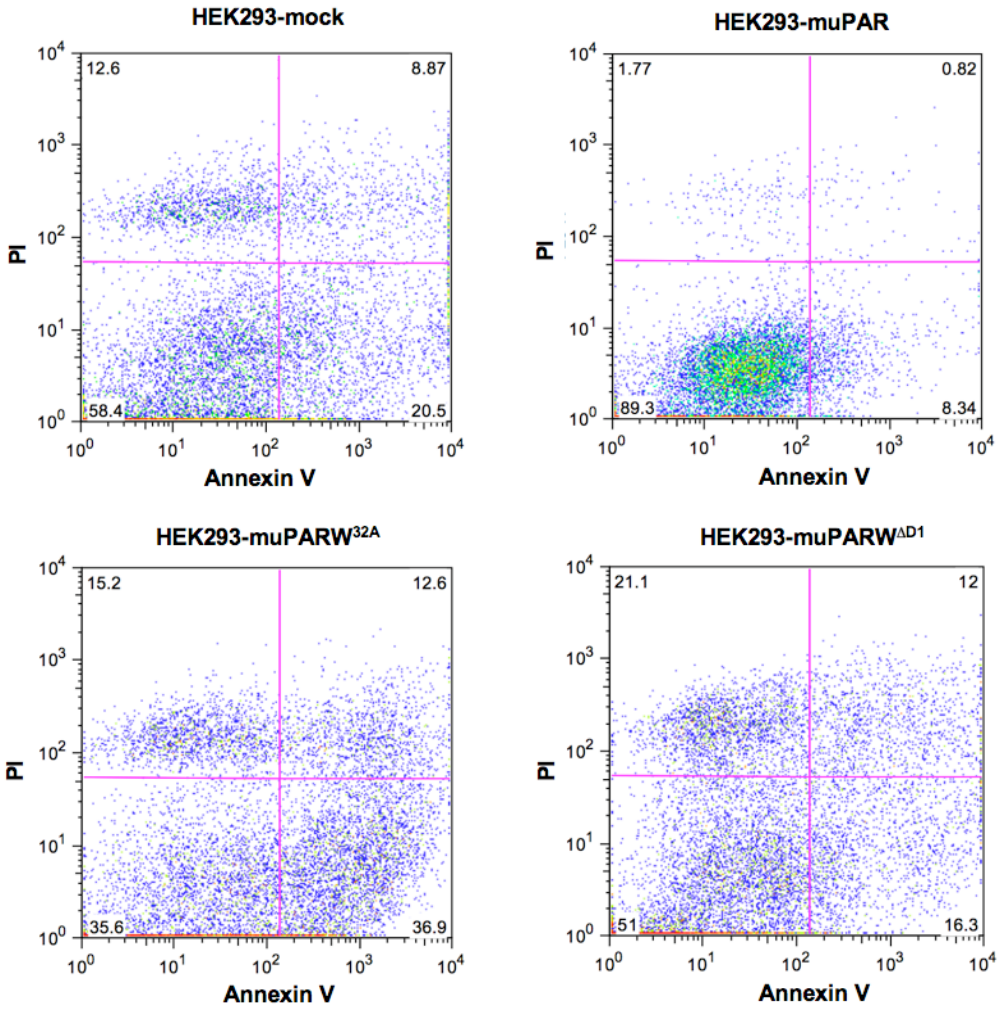

Figure 21: muPAR expression preserves cells from apoptosis.

Contour diagram of Annexin V/PI flow cytometry: Lower left quadrants of each panels show the viable cells, which exclude PI and are negative for Annexin V binding. The upper right quadrants contain the

non-viable, necrotic cells, positive for PI uptake and Annexin V binding. The lower right quadrants represent the apoptotic cells, PI negative and Annexin V positive, demonstrating cytoplasmic membrane integrity. One representative experiment out of three is shown.

Expression of Wt muPAR on the cell surface prevented HEK293 cells from apoptosis. This phenomenon did not happen in absence of uPAR-VN interaction. The loss of cell VN-binding in HEK293muPAR^{W32A}, in fact, induce a shift in Annexin fluorescence intensity. Interestingly, muPAR^{W32A} expressing cells showed a slight increase in the Annexin V staining respect to the control cells. On the contrary, the Annexin V/PI staining of HEK293muPAR$^{\Delta D1}$ and mock cells were comparable (Fig. 21). Further experiment are needed to clarify the difference observed in this apoptosis assay, in particular among the muPAR^{W32A}, muPAR$^{\Delta D1}$ and mock transfected cells.

As previously reported, uPAR-VN interaction is responsible for cell morphology changes and cell migration (Madsen et al., 2007).

To monitor the morphology changes upon uPAR-VN interaction, we quantified the area of individual cells through DIC microscopy and image analysis. When grown under serum containing conditions the expression of muPAR, but not of uPAR^{W32A} or muPAR$^{\Delta D1}$, resulted in increased cell spreading (~2.5-fold) as compared to mock-transfected cells (Fig. 22). To see whether these uPAR-VN induced morphology chances could result in different cell motility we performed migration assays, testing the migratory capacity of uPAR receptor variants. As expected, muPAR expression resulted in an increased migration speed compared to the other cells (Fig. 23). The increased cell spreading observed in muPAR expressing cells translated into enhanced cell migration.

Consistently the lack of uPAR-VN interaction resulted in a migration speed comparable to mock transfected cells.

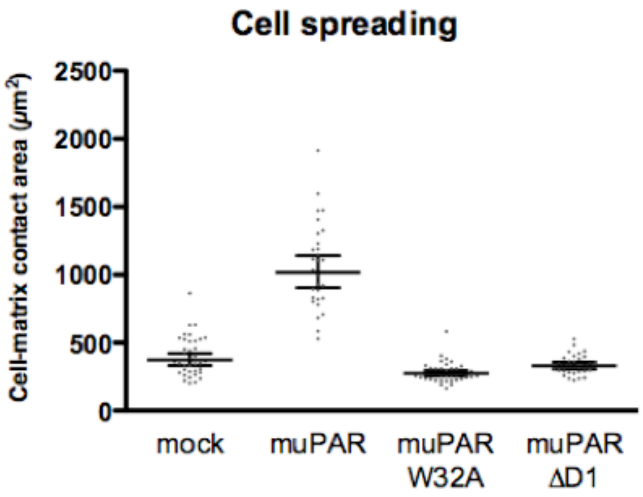

Figure 22: Increased cell-matrix contact area upon muPAR mediated VN adhesion.

Cell-matrix contact area was quantified by cell spreading assay: Sparse cells were grown for 24h. After fixation DIC images were taken and cell areas were quantified using ImageJ software. Columns are mean ± 95% confidence interval, n=50, two independent experiments. Average do not represents the area of one single cell.

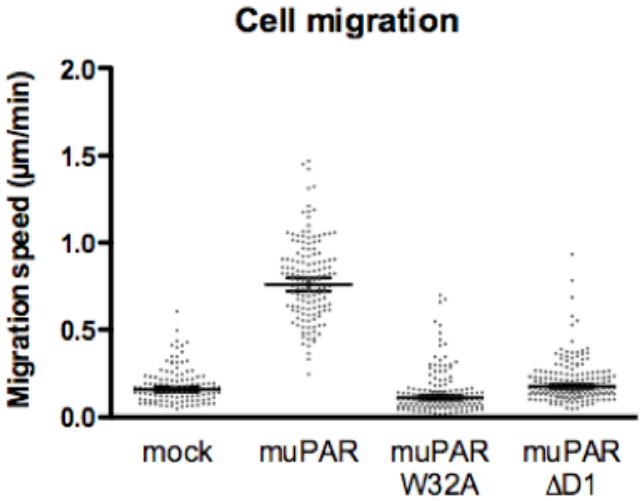

Figure 23: muPAR-VN interaction promotes cell migration.

HEK293/mock, HEK293/muPAR, HEK293/muPAR^{W32A} and muPAR$^{\Delta D1}$ cells were seeded at sparse conditions and allowed to adhere for 24h. Cells were monitored for 5h (1 frame every 5 min.) by phase-contrast time-lapse recordings. Cell migration speed was quantified by manual cell tracking using ImageJ software. Columns are mean ± 95% confidence interval, n=25, two independent experiments.

We further analyzed the signal transduction pathway that could be responsible for enhanced cell spreading and migration. Thus the phosphorylation of p130Cas, involved in cell spreading and migration, was assayed through immune blotting and quantified with densitometry. Serum starved muPAR cells displayed an increased p130Cas substrate domain (SD) phosphorylation, compared to mock and receptor variants transfected cells (Fig. 24).

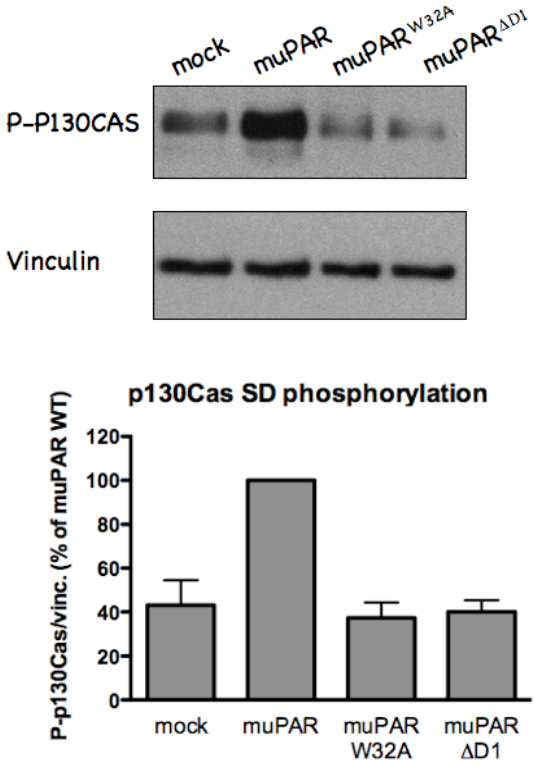

Figure 24: muPAR-VN interaction induces P130Cas phosphorylation.

muPAR, muPAR^{W32A}, muPAR$^{\Delta D1}$ and mock HEK293 cells were serum starved for 4 hours and prior to lysis. Blots were first probed for phosphorylated p130Cas (top blot) then stripped and reprobed for vinculin (bottom blot). The graph shows the mean ± s.e.m. in the ratio between phosphorylated and total protein (n=5). Ratio of muPAR wild type (WT) untreated cells was set as 100%. Representative western blots are shown.

As reported by other studies, P130Cas phosphorylation triggers lamellipodia protrusion and cell migration through the upregulation of Rac1 activity (Smith et al., 2008).

In summary, these data show that the ability of uPAR to induce changes in HEK293 cells morphology is a two-step process in which uPAR, through the direct interaction with VN triggers cell attachment to the matrix. Consequently this initial adhesion is followed by engagement of integrins with matrix VN, triggering changes in cell morphology and migration.

HEK293 tumorigenesis in SCID mice

The differences observed in the *in vitro* assays could suggest that uPAR-VN interaction may modulate tumor growth and metastasis dissemination in a xenotransplanted in vivo system.

To test this possibility, all the four cell lines, previously characterized, were inoculated into mammary fat pads in immunodeficient SCID mice. Tumor growth was followed by caliper measurements until the primary tumor mass reached a size of about 2 cm^3. Each cell line formed palpable tumours independently of the construct expressed. Importantly, muPAR expression induced an earlier formation of the primary tumor mass (about 1 week earlier) (Fig. 25, left panel) respect to mock transfected cells, in accordance with the enhanced proliferative capability of these cells. The observed effects are specifically related to ability of uPAR in inducing VN adhesion. Consistently, $muPAR^{W32A}$ expression, a mutant defective in VN-binding, significantly slowed down the tumor growth. Interestingly, tumor mass formed by HEK293$muPAR^{W32A}$ showed an impaired growth even when compared to mock cells (Fig. 25, right panel). No changes in the tumor formation and growth rate were induced by the expression of $muPAR^{\Delta D1}$, defective in both VN and uPA binding, if compared to

mock transfected cells (Fig. 25). These data indicates that uPAR-VN interaction accelerates the process of tumor formation.

The fact that muPAR^{W32A} expressing cells display an impaired tumor formation, respect to mock transfected cells, could indicate uPA to be a negative regulator of cancer growth rate. Consistently, cells expressing a receptor variant, in which the removed-D1 prevents uPA interaction, display the same growth rate of mock cells.

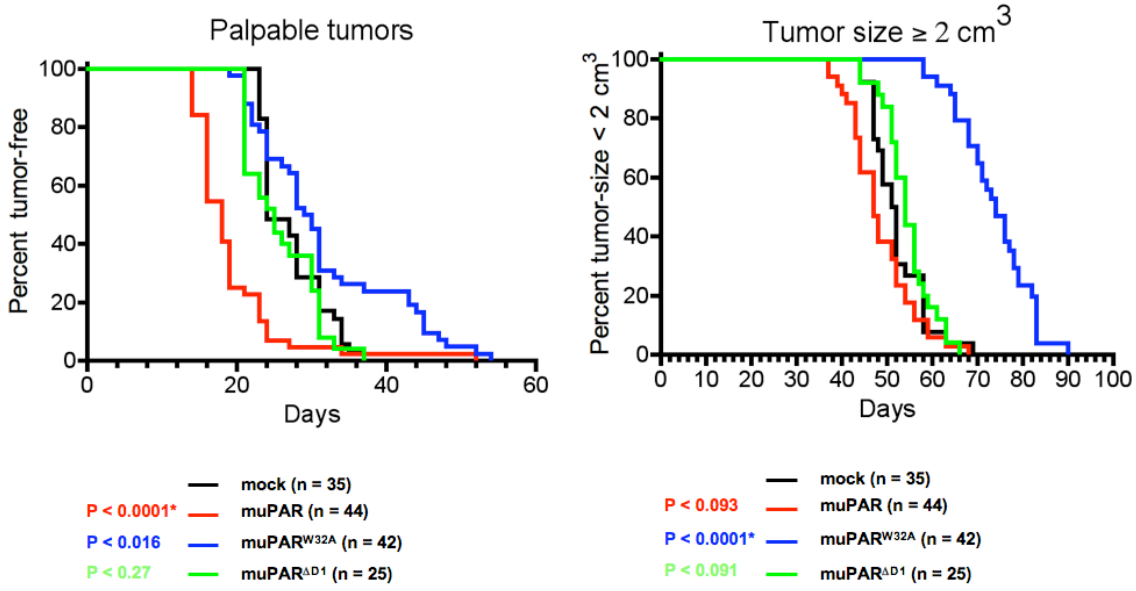

Figure 25: Effect of uPAR-VN interaction on xenograft growth rate in SCID mice.

Primary tumor growth and size were monitored using calipers until the size of tumor reached a maximum diameter of 2 cm. Number of mice used for each cell line are indicated (n). The curves plot the percent of tumor free mice (left panel) or the percent of tumor size ≥ 2 cm^3 (right panel) as a function of time.

HEK293 cells-induced tumors do not form macro-metastasis

Mice were euthanized when the primary tumor reached 2 cm^3. In no case we observed changes in animal behavior to indicate discomfort. Xenografts and lungs were recovered and examined using a fluorescent stereomicroscope.

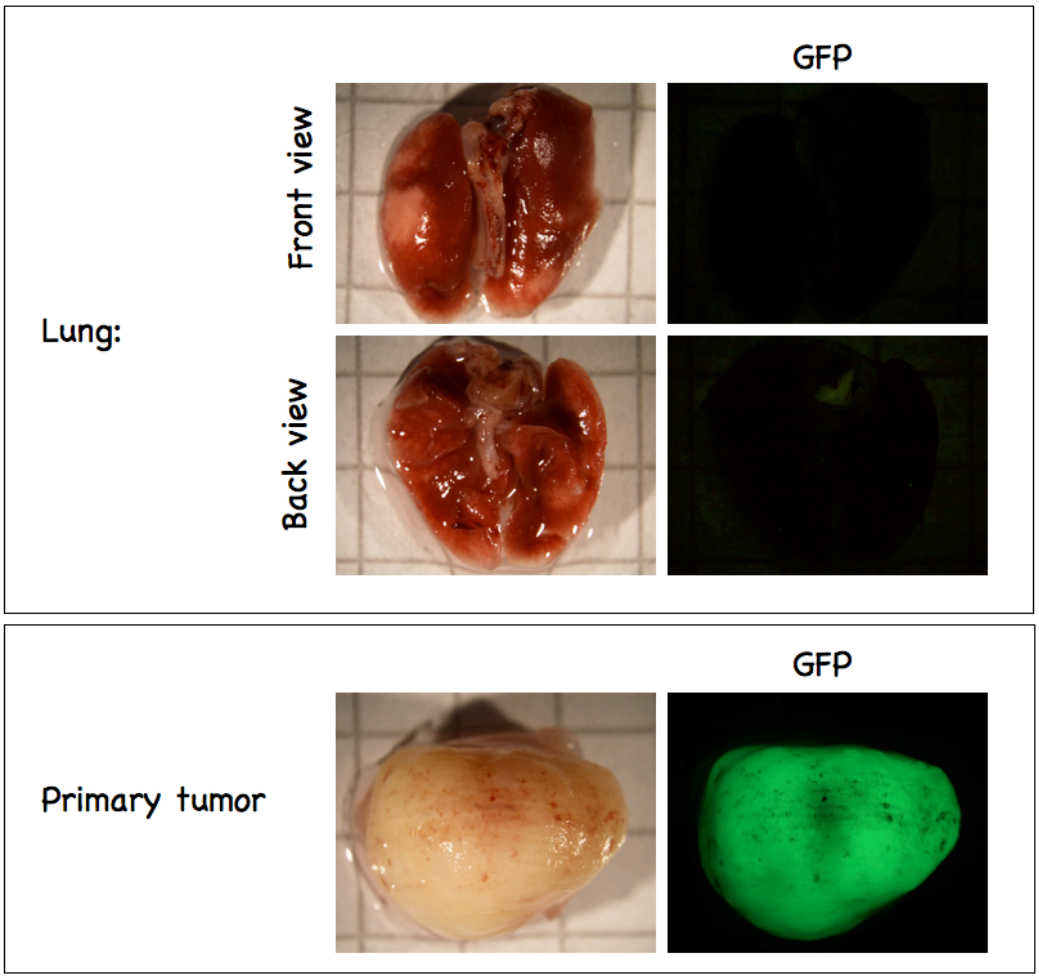

Figure 26: Lungs of HEK293 cells inoculated mice doesn't present metastasis foci.

Xenografts and lungs were collected from euthanized mice, fixed in 4% PFA 24 h and analyzed under fluorescent microscope. Representative images of lungs front and back views (upper panel) and of xenografted primary tumor (lower panel) are shown.

No metastasis were identified by the presence of green-fluorescent foci on the surface of the lungs. An example of lungs appearance is shown in figure 26, upper panel. The absence of green-fluorescent foci was not due to a loss of the GFP expression within the cells, as the excised tumor retains the fluorescence (Fig. 26, lower panel). However these results are not conclusive and may not exclude the presence of micrometastasis all over the body. Further experiments will be needed in order to clarify the role of uPAR-VN interaction in metastasis formation.

Mechanisms underlying the function of the uPAR-VN interaction *in vivo*

Although the function of the uPAR/VN-interaction in cell adhesion and migration has been extensively documented *in vitro*, it is not clear if and how this interaction may occur *in vivo*. It is straightforward to speculate that over-expression of uPAR by cancer cells may empower their migration/invasion in a VN-containing matrix, possibly in the tumor stroma, as demonstrated by the dramatic changes in cell migration on serum coated surfaces documented above. We have however decided to experimentally address also an alternative mechanism, which may explain a possible functional role the uPAR/VN-interaction *in vivo*. The rationale behind these experiments derives from the fact that the binding sites for uPAR and integrins in VN are non-overlapping, thus possibly allowing for the contemporary binding of both receptors. If the two receptor types are expressed on different cell types (i.e. uPAR on activated leukocytes and VN-integrin on endothelial cells) VN may promote cell-to-cell adhesion in processes such as leukocyte or cancer cell extravasation.

To establish whether uPAR and integrins may bind contemporarily to a single molecule of VN we conducted *in vitro* binding experiments (IVB) using purified components. In these experiments purified integrin ($\alpha_V\beta_3$) was immobilized and subsequently incubated with the monomeric SMB-RGD-domain of VN (which includes the specific uPAR and integrin binding sites) and soluble uPAR in the presence or absence of uPA (Fig. 27). The absence of absence of SMB and/or uPA resulted in no suPAR-integrin interaction, demonstrating that uPAR does not bind directly to $\alpha_V\beta_3$. On the contrary, the presence of both uPA and SMB-RGD-domain of VN promoted the binding of suPAR to the integrin. These findings suggest that VN acts as a bridge connecting uPAR to integrin. In particular integrins engage VN in the specific RGD motif while suPAR, occupied by uPA, interacts at the same time with the SMB domain.

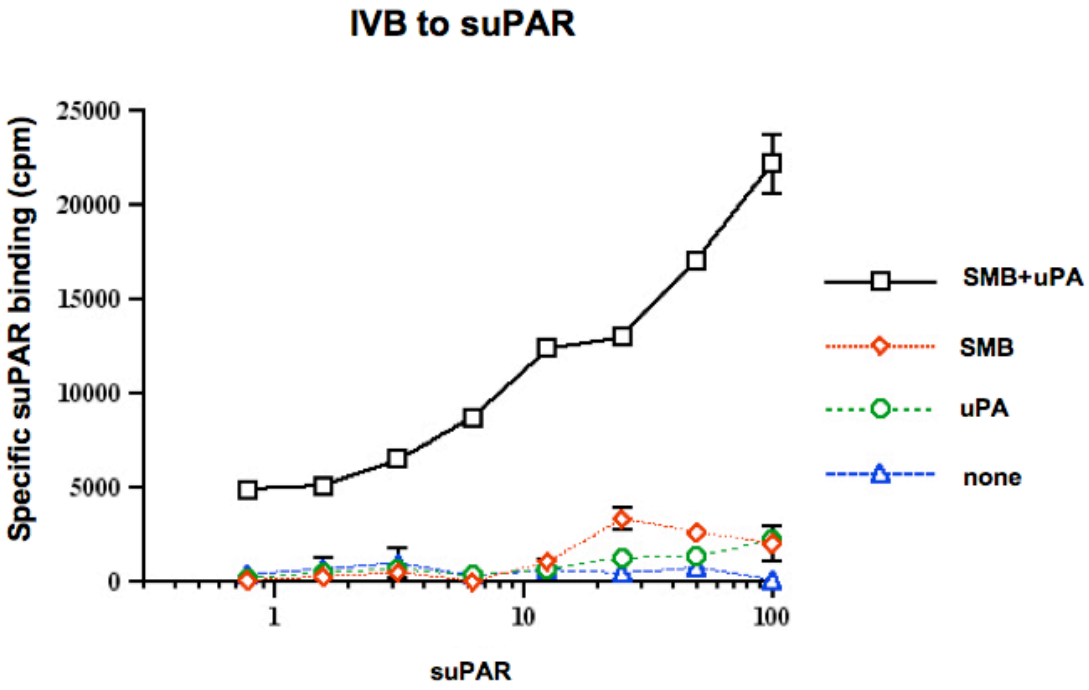

Figure 27: SMB- and uPA-dependent suPAR binding to $\alpha_V\beta_3$.

Binding of purified soluble uPAR to immobilized $\alpha_v\beta_3$-integrin. 96-well plates were coated with purified $\alpha_v\beta_3$-integrin, blocked with BSA, and incubated with a GFP-tagged SMB-domain. After washing away unbound SMB the wells were incubated with increasing concentrations of soluble uPAR (uPAR/Fc) in the presence or absence of pro-uPA (100 nM). Non-specific binding was determined in BSA-coated wells treated in the same way.

The ability of VN to connect uPAR molecule to a cell expressing $\alpha_V\beta_3$ integrin was tested in complementary experiments by adhesion assay. In these experiments purified suPAR was immobilized and subsequently incubated with the monomeric SMB domain of VN. The adhesion of cells expressing $\alpha_V\beta_3$ integrin was analyzed in presence or absence of uPA. In a first experiment, the adhesion of Rat smooth muscle cells (RSMC) was assayed. As for the IVB, the obtained results demonstrated that both SMB and uPA are required for uPAR/integrin interaction and, more importantly, that this "bridging" effect of the SMB is not mediated by direct uPAR/integrin interactions (Fig. 28).

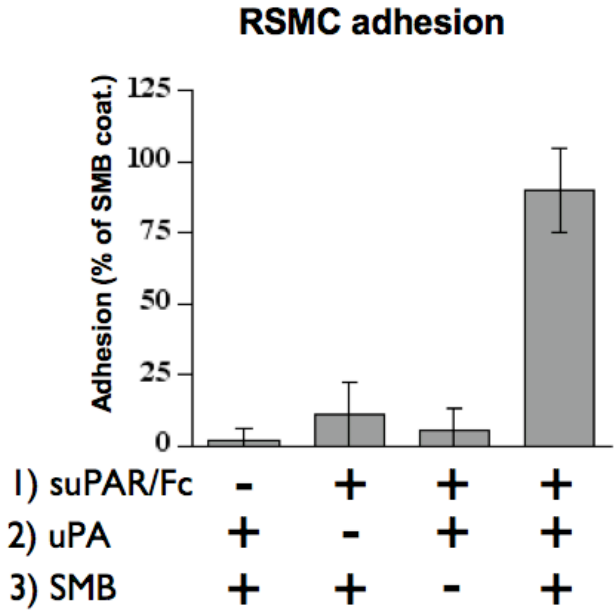

Figure 28: β_3 mediated RSMC adhesion to uPAR/uPA/VN-complexes.

Adhesion of $\alpha_V\beta_3$ expressing rat smooth muscle cells (RSMC) to immobilized suPAR. 96-well plates were coated with suPAR and incubated with SMB (30 nM) and uPA (20 nM) as indicated. Cells were allowed to adhere for 30 minutes and quantified by crystal violet staining. Background adhesion was determined using BSA-coated wells. The extend of adhesion is presented as percentage of direct adhesion to an immobilized SMB-domain.

These data were confirmed by a second experiment where adhesion of HEK293 cells expressing β_3 integrin (β_3^{WT}), activated by manganese (β_3^{WT}+Mn^{2+}), or a constitutively activated β_3 integrin (β_3^{303T}) (Luo et al., 2003) were used in replacement of RSMC. Importantly the endogenous array of integrin receptors expressed by HEK293 cells is not proficient in inducing a detectable adhesion in this kind of assay (Fig. 29). Indeed mock transfected cells adhered poorly to VN in an $\alpha_v\beta_5$ dependent fashion (Madsen et al., 2007).

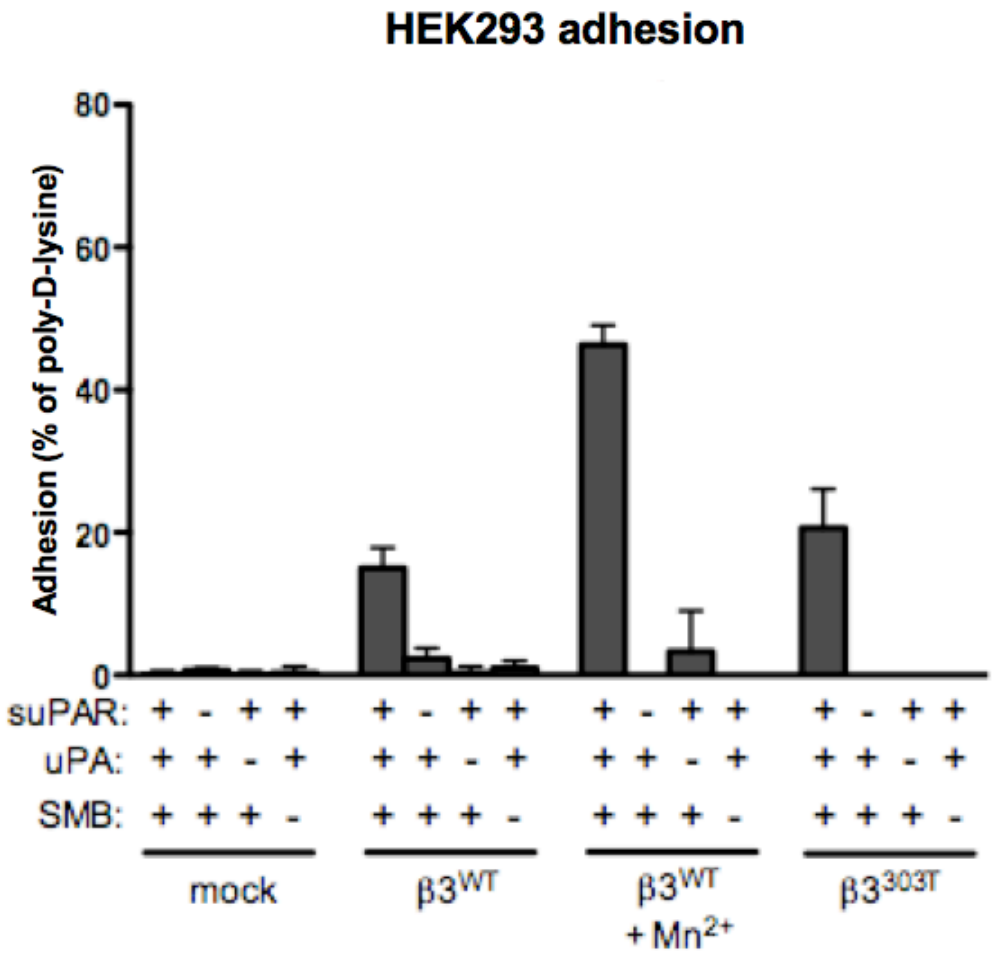

Figure 29: β_3 mediated cell adhesion to uPAR/uPA/VN-complexes.

Adhesion assay of HEK293 cells overexpressing β3 integrin, β3 integrin activated by Mn2+ or $\beta3^{303T}$ activated integrin to immobilized suPAR (20 nM), in presence/absence of uPA (20 nM) and SMB (30

nM). Adherent cells were fixed and stained with crystal violet. Cell adhesion to poly-D-lysine was set as 100% for each cell line. Data are expressed as mean ± s.e.m., n=3. HEK293 cells over expressing β3 and $\beta3^{303T}$ integrin were generated in the laboratory (Sarra Ferraris et al., unpublished).

Taken together these data strongly support the notion that VN may promote adhesion between cells expressing uPAR and VN-integrins, suggesting a possible role of the uPAR/VN-interaction also in cell-to-cell adhesion.

An unexpected result was the finding that VN could also connect two uPAR molecules.

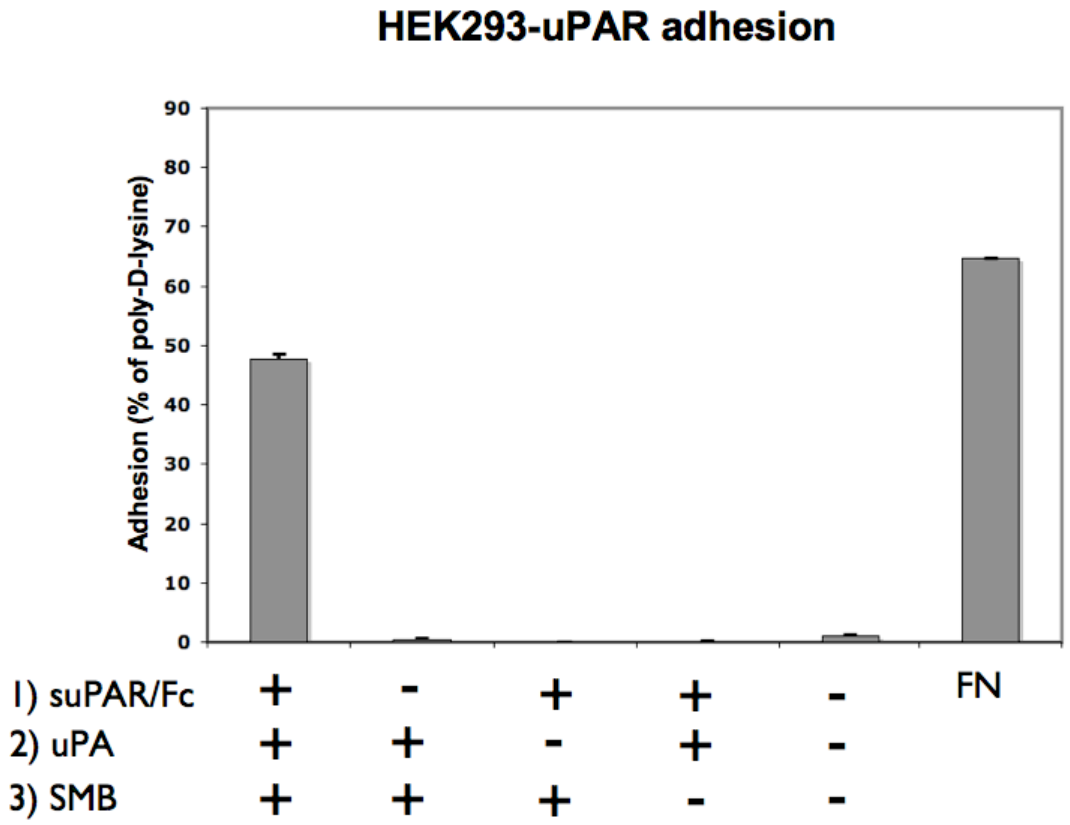

Figure 30: uPAR-mediated cell adhesion to uPAR/uPA/VN-complexes.

Adhesion assay of HEK293 cells expressing human uPAR to immobilized suPAR, (20 nM) in presence/absence of uPA (20 nM) and SMB (30 nM). Adherent cells were fixed and stained with crystal violet. Cell adhesion to poly-D-lysine was set as 100% for each cell line. Data are expressed as mean ± s.e.m., n=3.

In the performed experiment uPAR expressing HEK293 cells were allowed to adhere to immobilized suPAR, in presence or absence of SMB/uPA. Interestingly, SMB promoted adhesion of cells expressing uPAR to the immobilized suPAR incubated with both SMB and uPA (Fig. 30). The lack of either uPA or SMB resulted in no cell adhesion to immobilized suPAR. These findings could suggest that the SMB domain of VN molecule could be engaged by at least two uPAR molecules at the same time.

Derivation and characterization of endothelial cells and Bone marrow-derived macrophages from uPAR Wt and null mice

With the future aim of investigate the "bridging" capacity of VN to connect different cell types in a cell-to-cell adhesion assay, we derived macrophages and endothelial cells (EC) from uPAR Wt and knockout mice. Macrophages, which are in direct and constant contact with VN and are known to express high levels of uPAR when activated, interact indeed with EC expressing $\alpha_v\beta_3$ integrin, to reach the site of infection. Thus this could be an optimal system to test the physiological relevance of the VN "bridging" effect between these two cell types.

Endothelial cells were derived from lungs of two months old uPAR Wt and null mice and developed by direct infection with Polyoma middle T (PmT). To verify the purity of the endothelial population, the derived cells were stained for PECAM and VE-cadherin by immunofluorescence. PECAM (platelet endothelial cell adhesion molecule) is an adhesion molecule, expressed also in leukocytes and platelets (Dejana, 2004), that belongs to the immunoglobulin family. VE-cadherin (vascular endothelial cadherin) is a specific endothelial cell-to-cell adhesion molecule. uPAR Wt and the uPAR Ko derived

EC were positive for both the endothelial markers, strongly suggesting that we derived a pure endothelium (Fig. 31). Moreover, Figure 32 shows that uPAR Wt and uPAR Ko lung endothelial cells expressed the same amount of VE-cadherin.

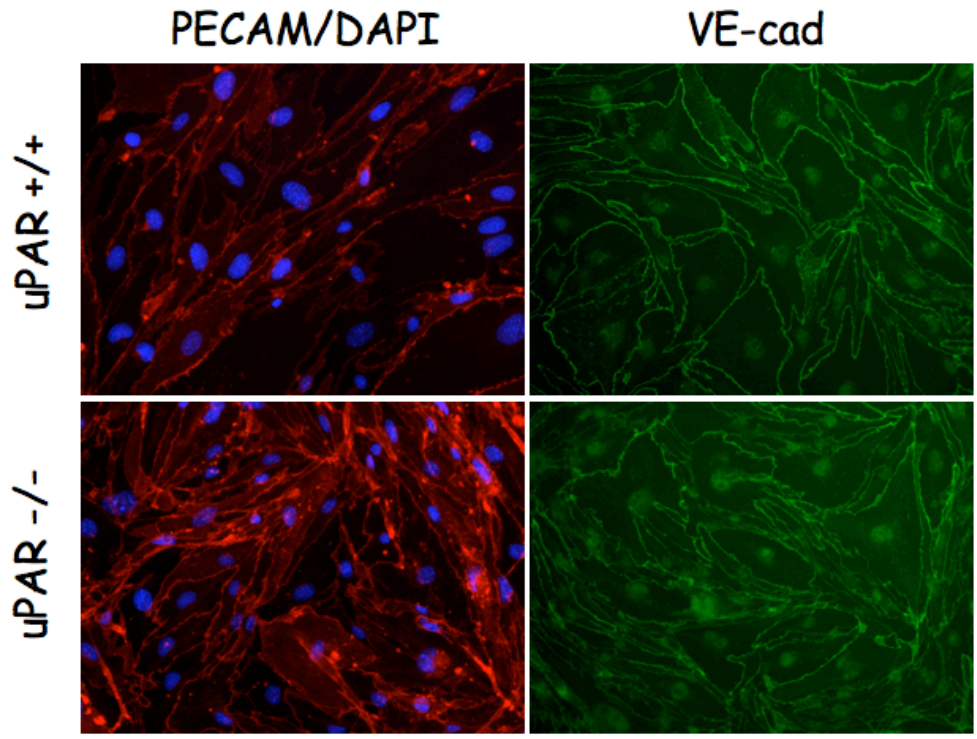

Figure 31: Immunofluorescence of lung-derived EC from uPAR+/+ and uPAR-/- mice.

Lung endothelial cells from uPAR+/+ (upper panel) and uPAR-/- mice (lower panel) were plated on 35mm plates pre-coated with 0.1% gelatin, let in culture for 2 days and starved overnight before fixation. Cells were then stained for PECAM (red) and VE-cadherin (green). The nuclear dye DAPI (blue) was used to counterstain cells. Representative images are shown.

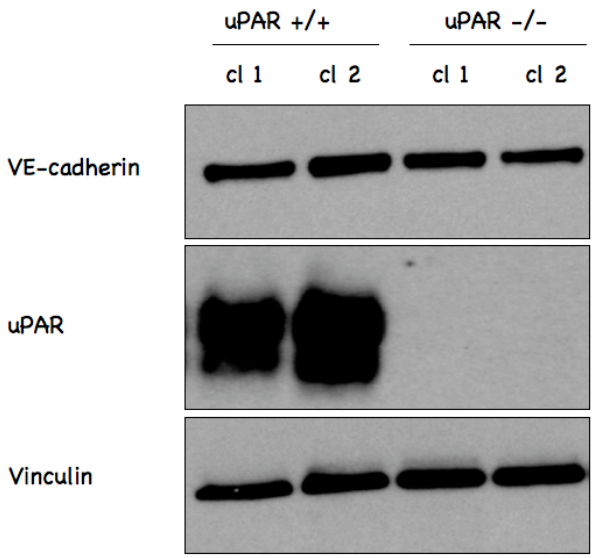

Figure 32: Western Blot analysis of EC derived from uPAR+/+ and uPAR-/- mice.

EC were cultured for two days and starved overnight before cell lysis and Western blot. Blots were probed for the endothelial cell-to-cell adhesion molecule VE-cadherin (top blot) and for uPAR (middle blot) then stripped and reprobed for vinculin as loading control (bottom blot). Two representative EC clones (cl) are shown for each genotype.

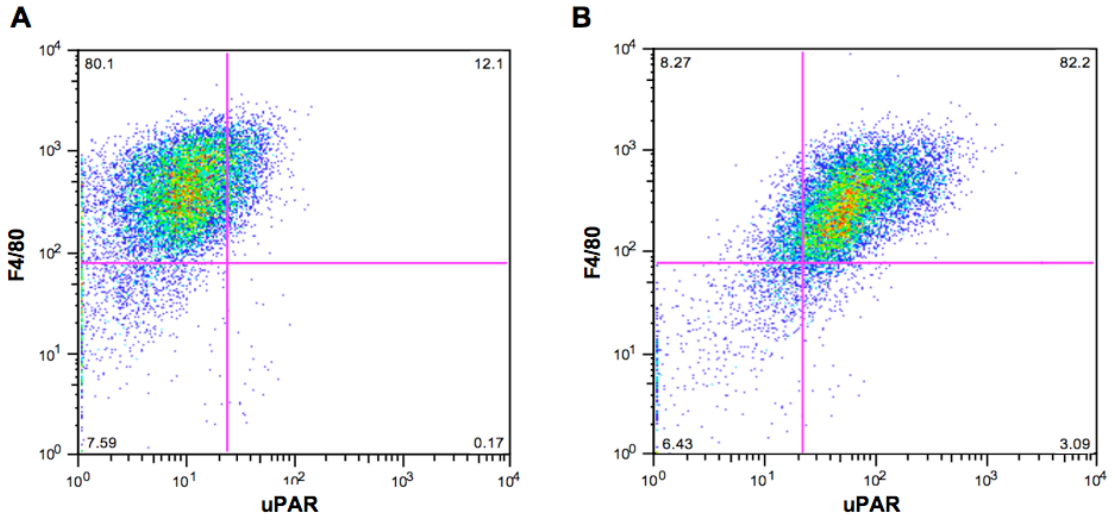

Figure 33: FACS analysis of BMM from uPAR+/+ and uPAR-/- mice.

Expression of macrophages specific antigen F4/80 (Y axis) and of uPAR (X axis) were evaluated by FACS analysis. **A**: BMM from uPAR -/- mice. **B**: BMM from uPAR+/+ mice.

Macrophages were derived from the bone marrow of uPAR+/+ and uPAR-/- mice.

The absence of uPAR didn't compromised macrophages differentiation. In fact, all the bone marrow-derived cells expressed the macrophage antigen F4/80 (Fig. 33).

Discussion

VN-binding epitope in mouse uPAR

Established models regarding the function of uPAR cancer implicate its activity as a protease receptor. Indeed, proteases activation and ECM remodeling are required in cell migration *in vivo*. However a secondary function of uPAR in orchestrating intracellular signaling, independently of its proteolytic activity has been suggested by a growing number of evidences. Considering the complexity of a tumor scenario, the proteolytic and non-proteolytic function of uPAR may synergistically cooperate in the process of tumor progression.

It has been demonstrated that the direct interaction between cell surface uPAR and the extra-cellular protein VN is required for the ability of uPAR to modulate changes in cell morphology and migration (Madsen et al., 2007). Moreover, it has been extensively documented that signal transduction initiated by uPAR-VN interaction occurs through the regulation of integrin signaling (Kjoller and Hall, 2001; Smith et al., 2008) and it does not involve a direct interaction between uPAR and integrins (Madsen et al., 2007).

Nevertheless the biological relevance of uPAR-VN interaction in cancer progression has never been investigated. In order to define the role of uPAR-VN interaction in this process we generated a simple cell system that will be finally used in xenotransplanted tumor model. This cell system will take advantage of the previous extensive characterization of the interaction interface between uPAR and VN. Indeed VN-binding epitope in human uPAR has been previously identified (Gardsvoll and Ploug, 2007; Madsen et al., 2007). It is constituted of 3 residues (W32, R58A, I63A) of

the D1 and 2 residues (R91, Y92) localized in the linker region between D1 and D2. Given the fully conservation of the VN binding epitope of uPAR in the mouse system, we introduced corresponding mutations by site directed mutagenesis in the murine receptor, which resulted in impaired uPAR-VN interaction. All the mutant receptors resulted to impair cell attachment to VN in an integrin-independent fashion, preserving the ability to bind to uPAR natural ligand uPA. More importantly, the absent uPAR-VN interaction that characterized all the receptor variants abolished those morphological chances such as loss of stress fibers and an accelerate FA turnover observed in the Wt receptor (muPAR). These results are completely in agreement with the published data obtained from the characterization of VN-binding epitope in human uPAR (Madsen et al., 2007).

In addition, uPAR has been reported to modulate integrin-mediated adhesion by a direct interaction (Wei et al., 2005). However, in our system, uPAR expression didn't result in an increased integrin-mediated VN or FN adhesion. This difference could be due to the different cell line used by Wei et al. in their cell adhesion assays. In fact, the authors use a cancer cell line that could express different levels of uPAR as well as uPAR-interacting factors respect to HEK293 Flp-In cells. It is also known that many cancer cells produce ECM factors that could have an effect in experiments performed on purified substrates. Moreover the different experimental conditions such as extensive washing of the cells, cell-adhesion timing, the different media used and the solution used to block the coated plated could influence the output of the experiments. Importantly, in Wei et al. paper cell adhesion is not quantified and normalized but it is shown as representative picture of stained plates.

uPAR and cell migration

Cell migration is the locomotion of cell over an ECM substratum. It involves extension at the leading edge and retraction at the trailing edge of the cell. Extension of the leading edge of the cell is associated with cell adhesion, which is induced by integrin binding to ECM ligands, triggering the anchoring of new polymerized actin to the integrins to form focal adhesion. Many studies have implicated uPAR as an important regulator in cell motility. Several studies support the uPA dependency of uPAR-induced migration. In fact, antibody against uPA inhibited migration of some cell types, while ATF stimulated migration in a proteolysis independent fashion (Andreasen et al., 1997). Other studies emphasize how uPAR-induced migration is uPA-independent. Indeed, expression of uPAR in Swiss 3T3 cells enhances cell migration, depending on the interaction between uPAR and VN (Kjoller and Hall, 2001). The effect of uPA on cell migration may be caused by its proteolytic function *in vivo*. Indeed proteolytic degradation of ECM is an hallmark of mesenchymal cell-migration (Friedl, 2004). Moreover, uPAR, upon uPA interaction increases its affinity to VN (Sidenius et al., 2002). As a consequence, cell lines expressing low uPAR levels will be dependent on uPA interaction for efficient VN adhesion whereas high levels of uPAR expression is sufficient to directly mediate VN cell adhesion independently of uPA.

In our *in vitro* studies, muPAR overexpression resulted in enhanced cell adhesion and migration without requiring uPA interaction. This effect was lost in the absence of uPAR-VN interaction, as cell contact area and migration of HEK293muPAR^{W32A} and HEK293$^{\Delta D1}$ were comparable to mock counterparts.

In agreement with previous studies (Kjoller and Hall, 2001; Smith et al., 2008), uPAR-VN interaction promotes P130Cas phosphorylation, leading to increased Rac1 activity that promotes ruffling and lamellipodia protrusion. In this way the enhanced

P130Cas phosphorylation that we observed upon uPAR-VN interaction can be linked to the pro-migratory phenotype that characterizes muPAR Wt expressing cells.

The uPAR-system and proliferation/apoptosis

The ability of tumor cells to migrate and invade through the basement membrane into surrounding tissues is one of the essential hallmarks of cancer and a prerequisite for both local tumor progression and metastasis. But transformation, migration and invasion of tumor cells requires their resistance to the endogenous death program once the cell has detached from the primary tumor tissue. Indeed, many cell types derived from human malignancies, such as gastric cancer, breast cancer, colon cancer, osteosarcomas, and lung cancer, are resistant to anoikis.

Recent studies demonstrate a close correlation between the uPA/uPAR-system and cell sensitivity to programmed cell death. Yanamandra and coworkers reported that SNB19 glioblastoma cells expressing antisense uPAR constructs are less invasive than parental cells when injected in vivo. They found that *in vivo* inhibition of tumor growth is associated with activation of caspase-9 and subsequent apoptosis (Yanamandra et al., 2000).

Differences in cell growth can be accounted to different processes: increased cell proliferation or decreased apoptosis. Accordingly to previous findings, our data show that muPAR expression in HEK293 cells prevent programmed cell death. In parallel the proliferation assay showed an increased growth rate upon uPAR-VN interaction. On the other hand, cells expressing the muPAR^{W32A} are not protected from apoptosis and showed a growth rate comparable to the mock-transfected cells.

The lack of uPAR-VN interaction resulted in a diminished cell proliferation and an enhanced apoptosis.

The decrease of apoptosis/increased growth rate correlates with enhanced ERK1/2 activation in muPAR Wt expressing cells. Importantly, the mitogenic signal downstream of uPAR is dependent on its interaction with VN. Indeed HEK293muPAR^{W32A} and HEK293$^{\Delta D1}$ cells do not displayed major upregulation in MAPK activation respect to mock-transfected cells. Consistently, MAPK signaling rules the transcriptional program that regulates DNA synthesis and contrasts apoptotic processes (Hildenbrand et al., 2008). These evidences could also explain the behavior of the cells injected into mice in our xenograft model.

Importance of uPAR-VN interaction in cancer

Several molecular components involved in ECM degradation are strong prognostic markers in several types of cancer, and inhibition of extracellular proteolysis is recognized as a valid approach to cancer therapy. However, the proteases have many functions in the normal organism. It is therefore inevitable that efficient inhibition will have toxic effects. Moreover the functional overlap between different proteases system means that combination of inhibitors must be used in order to obtain efficient anti-invasive therapy. This combination will additionally increase the toxicity.

Numerous reports documented the involvement of uPAR and uPA levels in cancer. However the loss of uPAR in the host did not prevent tumor growth (Bajou et al., 2001), but the use of antagonists of uPA or uPAR prevented growth invasiveness and metastasis of tumors (Crowley et al., 1993; Lakka et al., 2001; Min et al., 1996). These evidences suggest that in tumor scenario a major role is played by uPAR expressed by the tumor cells and not by the host, although uPAR expression has been found also in tumor-associated macrophages (see introduction). In this study we confirmed the importance of uPAR expression on cancer cells to induce and accelerate

tumor formation, as mice xenografted with muPAR expressing cells showed a premature primary tumor formation respect to mock injected mice. More important we found that uPAR-effect on cancer cells can be impaired by blocking its interaction with the ECM protein VN. Indeed the complete depletion of D1 (involved in VN and uPA binding (Sidenius and Blasi, 2000) or the specific mutation of the VN binding epitope abolished the uPAR-mediated effect on tumor formation. Surprisingly, an uPAR variant ($muPAR^{W32A}$) that can only interact with uPA, negatively regulated tumor formation, indicating that uPAR-uPA interaction could impaired cancer cell proliferation.

The effect that uPAR exerts on cancer cell proliferation was not observed in a similar study by Jo et al. (Jo et al., 2009). The authors transfected HEK293 cells expressing either human or mouse uPAR to express GFP and injected these cells in the fourth mammary fat pad of SCID mice. Tumor growth measurement and time of mice euthanization were similar to the ones we described. They found that uPAR expression was not associated with a significant change in the growth rate of the primary tumor. Moreover both human and mouse uPAR promoted lung metastasis (Fig. 8). Because of the activity of human uPAR they conclude uPAR-promoting cancer metastasis is uPA-independent.

Although the uPAR-uPA interaction shows species specificity, the binding between the mouse uPA and the human receptor occurs just with a lower affinity. The uPA concentration in a living system could be high enough to compensate the impaired affinity between the receptor and ligand of different species.

A possible explanation for the discrepancy between our and Jo et al. results can be found in the different cell line and method of transfection used. Jo et al. used HEK293 cells, transfected to express uPAR or the empty vector and subjected to single cell cloning. These cells were further transfected to express GFP and again subjected to single cell cloning. Differently, we used HEK293 Flp-In cells that have been first

transfected to express GFP and subjected to single cell cloning. The selected GFP clone was further transfected with muPAR variants or empty vector, taken advantage of the Flp-In system that generates pools of isogenic transfectants carrying a single copy of the expression cassette, thus by eliminating potential artifacts caused by clonal differences or heterogeneous expression levels. The absence of metastasis foci in our mice could be also due to the no metastatic potential of the GFP clone that we have selected.

Additionally, our results show that uPA can be a negative regulator of tumor growth. Indeed cell expressing muPAR^{W32A}, that cannot interact with VN but retains uPA-binding activity, displayed an impaired growth rate respect to mock transfected cells. Consistently cells expressing muPAR$^{\Delta D1}$, in which the interaction with both VN and uPA is blunted, behaved like uPAR-negative cells. The negative role of uPA in tumor cell growth should be clarified by further experiments, maybe taking advantage of a mutant form of uPAR where just uPA binding is impaired. However, the generation of this mutant variant is quite difficult, since uPA-binding interest all the three domains of uPAR.

Role of uPAR-VN interaction in Inflammation and cancer

Substantial evidences suggest a role of uPAR in leukocyte recruitment. uPAR-deficient mice showed an impaired neutrophils recruitment in response to Pulmonary *Pseudomonas aeruginosa* infection (Fig. 10) (Gyetko et al., 2000). Thioglycolate-elicited leukocyte recruitment to the peritoneal cavity is reduced in uPAR-deficient mice (May et al., 1998). In addition, macrophages from uPAR-deficient mice showed a defective adhesion to pulmonary capillary endothelial cell monolayers respect to Wt counterpart (Gyetko et al., 2000). In all these studies the absence of uPAR did not abrogate completely leukocyte recruitment; possibly because uPAR is a modulator of β_2

integrin (Cao et al., 1995) and β_2 integrin can still engage its specific ligands even in absence of uPAR. Consistently, Wt mice had diminished neutrophil recruitment to the lung when an anti-CD11b mAb is given before inoculation with the pathogen, while recruitment of uPAR-/- neutrophils is unaffected (Gyetko et al., 2000). Probably the combined blockage of both uPAR and β_2 integrin would result in complete depletion of leukocytes migratory capacity.

Up to now there are no studies investigating the role of uPAR-VN interaction in inflammation. We demonstrated that uPA-VN could act as a bridge, connecting uPAR to purified $\alpha_v\beta_3$ integrin protein or to cell expressing $\alpha_v\beta_3$ integrin. These results strongly support the idea that the crosstalk between uPAR and VN-$\alpha_v\beta_3$ could play a role in leukocytes recruitment in the site of infection and, in particular, in intravasation and extravasation processes. Indeed uPAR is expressed on activated leukocytes and $\alpha_v\beta_3$ integrin is expressed on endothelial cells. A cell to cell adhesion assay between macrophages and endothelial cells will help us to test our hypothesis, with particular attention to the VN-bridge function. For this purpose macrophages and endothelial cells were derived from uPAR+/+ and uPAR-/- mice. More in particular, Macrophages were derived from mouse bone marrow, while endothelial cells from mouse lungs. Both Wt and uPAR Ko macrophages showed no problem in their differentiation. A better morphological characterization of macrophages and endothelial cells is required in view of future experiments.

Madsen et al. demonstrated that VN-uPAR interaction provides the key to induce adhesion and cell migration (Madsen et al., 2007). Is our thought that cancer cells could mimic the leukocyte capacity to over-express uPAR to enter the tumor blood vessels and to reach the site of metastatization. After vascular leakage at the site of tumor, in fact, VN could get in contact with cancer cells expressing uPAR on the cell surface, thus promoting such morphological chances responsible for cell migration.

Interestingly, VN deposition was found in several tumor sites (Gladson and Cheresh, 1991; Gladson et al., 1995; Maenpaa et al., 1997). Consequently, uPAR expressed by cancer cells could interact with VN associated to $\alpha_v\beta_3$ integrin of endothelial cell to exit the blood vessel and reach the site of metastasis formation. To study the role of uPAR-VN interaction in cancer cell invasion and extravasation it is our intention to perform trans-endothelial migration of uPAR expressing tumor cell lines.

FUTURE PERSPECTIVES

uPAR appears to be strongly upregulated in many inflammatory diseases and in practically all types of cancer. Stromal cells and cancer cells in the invasive front of human tumors often exhibit a specific and high expression of uPAR, pointing to an important role during tumor dissemination. In the context of cancer dissemination, proteolytic remodeling of the ECM is often regarded as an advantage for invasive tumors although proteolysis-independent cancer invasion have been observed by the power of cancer cells to interconvert from a collective or mesenchymal mode of motility to an amoeboid type of migration surpassing the need of ECM degradation. Proteolytic degradation of the ECM can be executed by cancer and stromal cells, such as tumor associated macrophages and fibroblasts. The ability of uPAR to initiate extracellular proteolysis and to launch a broad range of signals regulating cell migration and proliferation places uPAR as a promising therapeutic target for tumor prevention.

The proteolytic function of uPAR during cancer progression has to some extent been evaluated in mice while the non-proteolytic function scarcely has been assessed. The newly characterized binding-interface between mouse uPAR and VN now permits the evaluation of this interaction to be scrutinized in more details *in vivo*. Of particular interest is the interplay between uPAR and VN during disease progression and during activation of the innate immune system. It is of great interest to establish whether VN incorporation into specific niches supports retention and recruitment of uPAR expressing cancer cells, immune cells and stem cells. The ability of uPAR-VN to fire up the activation of Rac1 and ERK1/2 *in vitro* may also have great impact on cancer cell invasion and growth *in vivo*.

It is becoming clear that unraveling the molecular mechanism(s) underlying non-proteolytic uPAR signaling is of fundamental importance. However, the non-

proteolytic function of uPAR has already received much "*in vitro attention"* and with that in mind it is now imperative to re-evaluate the available set of information through experimental *in vivo* enquiries. Further studies taking advantage of cancer cell lines, modulated for uPAR interaction with different binding proteins, in a mouse system were uPAR, uPA, VN, or integrin has been knocked-out will provide fundamental information regarding the uPAR interaction network and its *in vivo* implication(s).

References

Aguirre Ghiso, J.A., K. Kovalski, and L. Ossowski. 1999. Tumor dormancy induced by downregulation of urokinase receptor in human carcinoma involves integrin and MAPK signaling. *J Cell Biol*. 147:89-104.

Aguirre-Ghiso, J.A., D. Liu, A. Mignatti, K. Kovalski, and L. Ossowski. 2001. Urokinase receptor and fibronectin regulate the ERK(MAPK) to p38(MAPK) activity ratios that determine carcinoma cell proliferation or dormancy in vivo. *Mol Biol Cell*. 12:863-79.

Almholt, K., L.R. Lund, J. Rygaard, B.S. Nielsen, K. Dano, J. Romer, and M. Johnsen. 2005. Reduced metastasis of transgenic mammary cancer in urokinase-deficient mice. *Int J Cancer*. 113:525-32.

Andolfo, A., W.R. English, M. Resnati, G. Murphy, F. Blasi, and N. Sidenius. 2002. Metalloproteases cleave the urokinase-type plasminogen activator receptor in the D1-D2 linker region and expose epitopes not present in the intact soluble receptor. *Thromb Haemost*. 88:298-306.

Andreasen, P.A., L. Kjoller, L. Christensen, and M.J. Duffy. 1997. The urokinase-type plasminogen activator system in cancer metastasis: a review. *Int J Cancer*. 72:1-22.

Anichini, E., G. Fibbi, M. Pucci, R. Caldini, M. Chevanne, and M. Del Rosso. 1994. Production of second messengers following chemotactic and mitogenic urokinase-receptor interaction in human fibroblasts and mouse fibroblasts transfected with human urokinase receptor. *Exp Cell Res*. 213:438-48.

Artym, V.V., A.L. Kindzelskii, W.T. Chen, and H.R. Petty. 2002. Molecular proximity of seprase and the urokinase-type plasminogen activator receptor on malignant melanoma cell membranes: dependence on beta1 integrins and the cytoskeleton. *Carcinogenesis*. 23:1593-601.

Aumailley, M., and B. Gayraud. 1998. Structure and biological activity of the extracellular matrix. *J Mol Med*. 76:253-65.

Bajou, K., V. Masson, R.D. Gerard, P.M. Schmitt, V. Albert, M. Praus, L.R. Lund, T.L. Frandsen, N. Brunner, K. Dano, N.E. Fusenig, U. Weidle, G. Carmeliet, D. Loskutoff, D. Collen, P. Carmeliet, J.M. Foidart, and A. Noel. 2001. The plasminogen activator inhibitor PAI-1 controls in vivo tumor vascularization by interaction with proteases, not vitronectin. Implications for antiangiogenic strategies. *J Cell Biol*. 152:777-84.

Balabanov, R., D. Lisak, T. Beaumont, R.P. Lisak, and P. Dore-Duffy. 2001. Expression of urokinase plasminogen activator receptor on monocytes from

patients with relapsing-remitting multiple sclerosis: effect of glatiramer acetate (copolymer 1). *Clin Diagn Lab Immunol*. 8:1196-203.

Barinka, C., G. Parry, J. Callahan, D.E. Shaw, A. Kuo, K. Bdeir, D.B. Cines, A. Mazar, and J. Lubkowski. 2006. Structural basis of interaction between urokinase-type plasminogen activator and its receptor. *J Mol Biol*. 363:482-95.

Bauer, T.W., W. Liu, F. Fan, E.R. Camp, A. Yang, R.J. Somcio, C.D. Bucana, J. Callahan, G.C. Parry, D.B. Evans, D.D. Boyd, A.P. Mazar, and L.M. Ellis. 2005. Targeting of urokinase plasminogen activator receptor in human pancreatic carcinoma cells inhibits c-Met- and insulin-like growth factor-I receptor-mediated migration and invasion and orthotopic tumor growth in mice. *Cancer Res*. 65:7775-81.

Beaufort, N., D. Leduc, J.C. Rousselle, V. Magdolen, T. Luther, A. Namane, M. Chignard, and D. Pidard. 2004. Proteolytic regulation of the urokinase receptor/CD87 on monocytic cells by neutrophil elastase and cathepsin G. *J Immunol*. 172:540-9.

Behrendt, N., M. Ploug, L. Patthy, G. Houen, F. Blasi, and K. Dano. 1991. The ligand-binding domain of the cell surface receptor for urokinase-type plasminogen activator. *J Biol Chem*. 266:7842-7.

Behrendt, N., E. Ronne, M. Ploug, T. Petri, D. Lober, L.S. Nielsen, W.D. Schleuning, F. Blasi, E. Appella, and K. Dano. 1990. The human receptor for urokinase plasminogen activator. NH2-terminal amino acid sequence and glycosylation variants. *J Biol Chem*. 265:6453-60.

Bianchi, E., E. Ferrero, F. Fazioli, F. Mangili, J. Wang, J.R. Bender, F. Blasi, and R. Pardi. 1996. Integrin-dependent induction of functional urokinase receptors in primary T lymphocytes. *J Clin Invest*. 98:1133-41.

Blasi, F. 1993. Urokinase and urokinase receptor: a paracrine/autocrine system regulating cell migration and invasiveness. *Bioessays*. 15:105-11.

Blasi, F. 1999. The urokinase receptor. A cell surface, regulated chemokine. *APMIS*. 107:96-101.

Blasi, F., and P. Carmeliet. 2002. uPAR: a versatile signalling orchestrator. *Nat Rev Mol Cell Biol*. 3:932-43.

Borglum, A.D., A. Byskov, P. Ragno, A.L. Roldan, P. Tripputi, G. Cassani, K. Dano, F. Blasi, L. Bolund, and T.A. Kruse. 1992. Assignment of the urokinase-type plasminogen activator receptor gene (PLAUR) to chromosome 19q13.1-q13.2. *Am J Hum Genet*. 50:492-7.

Brooks, P.C., R.A. Clark, and D.A. Cheresh. 1994a. Requirement of vascular integrin alpha v beta 3 for angiogenesis. *Science*. 264:569-71.

Brooks, P.C., A.M. Montgomery, M. Rosenfeld, R.A. Reisfeld, T. Hu, G. Klier, and D.A. Cheresh. 1994b. Integrin alpha v beta 3 antagonists promote tumor regression by inducing apoptosis of angiogenic blood vessels. *Cell*. 79:1157-64.

Brooks, P.C., S. Stromblad, R. Klemke, D. Visscher, F.H. Sarkar, and D.A. Cheresh. 1995. Antiintegrin alpha v beta 3 blocks human breast cancer growth and angiogenesis in human skin. *J Clin Invest*. 96:1815-22.

Bugge, T.H., M.J. Flick, M.J. Danton, C.C. Daugherty, J. Romer, K. Dano, P. Carmeliet, D. Collen, and J.L. Degen. 1996. Urokinase-type plasminogen activator is effective in fibrin clearance in the absence of its receptor or tissue-type plasminogen activator. *Proc Natl Acad Sci U S A*. 93:5899-904.

Bugge, T.H., T.T. Suh, M.J. Flick, C.C. Daugherty, J. Romer, H. Solberg, V. Ellis, K. Dano, and J.L. Degen. 1995. The receptor for urokinase-type plasminogen activator is not essential for mouse development or fertility. *J Biol Chem*. 270:16886-94.

Cao, D., I.F. Mizukami, B.A. Garni-Wagner, A.L. Kindzelskii, R.F. Todd, 3rd, L.A. Boxer, and H.R. Petty. 1995. Human urokinase-type plasminogen activator primes neutrophils for superoxide anion release. Possible roles of complement receptor type 3 and calcium. *J Immunol*. 154:1817-29.

Cardin, A.D., and H.J. Weintraub. 1989. Molecular modeling of protein-glycosaminoglycan interactions. *Arteriosclerosis*. 9:21-32.

Carmeliet, P., L. Schoonjans, L. Kieckens, B. Ream, J. Degen, R. Bronson, R. De Vos, J.J. van den Oord, D. Collen, and R.C. Mulligan. 1994. Physiological consequences of loss of plasminogen activator gene function in mice. *Nature*. 368:419-24.

Carriero, M.V., S. Del Vecchio, P. Franco, M.I. Potena, F. Chiaradonna, G. Botti, M.P. Stoppelli, and M. Salvatore. 1997. Vitronectin binding to urokinase receptor in human breast cancer. *Clin Cancer Res*. 3:1299-308.

Chain, D., T. Kreizman, H. Shapira, and S. Shaltiel. 1991. Plasmin cleavage of vitronectin. Identification of the site and consequent attenuation in binding plasminogen activator inhibitor-1. *FEBS Lett*. 285:251-6.

Coleman, J.L., J.A. Gebbia, and J.L. Benach. 2001. Borrelia burgdorferi and other bacterial products induce expression and release of the urokinase receptor (CD87). *J Immunol*. 166:473-80.

Collen, D., and H.R. Lijnen. 1991. Basic and clinical aspects of fibrinolysis and thrombolysis. *Blood*. 78:3114-24.

Connolly, B.M., E.Y. Choi, H. Gardsvoll, A.L. Bey, B.M. Currie, T. Chavakis, S. Liu, A. Molinolo, M. Ploug, S.H. Leppla, and T.H. Bugge. 2010. Selective

abrogation of the uPA-uPAR interaction in vivo reveals a novel role in suppression of fibrin-associated inflammation. *Blood*. 116:1593-603.

Crowley, C.W., R.L. Cohen, B.K. Lucas, G. Liu, M.A. Shuman, and A.D. Levinson. 1993. Prevention of metastasis by inhibition of the urokinase receptor. *Proc Natl Acad Sci U S A*. 90:5021-5.

Cubellis, M.V., P. Andreasen, P. Ragno, M. Mayer, K. Dano, and F. Blasi. 1989. Accessibility of receptor-bound urokinase to type-1 plasminogen activator inhibitor. *Proc Natl Acad Sci U S A*. 86:4828-32.

Cubellis, M.V., T.C. Wun, and F. Blasi. 1990. Receptor-mediated internalization and degradation of urokinase is caused by its specific inhibitor PAI-1. *EMBO J*. 9:1079-85.

Cunningham, O., A. Andolfo, M.L. Santovito, L. Iuzzolino, F. Blasi, and N. Sidenius. 2003. Dimerization controls the lipid raft partitioning of uPAR/CD87 and regulates its biological functions. *EMBO J*. 22:5994-6003.

Daci, E., N. Udagawa, T.J. Martin, R. Bouillon, and G. Carmeliet. 1999. The role of the plasminogen system in bone resorption in vitro. *J Bone Miner Res*. 14:946-52.

Dano, K., N. Behrendt, G. Hoyer-Hansen, M. Johnsen, L.R. Lund, M. Ploug, and J. Romer. 2005. Plasminogen activation and cancer. *Thromb Haemost*. 93:676-81.

Dano, K., J. Romer, B.S. Nielsen, S. Bjorn, C. Pyke, J. Rygaard, and L.R. Lund. 1999. Cancer invasion and tissue remodeling--cooperation of protease systems and cell types. *APMIS*. 107:120-7.

De Petro, G., D. Tavian, A. Copeta, N. Portolani, S.M. Giulini, and S. Barlati. 1998. Expression of urokinase-type plasminogen activator (u-PA), u-PA receptor, and tissue-type PA messenger RNAs in human hepatocellular carcinoma. *Cancer Res*. 58:2234-9.

Dejana, E. 2004. Endothelial cell-cell junctions: happy together. *Nat Rev Mol Cell Biol*. 5:261-70.

Del Rosso, M., G. Fibbi, and M. Matucci Cerinic. 1999. The urokinase-type plasminogen activator system and inflammatory joint diseases. *Clin Exp Rheumatol*. 17:485-98.

Deng, G., S.A. Curriden, S. Wang, S. Rosenberg, and D.J. Loskutoff. 1996. Is plasminogen activator inhibitor-1 the molecular switch that governs urokinase receptor-mediated cell adhesion and release? *J Cell Biol*. 134:1563-71.

Desgrosellier, J.S., and D.A. Cheresh. Integrins in cancer: biological implications and therapeutic opportunities. *Nat Rev Cancer*. 10:9-22.

Dewerchin, M., A.V. Nuffelen, G. Wallays, A. Bouche, L. Moons, P. Carmeliet, R.C. Mulligan, and D. Collen. 1996. Generation and characterization of urokinase receptor-deficient mice. *J Clin Invest*. 97:870-8.

Ellis, V., and K. Dano. 1991. Plasminogen activation by receptor-bound urokinase. *Semin Thromb Hemost*. 17:194-200.

Ellis, V., M.F. Scully, and V.V. Kakkar. 1989. Plasminogen activation initiated by single-chain urokinase-type plasminogen activator. Potentiation by U937 monocytes. *J Biol Chem*. 264:2185-8.

Ellis, V., T.C. Wun, N. Behrendt, E. Ronne, and K. Dano. 1990. Inhibition of receptor-bound urokinase by plasminogen-activator inhibitors. *J Biol Chem*. 265:9904-8.

Estreicher, A., J. Muhlhauser, J.L. Carpentier, L. Orci, and J.D. Vassalli. 1990. The receptor for urokinase type plasminogen activator polarizes expression of the protease to the leading edge of migrating monocytes and promotes degradation of enzyme inhibitor complexes. *J Cell Biol*. 111:783-92.

Fawcett, J., C.L. Holness, L.A. Needham, H. Turley, K.C. Gatter, D.Y. Mason, and D.L. Simmons. 1992. Molecular cloning of ICAM-3, a third ligand for LFA-1, constitutively expressed on resting leukocytes. *Nature*. 360:481-4.

Fazioli, F., M. Resnati, N. Sidenius, Y. Higashimoto, E. Appella, and F. Blasi. 1997. A urokinase-sensitive region of the human urokinase receptor is responsible for its chemotactic activity. *EMBO J*. 16:7279-86.

Festuccia, C., A. Angelucci, G.L. Gravina, L. Biordi, D. Millimaggi, P. Muzi, C. Vicentini, and M. Bologna. 2005. Epidermal growth factor modulates prostate cancer cell invasiveness regulating urokinase-type plasminogen activator activity. EGF-receptor inhibition may prevent tumor cell dissemination. *Thromb Haemost*. 93:964-75.

Friedl, P. 2004. Prespecification and plasticity: shifting mechanisms of cell migration. *Curr Opin Cell Biol*. 16:14-23.

Ganesh, S., C.F. Sier, M.M. Heerding, G. Griffioen, C.B. Lamers, and H.W. Verspaget. 1994. Urokinase receptor and colorectal cancer survival. *Lancet*. 344:401-2.

Gardsvoll, H., B. Gilquin, M.H. Le Du, A. Menez, T.J. Jorgensen, and M. Ploug. 2006. Characterization of the functional epitope on the urokinase receptor. Complete alanine scanning mutagenesis supplemented by chemical cross-linking. *J Biol Chem*. 281:19260-72.

Gardsvoll, H., and M. Ploug. 2007. Mapping of the vitronectin-binding site on the urokinase receptor: involvement of a coherent receptor interface consisting of residues from both domain I and the flanking interdomain linker region. *J Biol Chem*. 282:13561-72.

Gargiulo, L., I. Longanesi-Cattani, K. Bifulco, P. Franco, R. Raiola, P. Campiglia, P. Grieco, G. Peluso, M.P. Stoppelli, and M.V. Carriero. 2005. Cross-talk between fMLP and vitronectin receptors triggered by urokinase receptor-derived SRSRY peptide. *J Biol Chem*. 280:25225-32.

Garlanda, C., C. Parravicini, M. Sironi, M. De Rossi, R. Wainstok de Calmanovici, F. Carozzi, F. Bussolino, F. Colotta, A. Mantovani, and A. Vecchi. 1994. Progressive growth in immunodeficient mice and host cell recruitment by mouse endothelial cells transformed by polyoma middle-sized T antigen: implications for the pathogenesis of opportunistic vascular tumors. *Proc Natl Acad Sci U S A*. 91:7291-5.

Gladson, C.L., and D.A. Cheresh. 1991. Glioblastoma expression of vitronectin and the alpha v beta 3 integrin. Adhesion mechanism for transformed glial cells. *J Clin Invest*. 88:1924-32.

Gladson, C.L., J.N. Wilcox, L. Sanders, G.Y. Gillespie, and D.A. Cheresh. 1995. Cerebral microenvironment influences expression of the vitronectin gene in astrocytic tumors. *J Cell Sci*. 108 (Pt 3):947-56.

Graham, F.L., J. Smiley, W.C. Russell, and R. Nairn. 1977. Characteristics of a human cell line transformed by DNA from human adenovirus type 5. *J Gen Virol*. 36:59-74.

Grondahl-Hansen, J., H.A. Peters, W.L. van Putten, M.P. Look, H. Pappot, E. Ronne, K. Dano, J.G. Klijn, N. Brunner, and J.A. Foekens. 1995. Prognostic significance of the receptor for urokinase plasminogen activator in breast cancer. *Clin Cancer Res*. 1:1079-87.

Gutierrez, L.S., A. Schulman, T. Brito-Robinson, F. Noria, V.A. Ploplis, and F.J. Castellino. 2000. Tumor development is retarded in mice lacking the gene for urokinase-type plasminogen activator or its inhibitor, plasminogen activator inhibitor-1. *Cancer Res*. 60:5839-47.

Gyetko, M.R., E.A. Libre, J.A. Fuller, G.H. Chen, and G. Toews. 1999. Urokinase is required for T lymphocyte proliferation and activation in vitro. *J Lab Clin Med*. 133:274-88.

Gyetko, M.R., S. Sud, G.H. Chen, J.A. Fuller, S.W. Chensue, and G.B. Toews. 2002. Urokinase-type plasminogen activator is required for the generation of a type 1 immune response to pulmonary Cryptococcus neoformans infection. *J Immunol*. 168:801-9.

Gyetko, M.R., S. Sud, and S.W. Chensue. 2004. Urokinase-deficient mice fail to generate a type 2 immune response following schistosomal antigen challenge. *Infect Immun*. 72:461-7.

Gyetko, M.R., S. Sud, T. Kendall, J.A. Fuller, M.W. Newstead, and T.J. Standiford. 2000. Urokinase receptor-deficient mice have impaired neutrophil recruitment in

response to pulmonary Pseudomonas aeruginosa infection. *J Immunol*. 165:1513-9.

Gyetko, M.R., S. Sud, J. Sonstein, T. Polak, A. Sud, and J.L. Curtis. 2001. Antigen-driven lymphocyte recruitment to the lung is diminished in the absence of urokinase-type plasminogen activator (uPA) receptor, but is independent of uPA. *J Immunol*. 167:5539-42.

Gyetko, M.R., R.F. Todd, 3rd, C.C. Wilkinson, and R.G. Sitrin. 1994. The urokinase receptor is required for human monocyte chemotaxis in vitro. *J Clin Invest*. 93:1380-7.

Hayman, E.G., M.D. Pierschbacher, Y. Ohgren, and E. Ruoslahti. 1983. Serum spreading factor (vitronectin) is present at the cell surface and in tissues. *Proc Natl Acad Sci U S A*. 80:4003-7.

Hetland, G., H.B. Pettersen, T.E. Mollnes, and E. Johnson. 1989. S-protein is synthesized by human monocytes and macrophages in vitro. *Scand J Immunol*. 29:15-21.

Hildenbrand, R., M. Gandhari, P. Stroebel, A. Marx, H. Allgayer, and N. Arens. 2008. The urokinase-system--role of cell proliferation and apoptosis. *Histol Histopathol*. 23:227-36.

Holmes, R. 1967. Preparation from human serum of an alpha-one protein which induces the immediate growth of unadapted cells in vitro. *J Cell Biol*. 32:297-308.

Hoyer-Hansen, G., M. Ploug, N. Behrendt, E. Ronne, and K. Dano. 1997. Cell-surface acceleration of urokinase-catalyzed receptor cleavage. *Eur J Biochem*. 243:21-6.

Huai, Q., A.P. Mazar, A. Kuo, G.C. Parry, D.E. Shaw, J. Callahan, Y. Li, C. Yuan, C. Bian, L. Chen, B. Furie, B.C. Furie, D.B. Cines, and M. Huang. 2006. Structure of human urokinase plasminogen activator in complex with its receptor. *Science*. 311:656-9.

Huai, Q., A. Zhou, L. Lin, A.P. Mazar, G.C. Parry, J. Callahan, D.E. Shaw, B. Furie, B.C. Furie, and M. Huang. 2008. Crystal structures of two human vitronectin, urokinase and urokinase receptor complexes. *Nat Struct Mol Biol*. 15:422-3.

Hudson, M.A., and L.M. McReynolds. 1997. Urokinase and the urokinase receptor: association with in vitro invasiveness of human bladder cancer cell lines. *J Natl Cancer Inst*. 89:709-17.

Humphries, J.D., A. Byron, and M.J. Humphries. 2006. Integrin ligands at a glance. *J Cell Sci*. 119:3901-3.

Izumi, M., T. Shimo-Oka, N. Morishita, I. Ii, and M. Hayashi. 1988. Identification of the collagen-binding domain of vitronectin using monoclonal antibodies. *Cell Struct Funct*. 13:217-25.

Izumi, M., K.M. Yamada, and M. Hayashi. 1989. Vitronectin exists in two structurally and functionally distinct forms in human plasma. *Biochim Biophys Acta*. 990:101-8.

Jenne, D., A. Hille, K.K. Stanley, and W.B. Huttner. 1989. Sulfation of two tyrosine-residues in human complement S-protein (vitronectin). *Eur J Biochem*. 185:391-5.

Jenne, D., and K.K. Stanley. 1987. Nucleotide sequence and organization of the human S-protein gene: repeating peptide motifs in the "pexin" family and a model for their evolution. *Biochemistry*. 26:6735-42.

Jing, Y., C. Tong, J. Zhang, T. Nakamura, I. Iankov, S.J. Russell, and J.R. Merchan. 2009. Tumor and vascular targeting of a novel oncolytic measles virus retargeted against the urokinase receptor. *Cancer Res*. 69:1459-68.

Jo, M., S. Takimoto, V. Montel, and S.L. Gonias. 2009. The urokinase receptor promotes cancer metastasis independently of urokinase-type plasminogen activator in mice. *Am J Pathol*. 175:190-200.

Kirchheimer, J.C., J. Wojta, G. Christ, and B.R. Binder. 1989. Functional inhibition of endogenously produced urokinase decreases cell proliferation in a human melanoma cell line. *Proc Natl Acad Sci U S A*. 86:5424-8.

Kjoller, L., and A. Hall. 2001. Rac mediates cytoskeletal rearrangements and increased cell motility induced by urokinase-type plasminogen activator receptor binding to vitronectin. *J Cell Biol.* 152:1145-57.

Knudsen, B.S., and R.L. Nachman. 1988. Matrix plasminogen activator inhibitor. Modulation of the extracellular proteolytic environment. *J Biol Chem*. 263:9476-81.

Kobayashi, H., J. Gotoh, M. Fujie, H. Shinohara, N. Moniwa, and T. Terao. 1994. Inhibition of metastasis of Lewis lung carcinoma by a synthetic peptide within growth factor-like domain of urokinase in the experimental and spontaneous metastasis model. *Int J Cancer*. 57:727-33.

Kost, C., W. Stuber, H.J. Ehrlich, H. Pannekoek, and K.T. Preissner. 1992. Mapping of binding sites for heparin, plasminogen activator inhibitor-1, and plasminogen to vitronectin's heparin-binding region reveals a novel vitronectin-dependent feedback mechanism for the control of plasmin formation. *J Biol Chem*. 267:12098-105.

Kratzschmar, J., B. Haendler, S. Kojima, D.B. Rifkin, and W.D. Schleuning. 1993. Bovine urokinase-type plasminogen activator and its receptor: cloning and induction by retinoic acid. *Gene*. 125:177-83.

Kristensen, P., J. Eriksen, F. Blasi, and K. Dano. 1991. Two alternatively spliced mouse urokinase receptor mRNAs with different histological localization in the gastrointestinal tract. *J Cell Biol*. 115:1763-71.

Kruger, A., R. Soeltl, V. Lutz, O.G. Wilhelm, V. Magdolen, E.E. Rojo, P.A. Hantzopoulos, H. Graeff, B. Gansbacher, and M. Schmitt. 2000. Reduction of breast carcinoma tumor growth and lung colonization by overexpression of the soluble urokinase-type plasminogen activator receptor (CD87). *Cancer Gene Ther*. 7:292-9.

Kunigal, S., S.S. Lakka, C.S. Gondi, N. Estes, and J.S. Rao. 2007. RNAi-mediated downregulation of urokinase plasminogen activator receptor and matrix metalloprotease-9 in human breast cancer cells results in decreased tumor invasion, angiogenesis and growth. *Int J Cancer*. 121:2307-16.

Lakka, S.S., R. Rajagopal, M.K. Rajan, P.M. Mohan, Y. Adachi, D.H. Dinh, W.C. Olivero, M. Gujrati, F. Ali-Osman, J.A. Roth, W.K. Yung, A.P. Kyritsis, and J.S. Rao. 2001. Adenovirus-mediated antisense urokinase-type plasminogen activator receptor gene transfer reduces tumor cell invasion and metastasis in non-small cell lung cancer cell lines. *Clin Cancer Res*. 7:1087-93.

Lanza, F., G.L. Castoldi, B. Castagnari, R.F. Todd, 3rd, S. Moretti, S. Spisani, A. Latorraca, E. Focarile, M.G. Roberti, and S. Traniello. 1998. Expression and functional role of urokinase-type plasminogen activator receptor in normal and acute leukaemic cells. *Br J Haematol*. 103:110-23.

Li, H., H. Lu, F. Griscelli, P. Opolon, L.Q. Sun, T. Ragot, Y. Legrand, D. Belin, J. Soria, C. Soria, M. Perricaudet, and P. Yeh. 1998. Adenovirus-mediated delivery of a uPA/uPAR antagonist suppresses angiogenesis-dependent tumor growth and dissemination in mice. *Gene Ther*. 5:1105-13.

Liang, O.D., S. Rosenblatt, G.S. Chhatwal, and K.T. Preissner. 1997. Identification of novel heparin-binding domains of vitronectin. *FEBS Lett*. 407:169-72.

Limongi, P., M. Resnati, L. Hernandez-Marrero, O. Cremona, F. Blasi, and F. Fazioli. 1995. Biosynthesis and apical localization of the urokinase receptor in polarized MDCK epithelial cells. *FEBS Lett*. 369:207-11.

Lin, L., H. Gardsvoll, Q. Huai, M. Huang, and M. Ploug. 2010. Structure-based engineering of species selectivity in the interaction between urokinase and its receptor: implication for preclinical cancer therapy. *J Biol Chem*. 285:10982-92.

Liotta, L.A., and E.C. Kohn. 2001. The microenvironment of the tumour-host interface. *Nature*. 411:375-9.

Liu, S., T.H. Bugge, and S.H. Leppla. 2001. Targeting of tumor cells by cell surface urokinase plasminogen activator-dependent anthrax toxin. *J Biol Chem*. 276:17976-84.

Liu, S., V. Redeye, J.G. Kuremsky, M. Kuhnen, A. Molinolo, T.H. Bugge, and S.H. Leppla. 2005. Intermolecular complementation achieves high-specificity tumor targeting by anthrax toxin. *Nat Biotechnol*. 23:725-30.

Llinas, P., M.H. Le Du, H. Gardsvoll, K. Dano, M. Ploug, B. Gilquin, E.A. Stura, and A. Menez. 2005. Crystal structure of the human urokinase plasminogen activator receptor bound to an antagonist peptide. *EMBO J*. 24:1655-63.

Loridon-Rosa, B., P. Vielh, C. Cuadrado, and P. Burtin. 1988. Comparative distribution of fibronectin and vitronectin in human breast and colon carcinomas. An immunofluorescence study. *Am J Clin Pathol*. 90:7-16.

Lund, L.R., V. Ellis, E. Ronne, C. Pyke, and K. Dano. 1995. Transcriptional and post-transcriptional regulation of the receptor for urokinase-type plasminogen activator by cytokines and tumour promoters in the human lung carcinoma cell line A549. *Biochem J*. 310 (Pt 1):345-52.

Lund, L.R., J. Romer, E. Ronne, V. Ellis, F. Blasi, and K. Dano. 1991a. Urokinase-receptor biosynthesis, mRNA level and gene transcription are increased by transforming growth factor beta 1 in human A549 lung carcinoma cells. *EMBO J*. 10:3399-407.

Lund, L.R., E. Ronne, A.L. Roldan, N. Behrendt, J. Romer, F. Blasi, and K. Dano. 1991b. Urokinase receptor mRNA level and gene transcription are strongly and rapidly increased by phorbol myristate acetate in human monocyte-like U937 cells. *J Biol Chem*. 266:5177-81.

Luo, B.H., T.A. Springer, and J. Takagi. 2003. Stabilizing the open conformation of the integrin headpiece with a glycan wedge increases affinity for ligand. *Proc Natl Acad Sci U S A*. 100:2403-8.

Lyons, R.M., L.E. Gentry, A.F. Purchio, and H.L. Moses. 1990. Mechanism of activation of latent recombinant transforming growth factor beta 1 by plasmin. *J Cell Biol*. 110:1361-7.

Madsen, C.D., G.M. Ferraris, A. Andolfo, O. Cunningham, and N. Sidenius. 2007. uPAR-induced cell adhesion and migration: vitronectin provides the key. *J Cell Biol*. 177:927-39.

Maenpaa, A., P.E. Kovanen, A. Paetau, J. Jaaskelainen, and T. Timonen. 1997. Lymphocyte adhesion molecule ligands and extracellular matrix proteins in gliomas and normal brain: expression of VCAM-1 in gliomas. *Acta Neuropathol*. 94:216-25.

Mantovani, A., and M.A. Pierotti. 2008. Cancer and inflammation: a complex relationship. *Cancer Lett*. 267:180-1.

May, A.E., S.M. Kanse, L.R. Lund, R.H. Gisler, B.A. Imhof, and K.T. Preissner. 1998. Urokinase receptor (CD87) regulates leukocyte recruitment via beta 2 integrins in vivo. *J Exp Med*. 188:1029-37.

Miles, L.A., and E.F. Plow. 1987. Receptor mediated binding of the fibrinolytic components, plasminogen and urokinase, to peripheral blood cells. *Thromb Haemost*. 58:936-42.

Min, H.Y., L.V. Doyle, C.R. Vitt, C.L. Zandonella, J.R. Stratton-Thomas, M.A. Shuman, and S. Rosenberg. 1996. Urokinase receptor antagonists inhibit angiogenesis and primary tumor growth in syngeneic mice. *Cancer Res*. 56:2428-33.

Moller, L.B., M. Ploug, and F. Blasi. 1992. Structural requirements for glycosyl-phosphatidylinositol-anchor attachment in the cellular receptor for urokinase plasminogen activator. *Eur J Biochem*. 208:493-500.

Morita, S., A. Sato, H. Hayakawa, H. Ihara, T. Urano, Y. Takada, and A. Takada. 1998. Cancer cells overexpress mRNA of urokinase-type plasminogen activator, its receptor and inhibitors in human non-small-cell lung cancer tissue: analysis by Northern blotting and in situ hybridization. *Int J Cancer*. 78:286-92.

Mustjoki, S., R. Alitalo, R.W. Stephens, and A. Vaheri. 1999. Plasminogen activation in human leukemia and in normal hematopoietic cells. *APMIS*. 107:144-9.

Naldini, L., L. Tamagnone, E. Vigna, M. Sachs, G. Hartmann, W. Birchmeier, Y. Daikuhara, H. Tsubouchi, F. Blasi, and P.M. Comoglio. 1992. Extracellular proteolytic cleavage by urokinase is required for activation of hepatocyte growth factor/scatter factor. *EMBO J*. 11:4825-33.

Niculescu, F., H.G. Rus, D. Porutiu, V. Ghiurca, and R. Vlaicu. 1989. Immunoelectron-microscopic localization of S-protein/vitronectin in human atherosclerotic wall. *Atherosclerosis*. 78:197-203.

Nielsen, B.S., F. Rank, M. Illemann, L.R. Lund, and K. Dano. 2007. Stromal cells associated with early invasive foci in human mammary ductal carcinoma in situ coexpress urokinase and urokinase receptor. *Int J Cancer*. 120:2086-95.

Nielsen, B.S., M. Sehested, S. Duun, F. Rank, S. Timshel, J. Rygaard, M. Johnsen, and K. Dano. 2001. Urokinase plasminogen activator is localized in stromal cells in ductal breast cancer. *Lab Invest*. 81:1485-501.

Nielsen, L.S., G.M. Kellerman, N. Behrendt, R. Picone, K. Dano, and F. Blasi. 1988. A 55,000-60,000 Mr receptor protein for urokinase-type plasminogen activator. Identification in human tumor cell lines and partial purification. *J Biol Chem*. 263:2358-63.

Niiya, K., T. Ozawa, T. Tsuzawa, S. Ueshima, O. Matsuo, and N. Sakuragawa. 1998. Transcriptional regulation of urokinase-type plasminogen activator receptor by

cyclic AMP in PL-21 human myeloid leukemia cells: comparison with the regulation by phorbol myristate acetate. *Thromb Haemost*. 79:574-8.

Nip, J., H. Shibata, D.J. Loskutoff, D.A. Cheresh, and P. Brodt. 1992. Human melanoma cells derived from lymphatic metastases use integrin alpha v beta 3 to adhere to lymph node vitronectin. *J Clin Invest*. 90:1406-13.

Nykjaer, A., M. Conese, E.I. Christensen, D. Olson, O. Cremona, J. Gliemann, and F. Blasi. 1997. Recycling of the urokinase receptor upon internalization of the uPA:serpin complexes. *EMBO J*. 16:2610-20.

Nykjaer, A., B. Moller, R.F. Todd, 3rd, T. Christensen, P.A. Andreasen, J. Gliemann, and C.M. Petersen. 1994. Urokinase receptor. An activation antigen in human T lymphocytes. *J Immunol*. 152:505-16.

Nykjaer, A., C.M. Petersen, E.I. Christensen, O. Davidsen, and J. Gliemann. 1990. Urokinase receptors in human monocytes. *Biochim Biophys Acta*. 1052:399-407.

Nykjaer, A., C.M. Petersen, B. Moller, P.A. Andreasen, and J. Gliemann. 1992. Identification and characterization of urokinase receptors in natural killer cells and T-cell-derived lymphokine activated killer cells. *FEBS Lett*. 300:13-7.

Okada, S.S., M.A. Golden, P.N. Raghunath, J.E. Tomaszewski, M.L. David, A. Kuo, K. Kariko, and E.S. Barnathan. 1998. Native atherosclerosis and vein graft arterialization: association with increased urokinase receptor expression in vitro and in vivo. *Thromb Haemost*. 80:140-7.

Olson, D., J. Pollanen, G. Hoyer-Hansen, E. Ronne, K. Sakaguchi, T.C. Wun, E. Appella, K. Dano, and F. Blasi. 1992. Internalization of the urokinase-plasminogen activator inhibitor type-1 complex is mediated by the urokinase receptor. *J Biol Chem*. 267:9129-33.

Ossowski, L., and E. Reich. 1983. Antibodies to plasminogen activator inhibit human tumor metastasis. *Cell*. 35:611-9.

Pedersen, H., N. Brunner, D. Francis, K. Osterlind, E. Ronne, H.H. Hansen, K. Dano, and J. Grondahl-Hansen. 1994. Prognostic impact of urokinase, urokinase receptor, and type 1 plasminogen activator inhibitor in squamous and large cell lung cancer tissue. *Cancer Res*. 54:4671-5.

Pedersen, N., M. Schmitt, E. Ronne, M.I. Nicoletti, G. Hoyer-Hansen, M. Conese, R. Giavazzi, K. Dano, W. Kuhn, F. Janicke, and et al. 1993. A ligand-free, soluble urokinase receptor is present in the ascitic fluid from patients with ovarian cancer. *J Clin Invest*. 92:2160-7.

Pepper, M.S., A.P. Sappino, R. Stocklin, R. Montesano, L. Orci, and J.D. Vassalli. 1993. Upregulation of urokinase receptor expression on migrating endothelial cells. *J Cell Biol*. 122:673-84.

Picone, R., E.L. Kajtaniak, L.S. Nielsen, N. Behrendt, M.R. Mastronicola, M.V. Cubellis, M.P. Stoppelli, S. Pedersen, K. Dano, and F. Blasi. 1989. Regulation of urokinase receptors in monocytelike U937 cells by phorbol ester phorbol myristate acetate. *J Cell Biol*. 108:693-702.

Pierleoni, C., G.B. Samuelsen, N. Graem, E. Ronne, B.S. Nielsen, P. Kaufmann, and M. Castellucci. 1998. Immunohistochemical identification of the receptor for urokinase plasminogen activator associated with fibrin deposition in normal and ectopic human placenta. *Placenta*. 19:501-8.

Plesner, T., N. Behrendt, and M. Ploug. 1997. Structure, function and expression on blood and bone marrow cells of the urokinase-type plasminogen activator receptor, uPAR. *Stem Cells*. 15:398-408.

Plesner, T., M. Ploug, V. Ellis, E. Ronne, G. Hoyer-Hansen, M. Wittrup, T.L. Pedersen, T. Tscherning, K. Dano, and N.E. Hansen. 1994a. The receptor for urokinase-type plasminogen activator and urokinase is translocated from two distinct intracellular compartments to the plasma membrane on stimulation of human neutrophils. *Blood*. 83:808-15.

Plesner, T., E. Ralfkiaer, M. Wittrup, H. Johnsen, C. Pyke, T.L. Pedersen, N.E. Hansen, and K. Dano. 1994b. Expression of the receptor for urokinase-type plasminogen activator in normal and neoplastic blood cells and hematopoietic tissue. *Am J Clin Pathol*. 102:835-41.

Ploug, M., and V. Ellis. 1994. Structure-function relationships in the receptor for urokinase-type plasminogen activator. Comparison to other members of the Ly-6 family and snake venom alpha-neurotoxins. *FEBS Lett*. 349:163-8.

Ploug, M., V. Ellis, and K. Dano. 1994. Ligand interaction between urokinase-type plasminogen activator and its receptor probed with 8-anilino-1-naphthalenesulfonate. Evidence for a hydrophobic binding site exposed only on the intact receptor. *Biochemistry*. 33:8991-7.

Ploug, M., S. Ostergaard, H. Gardsvoll, K. Kovalski, C. Holst-Hansen, A. Holm, L. Ossowski, and K. Dano. 2001. Peptide-derived antagonists of the urokinase receptor. affinity maturation by combinatorial chemistry, identification of functional epitopes, and inhibitory effect on cancer cell intravasation. *Biochemistry*. 40:12157-68.

Ploug, M., H. Rahbek-Nielsen, P.F. Nielsen, P. Roepstorff, and K. Dano. 1998. Glycosylation profile of a recombinant urokinase-type plasminogen activator receptor expressed in Chinese hamster ovary cells. *J Biol Chem*. 273:13933-43.

Ploug, M., E. Ronne, N. Behrendt, A.L. Jensen, F. Blasi, and K. Dano. 1991. Cellular receptor for urokinase plasminogen activator. Carboxyl-terminal processing and membrane anchoring by glycosyl-phosphatidylinositol. *J Biol Chem*. 266:1926-33.

Preissner, K.T. 1991. Structure and biological role of vitronectin. *Annu Rev Cell Biol*. 7:275-310.

Preissner, K.T., S. Holzhuter, C. Justus, and G. Muller-Berghaus. 1989. Identification of and partial characterization of platelet vitronectin: evidence for complex formation with platelet-derived plasminogen activator inhibitor-1. *Blood*. 74:1989-96.

Preissner, K.T., and D. Seiffert. 1998. Role of vitronectin and its receptors in haemostasis and vascular remodeling. *Thromb Res*. 89:1-21.

Preissner, K.T., R. Wassmuth, and G. Muller-Berghaus. 1985. Physicochemical characterization of human S-protein and its function in the blood coagulation system. *Biochem J*. 231:349-55.

Pyke, C., N. Graem, E. Ralfkiaer, E. Ronne, G. Hoyer-Hansen, N. Brunner, and K. Dano. 1993. Receptor for urokinase is present in tumor-associated macrophages in ductal breast carcinoma. *Cancer Res*. 53:1911-5.

Pyke, C., P. Kristensen, E. Ralfkiaer, J. Grondahl-Hansen, J. Eriksen, F. Blasi, and K. Dano. 1991. Urokinase-type plasminogen activator is expressed in stromal cells and its receptor in cancer cells at invasive foci in human colon adenocarcinomas. *Am J Pathol*. 138:1059-67.

Rabbani, S.A., and J. Gladu. 2002. Urokinase receptor antibody can reduce tumor volume and detect the presence of occult tumor metastases in vivo. *Cancer Res*. 62:2390-7.

Rabbani, S.A., J. Gladu, A.P. Mazar, J. Henkin, and D. Goltzman. 1997. Induction in human osteoblastic cells (SaOS2) of the early response genes fos, jun, and myc by the amino terminal fragment (ATF) of urokinase. *J Cell Physiol*. 172:137-45.

Rabbani, S.A., N. Rajwans, A. Achbarou, K.K. Murthy, and D. Goltzman. 1994. Isolation and characterization of multiple isoforms of the rat urokinase receptor in osteoblasts. *FEBS Lett*. 338:69-74.

Ramirez, F., and D.B. Rifkin. 2003. Cell signaling events: a view from the matrix. *Matrix Biol*. 22:101-7.

Reilly, J.T., and J.R. Nash. 1988. Vitronectin (serum spreading factor): its localisation in normal and fibrotic tissue. *J Clin Pathol*. 41:1269-72.

Remacle-Bonnet, M.M., F.L. Garrouste, and G.J. Pommier. 1997. Surface-bound plasmin induces selective proteolysis of insulin-like-growth-factor (IGF)-binding protein-4 (IGFBP-4) and promotes autocrine IGF-II bio-availability in human colon-carcinoma cells. *Int J Cancer*. 72:835-43.

Reuning, U., S.P. Little, E.P. Dixon, E.M. Johnstone, and N.U. Bang. 1993. Molecular cloning of cDNA for the bovine urokinase-type plasminogen activator receptor. *Thromb Res*. 72:59-70.

Ribatti, D., D. Leali, A. Vacca, R. Giuliani, A. Gualandris, L. Roncali, M.L. Nolli, and M. Presta. 1999. In vivo angiogenic activity of urokinase: role of endogenous fibroblast growth factor-2. *J Cell Sci*. 112 (Pt 23):4213-21.

Riittinen, L., P. Limongi, M.P. Crippa, M. Conese, L. Hernandez-Marrero, F. Fazioli, and F. Blasi. 1996. Removal of domain D2 or D3 of the human urokinase receptor does not affect ligand affinity. *FEBS Lett*. 381:1-6.

Rijneveld, A.W., S. Florquin, P. Bresser, M. Levi, V. De Waard, R. Lijnen, J.S. Van Der Zee, P. Speelman, P. Carmeliet, and T. Van Der Poll. 2003. Plasminogen activator inhibitor type-1 deficiency does not influence the outcome of murine pneumococcal pneumonia. *Blood*. 102:934-9.

Rijneveld, A.W., M. Levi, S. Florquin, P. Speelman, P. Carmeliet, and T. van Der Poll. 2002. Urokinase receptor is necessary for adequate host defense against pneumococcal pneumonia. *J Immunol*. 168:3507-11.

Roldan, A.L., M.V. Cubellis, M.T. Masucci, N. Behrendt, L.R. Lund, K. Dano, E. Appella, and F. Blasi. 1990. Cloning and expression of the receptor for human urokinase plasminogen activator, a central molecule in cell surface, plasmin dependent proteolysis. *EMBO J*. 9:467-74.

Romer, J., L.R. Lund, J. Eriksen, C. Pyke, P. Kristensen, and K. Dano. 1994. The receptor for urokinase-type plasminogen activator is expressed by keratinocytes at the leading edge during re-epithelialization of mouse skin wounds. *J Invest Dermatol*. 102:519-22.

Romer, J., L.R. Lund, J. Eriksen, E. Ralfkiaer, R. Zeheb, T.D. Gelehrter, K. Dano, and P. Kristensen. 1991. Differential expression of urokinase-type plasminogen activator and its type-1 inhibitor during healing of mouse skin wounds. *J Invest Dermatol*. 97:803-11.

Sahai, E., and C.J. Marshall. 2003. Differing modes of tumour cell invasion have distinct requirements for Rho/ROCK signalling and extracellular proteolysis. *Nat Cell Biol*. 5:711-9.

Saksela, O., and D.B. Rifkin. 1990. Release of basic fibroblast growth factor-heparan sulfate complexes from endothelial cells by plasminogen activator-mediated proteolytic activity. *J Cell Biol*. 110:767-75.

Sano, K., K. Asanuma-Date, F. Arisaka, S. Hattori, and H. Ogawa. 2007. Changes in glycosylation of vitronectin modulate multimerization and collagen binding during liver regeneration. *Glycobiology*. 17:784-94.

Schewe, D.M., J.H. Leupold, D.D. Boyd, E.R. Lengyel, H. Wang, K.U. Gruetzner, F.W. Schildberg, K.W. Jauch, and H. Allgayer. 2003. Tumor-specific transcription factor binding to an activator protein-2/Sp1 element of the urokinase-type plasminogen activator receptor promoter in a first large series of resected gastrointestinal cancers. *Clin Cancer Res*. 9:2267-76.

Schroeck, F., N. Arroyo de Prada, S. Sperl, M. Schmitt, and M. Viktor. 2002. Interaction of plasminogen activator inhibitor type-1 (PAI-1) with vitronectin (Vn): mapping the binding sites on PAI-1 and Vn. *Biol Chem*. 383:1143-9.

Schvartz, I., T. Kreizman, V. Brumfeld, Z. Gechtman, D. Seger, and S. Shaltiel. 2002. The PKA phosphorylation of vitronectin: effect on conformation and function. *Arch Biochem Biophys*. 397:246-52.

Schvartz, I., D. Seger, and S. Shaltiel. 1999. Vitronectin. *Int J Biochem Cell Biol*. 31:539-44.

Seger, D., Z. Gechtman, and S. Shaltiel. 1998. Phosphorylation of vitronectin by casein kinase II. Identification of the sites and their promotion of cell adhesion and spreading. *J Biol Chem*. 273:24805-13.

Seger, D., R. Seger, and S. Shaltiel. 2001. The CK2 phosphorylation of vitronectin. Promotion of cell adhesion via the alpha(v)beta 3-phosphatidylinositol 3-kinase pathway. *J Biol Chem*. 276:16998-7006.

Seiffert, D. 1997. Constitutive and regulated expression of vitronectin. *Histol Histopathol*. 12:787-97.

Seiffert, D., and D.J. Loskutoff. 1991. Evidence that type 1 plasminogen activator inhibitor binds to the somatomedin B domain of vitronectin. *J Biol Chem*. 266:2824-30.

Seiffert, D., and D.J. Loskutoff. 1996. Type 1 plasminogen activator inhibitor induces multimerization of plasma vitronectin. A suggested mechanism for the generation of the tissue form of vitronectin in vivo. *J Biol Chem*. 271:29644-51.

Seiffert, D., and R.R. Schleef. 1996. Two functionally distinct pools of vitronectin (Vn) in the blood circulation: identification of a heparin-binding competent population of Vn within platelet alpha-granules. *Blood*. 88:552-60.

Shetty, S., and S. Idell. 1998a. A urokinase receptor mRNA binding protein from rabbit lung fibroblasts and mesothelial cells. *Am J Physiol*. 274:L871-82.

Shetty, S., and S. Idell. 1998b. A urokinase receptor mRNA binding protein-mRNA interaction regulates receptor expression and function in human pleural mesothelioma cells. *Arch Biochem Biophys*. 356:265-79.

Shetty, S., A. Kumar, and S. Idell. 1997. Posttranscriptional regulation of urokinase receptor mRNA: identification of a novel urokinase receptor mRNA binding protein in human mesothelioma cells. *Mol Cell Biol*. 17:1075-83.

Shetty, S., H. Muniyappa, P.K. Halady, and S. Idell. 2004. Regulation of urokinase receptor expression by phosphoglycerate kinase. *Am J Respir Cell Mol Biol*. 31:100-6.

Sidenius, N., A. Andolfo, R. Fesce, and F. Blasi. 2002. Urokinase regulates vitronectin binding by controlling urokinase receptor oligomerization. *J Biol Chem*. 277:27982-90.

Sidenius, N., and F. Blasi. 2000. Domain 1 of the urokinase receptor (uPAR) is required for uPAR-mediated cell binding to vitronectin. *FEBS Lett*. 470:40-6.

Sidenius, N., and F. Blasi. 2003. The urokinase plasminogen activator system in cancer: recent advances and implication for prognosis and therapy. *Cancer Metastasis Rev*. 22:205-22.

Smith, H.W., P. Marra, and C.J. Marshall. 2008. uPAR promotes formation of the p130Cas-Crk complex to activate Rac through DOCK180. *J Cell Biol*. 182:777-90.

Smith, H.W., and C.J. Marshall. 2009. Regulation of cell signalling by uPAR. *Nat Rev Mol Cell Biol*. 11:23-36.

Solberg, H., M. Ploug, G. Hoyer-Hansen, B.S. Nielsen, and L.R. Lund. 2001. The murine receptor for urokinase-type plasminogen activator is primarily expressed in tissues actively undergoing remodeling. *J Histochem Cytochem*. 49:237-46.

Sperl, S., M.M. Mueller, O.G. Wilhelm, M. Schmitt, V. Magdolen, and L. Moroder. 2001. The uPA/uPA receptor system as a target for tumor therapy. *Drug News Perspect*. 14:401-11.

Speth, C., I. Pichler, G. Stockl, M. Mair, and M.P. Dierich. 1998. Urokinase plasminogen activator receptor (uPAR; CD87) expression on monocytic cells and T cells is modulated by HIV-1 infection. *Immunobiology*. 199:152-62.

Stefansson, S., E.J. Su, S. Ishigami, J.M. Cale, Y. Gao, N. Gorlatova, and D.A. Lawrence. 2007. The contributions of integrin affinity and integrin-cytoskeletal engagement in endothelial and smooth muscle cell adhesion to vitronectin. *J Biol Chem*. 282:15679-89.

Stephens, R.W., H.J. Nielsen, I.J. Christensen, O. Thorlacius-Ussing, S. Sorensen, K. Dano, and N. Brunner. 1999. Plasma urokinase receptor levels in patients with colorectal cancer: relationship to prognosis. *J Natl Cancer Inst*. 91:869-74.

Stockmann, A., S. Hess, P. Declerck, R. Timpl, and K.T. Preissner. 1993. Multimeric vitronectin. Identification and characterization of conformation-dependent self-association of the adhesive protein. *J Biol Chem*. 268:22874-82.

Stonehouse, T.J., V.E. Woodhead, P.S. Herridge, H. Ashrafian, M. George, B.M. Chain, and D.R. Katz. 1999. Molecular characterization of U937-dependent T-cell co-stimulation. *Immunology*. 96:35-47.

Taniguchi, T., A.K. Kakkar, E.G. Tuddenham, R.C. Williamson, and N.R. Lemoine. 1998. Enhanced expression of urokinase receptor induced through the tissue factor-factor VIIa pathway in human pancreatic cancer. *Cancer Res*. 58:4461-7.

Thiagarajan, P., and K.L. Kelly. 1988. Exposure of binding sites for vitronectin on platelets following stimulation. *J Biol Chem*. 263:3035-8.

Tjwa, M., N. Sidenius, R. Moura, S. Jansen, K. Theunissen, A. Andolfo, M. De Mol, M. Dewerchin, L. Moons, F. Blasi, C. Verfaillie, and P. Carmeliet. 2009. Membrane-anchored uPAR regulates the proliferation, marrow pool size, engraftment, and mobilization of mouse hematopoietic stem/progenitor cells. *J Clin Invest*. 119:1008-18.

Tomasini-Johansson, B.R., J. Milbrink, and G. Pejler. 1998. Vitronectin expression in rheumatoid arthritic synovia--inhibition of plasmin generation by vitronectin produced in vitro. *Br J Rheumatol*. 37:620-9.

Usher, P.A., O.F. Thomsen, P. Iversen, M. Johnsen, N. Brunner, G. Hoyer-Hansen, P. Andreasen, K. Dano, and B.S. Nielsen. 2005. Expression of urokinase plasminogen activator, its receptor and type-1 inhibitor in malignant and benign prostate tissue. *Int J Cancer*. 113:870-80.

Vaday, G.G., and O. Lider. 2000. Extracellular matrix moieties, cytokines, and enzymes: dynamic effects on immune cell behavior and inflammation. *J Leukoc Biol*. 67:149-59.

Vassalli, J.D., A.P. Sappino, and D. Belin. 1991. The plasminogen activator/plasmin system. *J Clin Invest*. 88:1067-72.

Walker, D.G., L.F. Lue, and T.G. Beach. 2002. Increased expression of the urokinase plasminogen-activator receptor in amyloid beta peptide-treated human brain microglia and in AD brains. *Brain Res*. 926:69-79.

Wang, G.J., M. Collinge, F. Blasi, R. Pardi, and J.R. Bender. 1998. Posttranscriptional regulation of urokinase plasminogen activator receptor messenger RNA levels by leukocyte integrin engagement. *Proc Natl Acad Sci U S A*. 95:6296-301.

Wang, H., J. Hicks, P. Khanbolooki, S.J. Kim, C. Yan, Y. Wang, and D. Boyd. 2003. Transgenic mice demonstrate novel promoter regions for tissue-specific expression of the urokinase receptor gene. *Am J Pathol*. 163:453-64.

Wang, Y. 2001. The role and regulation of urokinase-type plasminogen activator receptor gene expression in cancer invasion and metastasis. *Med Res Rev*. 21:146-70.

Wang, Y., J. Dang, L.K. Johnson, J.J. Selhamer, and W.F. Doe. 1995. Structure of the human urokinase receptor gene and its similarity to CD59 and the Ly-6 family. *Eur J Biochem*. 227:116-22.

Wang, Y., C.J. Jones, J. Dang, X. Liang, J.E. Olsen, and W.F. Doe. 1994. Human urokinase receptor expression is inhibited by amiloride and induced by tumor necrosis factor and phorbol ester in colon cancer cells. *FEBS Lett*. 353:138-42.

Wang, Y., X. Liang, S. Wu, G.A. Murrell, and W.F. Doe. 2001. Inhibition of colon cancer metastasis by a 3'- end antisense urokinase receptor mRNA in a nude mouse model. *Int J Cancer*. 92:257-62.

Wei, C., C.C. Moller, M.M. Altintas, J. Li, K. Schwarz, S. Zacchigna, L. Xie, A. Henger, H. Schmid, M.P. Rastaldi, P. Cowan, M. Kretzler, R. Parrilla, M. Bendayan, V. Gupta, B. Nikolic, R. Kalluri, P. Carmeliet, P. Mundel, and J. Reiser. 2008. Modification of kidney barrier function by the urokinase receptor. *Nat Med*. 14:55-63.

Wei, Y., R.P. Czekay, L. Robillard, M.C. Kugler, F. Zhang, K.K. Kim, J.P. Xiong, M.J. Humphries, and H.A. Chapman. 2005. Regulation of alpha5beta1 integrin conformation and function by urokinase receptor binding. *J Cell Biol*. 168:501-11.

Wei, Y., M. Lukashev, D.I. Simon, S.C. Bodary, S. Rosenberg, M.V. Doyle, and H.A. Chapman. 1996. Regulation of integrin function by the urokinase receptor. *Science*. 273:1551-5.

Wei, Y., D.A. Waltz, N. Rao, R.J. Drummond, S. Rosenberg, and H.A. Chapman. 1994. Identification of the urokinase receptor as an adhesion receptor for vitronectin. *J Biol Chem*. 269:32380-8.

Wilhelm, O.G., S. Wilhelm, G.M. Escott, V. Lutz, V. Magdolen, M. Schmitt, D.B. Rifkin, E.L. Wilson, H. Graeff, and G. Brunner. 1999. Cellular glycosylphosphatidylinositol-specific phospholipase D regulates urokinase receptor shedding and cell surface expression. *J Cell Physiol*. 180:225-35.

Wohn, K.D., S.M. Kanse, V. Deutsch, T. Schmidt, A. Eldor, and K.T. Preissner. 1997. The urokinase-receptor (CD87) is expressed in cells of the megakaryoblastic lineage. *Thromb Haemost*. 77:540-7.

Wolf, K., I. Mazo, H. Leung, K. Engelke, U.H. von Andrian, E.I. Deryugina, A.Y. Strongin, E.B. Brocker, and P. Friedl. 2003. Compensation mechanism in tumor cell migration: mesenchymal-amoeboid transition after blocking of pericellular proteolysis. *J Cell Biol*. 160:267-77.

Woodhead, V.E., T.J. Stonehouse, M.H. Binks, K. Speidel, D.A. Fox, A. Gaya, D. Hardie, A.J. Henniker, V. Horejsi, K. Sagawa, K.M. Skubitz, H. Taskov, R.F. Todd, 3rd, A. van Agthoven, D.R. Katz, and B.M. Chain. 2000. Novel molecular mechanisms of dendritic cell-induced T cell activation. *Int Immunol*. 12:1051-61.

Yamamoto, M., R. Sawaya, S. Mohanam, A.K. Bindal, J.M. Bruner, K. Oka, V.H. Rao, M. Tomonaga, G.L. Nicolson, and J.S. Rao. 1994. Expression and localization of urokinase-type plasminogen activator in human astrocytomas in vivo. *Cancer Res*. 54:3656-61.

Yanamandra, N., S.D. Konduri, S. Mohanam, D.H. Dinh, W.C. Olivero, M. Gujrati, G.L. Nicolson, M. Obeyeseke, and J.S. Rao. 2000. Downregulation of urokinase-type plasminogen activator receptor (uPAR) induces caspase-mediated cell death in human glioblastoma cells. *Clin Exp Metastasis*. 18:611-5.

Zheng, X., T.L. Saunders, S.A. Camper, L.C. Samuelson, and D. Ginsburg. 1995. Vitronectin is not essential for normal mammalian development and fertility. *Proc Natl Acad Sci U S A*. 92:12426-30.

Zhou, A., J.A. Huntington, N.S. Pannu, R.W. Carrell, and R.J. Read. 2003. How vitronectin binds PAI-1 to modulate fibrinolysis and cell migration. *Nat Struct Biol*. 10:541-4.

Zhu, F., S. Jia, G. Xing, L. Gao, L. Zhang, and F. He. 2001. cDNA transfection of amino-terminal fragment of urokinase efficiently inhibits cancer cell invasion and metastasis. *DNA Cell Biol*. 20:297-305.

Appendix A

Oligonucleotides used for cloning (5′-3′)

mupKpn:
gaagatctcggtaccgatctcaatatgggactcccaaggc

muPARre:
atatagtttagcggccgcatcaggtccagaggagga

mD1rev:
gccctgagggaaagcacggccgccctgggaggctgggacacaggtagt

mD1:
tgtgtcccagcctcccagggcggccgtgctttccctcagggccgtta

VN(1-66)u:
cggggtaccatggcacccctgagacccctttctcatactggccctgctggcatgggttgc
tctggctgaccaagagtcatgcaagggc

VN(1-66)d:
ccg ctc gag gtt ttt ctc ctc

FcU:
ggctcgagcccaaatcttgtgacaaaact

FcD:
tatagcggccgctcatttacccggagacaggga

Mouse uPAR mutant oligos (5′-3′)

W32A mutant:
FW : accgtgcttcgggaagcgcaagatgatagagag
RV : ctctctatcatcttgcgcttcccgaagcacggt

R58A mutant:
FW: aggaccatgagttacgccatgggctccatgatc
RV: gatcatggagcccatggcgtaactcatggtcct

R58E mutant:
FW: aggaccatgagttacgagatgggctccatgatc
RV: gatcatggagcccatctcgtaactcatggtcct

I63A mutant:
FW: cgcatgggctccatggccatcagcctgacagag
RV: ctctgtcaggctgatggccatggagcccatgcg

R92A mutant:
FW: gctttccctcagggcgcttacctcgagtgtgcg
RV: cgcacactcgaggtaagcgccctgagggaaagc

A284Stop:
FW: gggggcgccccctgttcagctgttacagccgct
RV: agcggctgtaacagctgaacaggggcgccccc

Acknowledgments

Special thanks goes to my group, to whom I shared good and hard times.

I would like to express all my gratitude to my boss, Nicolai Sidenius, who helped me to come out from a difficult family moment and to find in the lab a second home. You thought me to think with my brain, be creative and to express my ideas. This helped me to learn from my own mistakes and to set up the right experiments. You were always open to scientific and non-scientific discussion. That's a wonderful quality. I hope that I will get the possibility to work with you again in the future.

I am thankful to Gianmaria Sarra Ferraris for the amazing scientific discussions, but moreover for the many laughs and the funny gossip news I would have never discovered by myself. He is a great scientist, always ready to help you when you need it and always enthusiastic to make new experiments. It's been a pleasure to work with you in the lab.

Thanks to Carsten Schulte, who joined the group few years ago. He brought in the lab the Crazy Santa and the German Carnival, beer included. How can I thank you!

A special thanks goes to Annapaola Andolfo, who was always helpful and nice despite the many things she had to do. Thanks a lot!

Thanks to Chris Madsen. He is the crazy man with smart ideas that every lab must have. Always smiling, always ready for new exciting experiments and scientific discussion. We have missed you!

I would particularly like to express great gratitude to Francesco Blasi, a great scientist. He is really a nice and easygoing person; always happy and open to people of the lab. But more importantly he was helpful when I needed his advice. I really thank you!

A great thanks goes to my external supervisor, Thomas Bugge. Thank you for all advises and for always being helpful whenever I asked you for help. You are great!

I thank people of Lab F, especially Federica Alberghini, Federica, Zanardi, Gabriele Varano (the fined guy), Luis Fernandez Diaz, Elena Longobardi, Giorgio Iotti, Dima (our special and always welcome guest), and the undergraduate students Sara Girasoli, Chiara Quattri and Lara Sicouri for making the lab the most enjoyable place, for all the scientific and non-scientific discussions, laughter and fun.

A thank goes to my dear friends at the campus, especially Giovanni d'Ario, Marco Bonù, with whom I shared good chit chat at coffee breaks and Happy Hours! You are great and I wish you all the best!!

Special thanks goes to my University friend, and a special roommate Fabio Zani, who always supported me unreservedly and broke my balls asking me to look for papers ;-)). I love you!

Great thank to Anna Cattelino, a great woman of science. She was the person that gave me the first idea of how a real scientist should be. Thank you for having supported me during my first steps in the lab. You have been a great post doc and teacher!

Finally, I would like to thank Daniele, the love of my life. You have always believed in me and you have always supported me wholeheartedly; when I was sad, tired, worried, when I had problems with my family, whenever… Thank you for that! I love you!
A thanks goes also to your wonderful family, which I consider as my second family.

Last, but not least, a big thank you to my dear mother, who had to face with a hard time of life. You are a great fighter, I know. I'm proud of you and I will always love you!